10. SITE 703[1]

Shipboard Scientific Party[2]

HOLE 703A

Date occupied: 21 April 1987

Date departed: 25 April 1987

Time on hole: 4 days, 5 hr

Position: 47°03.042'S, 07°53.679'E

Bottom felt (rig floor; m; drill-pipe measurement): 1806.6

Distance between rig floor and sea level (m): 10.50

Water depth (drill-pipe measurement from sea level; corrected m): 1796.1

Total depth (rig floor; corrected m): 2184.0

Penetration (m): 377.4

Number of cores: 41

Total length of cored section (m): 377.4

Total core recovered (m): 192.29

Core recovery (%): 50

Oldest sediment cored:
Depth sub-bottom (m): 363.95
Nature: dolomite-bearing volcanic ash calcareous sand (turbidite)
Age: early middle Eocene

Basement:
Depth sub-bottom (m): 364.0
Nature: highly altered porphyritic basalt or basaltic andesite
Age: early middle Eocene?
Measured velocity range (km/s): 5.255

Principal results: Site 703 is located on the Meteor Rise (47°03.042'S, 07°53.679'E; water depth of 1796 m), an aseismic ridge extending southwest from the Agulhas Fracture Zone. The Islas Orcadas Rise (Site 702 location) and the Meteor Rise are both bounded by lower Eocene oceanic crust generated at the Mid-Atlantic Ridge. These rises were formed at the locus of a new spreading center following a Late Cretaceous westward shift of the ridge axis in the Agulhas Basin. The major objectives of drilling at this site were to determine the nature, age, and subsidence history of the rise and to investigate the influence of the shallow Paleogene Meteor Rise, Islas Orcadas Rise, and the adjacent fracture zones on oceanic communication between the high and temperate latitudes of the South Atlantic.

Site 703 was focused on the deep objectives and consists of a single hole, from which 15 cores were obtained with the advanced hydraulic piston corer (APC) to 137.9 m below seafloor (mbsf) (97.5% recovery), and 26 cores were obtained with the extended core barrel (XCB) system to a total depth of 377.4 mbsf (24.2% recovery), resulting in a total recovery of 51%. Further tests of the Navidrill coring system were carried out, but no sediments were obtained. The hole was logged with a single run using the Schlumberger sonic, dual induction, natural gamma-ray, and caliper tools. Drilling was hampered by heavy seas, and we spent 12 hr waiting on weather (maximum roll 15° and maximum pitch 10°).

The stratigraphic section at Site 703 consists of calcareous ooze and chalk, with intervals of mass flow deposits of clay, ooze, sand/gravel, and slightly to moderately porphyritic basalt or basaltic andesite and felsic pyroclastic rocks. The dominant lithologies and ages of the stratigraphic sequence are as follows:

0–71.4 mbsf: siliceous-foraminifer-bearing nannofossil ooze of latest early Oligocene to Quaternary age;
71.4–162.4 mbsf: foraminifer-bearing nannofossil ooze of latest middle Eocene to latest early Oligocene age;
162.4–228.9 mbsf: nannofossil ooze containing mass flow deposits of clay, foraminifer ooze, and gravelly sand of middle middle to latest middle Eocene age;
228.9–364.0 mbsf: nannofossil chalk containing mass flow deposits of gravel of middle Eocene age;
364.0–365.65 mbsf: slightly to moderately altered basalt, basaltic andesite, and felsic pyroclastic rocks.

Site 703 is between the Subtropical Convergence and the Antarctic Convergence Zone (ACZ) and has received predominantly calcareous biogenic sedimentation since the early Eocene, with significant biosiliceous input in the late Eocene, the late Oligocene/early Miocene, and particularly in the Pliocene and Quaternary. The middle Eocene through Oligocene sequence of this site was the sixth consecutive representation of Paleogene sediments recovered by Leg 114. An additional succession of paleomagnetic polarity zones was identified in the lower Oligocene to lower Miocene, where recovery was good (98.2%). Together with other Leg 114 sequences, this recovery of a major part of the Paleogene with a paleomagnetic polarity record allows calibration of biostratigraphic and paleoceanographic events to the geomagnetic polarity time scale (GPTS).

Sedimentation rates were ~9 m/m.y. during the late middle Eocene through early Oligocene. An evaluation of late Oligocene and early Miocene sedimentation rates awaits further biostratigraphic studies to determine the duration of bracketing hiatuses. The late Pliocene–Pleistocene sedimentation rate was ~ 3 m/m.y. Hiatuses span most of the upper Oligocene (~25–30 Ma) and a portion of the lower Miocene to upper Pliocene (~3.0 to 21.5–23.2 Ma). A minor hiatus (0.2 to 0.4 m.y. duration) occurs at the sediment/water interface.

Microfossil assemblages record a similar history of surface-water cooling during the middle Eocene to late Oligocene, as at the other Leg 114 sites. There is some indication at this more easterly site that surface waters remained warmer during the late Paleogene, although the general middle Eocene to late Oligocene cooling trend is the same.

Paleodepth estimates based on benthic foraminifer assemblages suggest a depth >600 m below sea level (mbsl) during the Eocene and >1000 mbsl during the Oligocene. Redeposited shallow-water microfossils occur throughout the Eocene and Oligocene section, and in the Eocene these include neritic diatoms, suggesting the presence of nearby islands.

The elevated position of this site makes the early middle Eocene age of basement an uncertain indicator of the age of the Meteor Rise. Redeposited microfossils are no older than Eocene, unlike at the Islas Orcadas Rise where Upper Cretaceous microfossils are reworked in the upper Paleocene.

BACKGROUND AND OBJECTIVES

Site 703 is located on the Meteor Rise, an aseismic ridge situated on lower Paleogene oceanic crust south of the Agulhas Fracture Zone (Fig. 1). The rise has a relief of 1–2 km and is over 350 km long, with a variable cross-strike width (100–170 km) (Fig. 2). The Meteor Rise parallels the north-northwest

[1] Ciesielski, P. F., Kristoffersen, Y., et al., 1988. *Proc. ODP, Init. Repts.*, 114: College Station, TX (Ocean Drilling Program).

[2] Shipboard Scientific Party is as given in the list of Participants preceding the contents, with the addition of M. Perfit, Department of Geology, University of Florida, Gainesville, FL 32611.

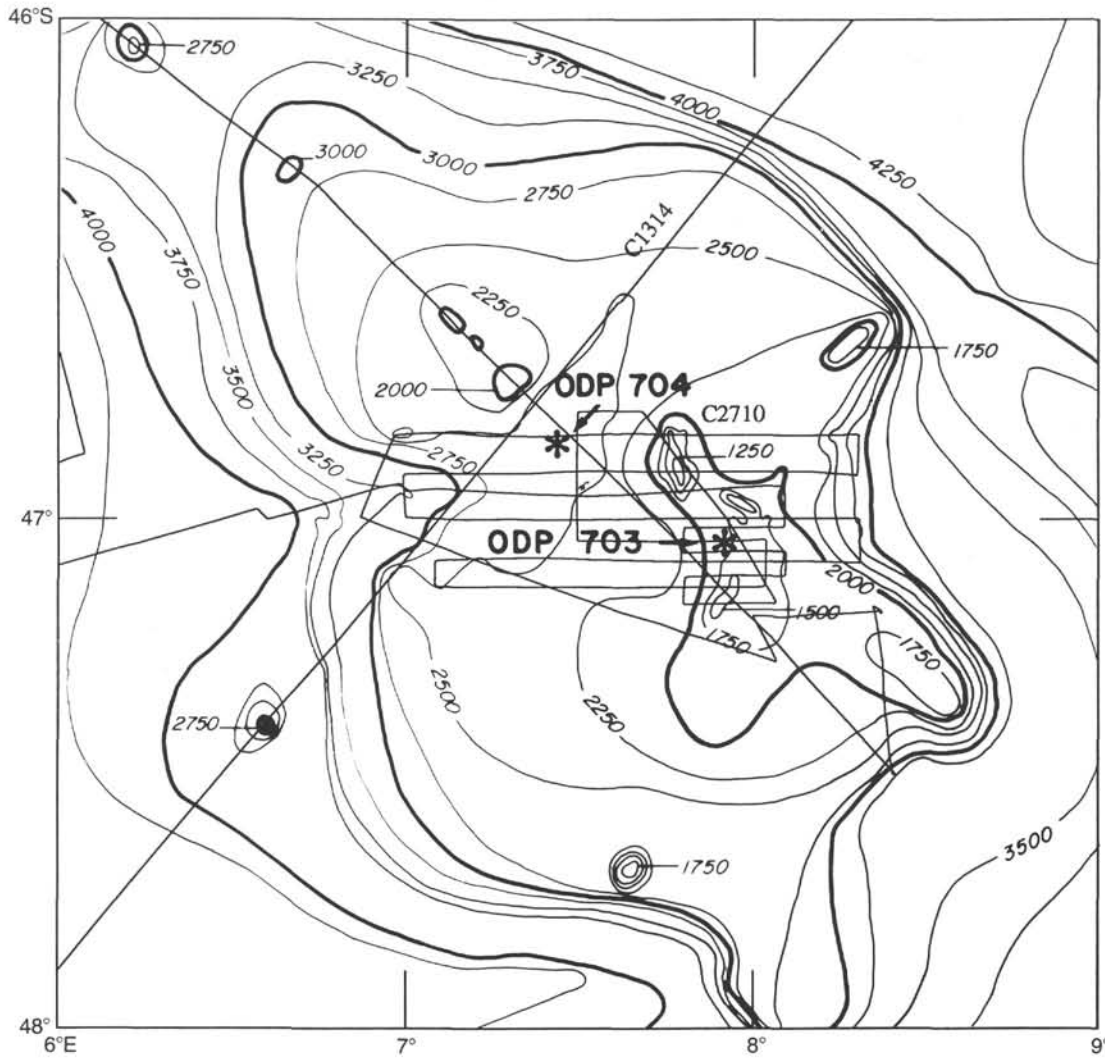

Figure 1. Regional bathymetry (in meters) of the Meteor Rise and vicinity, with locations of Sites 703 and 704 (from Raymond and LaBrecque, this volume).

trend of early Eocene (anomaly 24) and younger magnetic anomalies on the eastern flank of the Mid-Atlantic Ridge but is flanked to the east by an oblique trend of Late Cretaceous age (anomaly 34–32) magnetic lineations (LaBrecque, 1986). At the close of the Cretaceous, a discrete westward jump of the spreading center from the Agulhas Basin shortened the offset in the Falkland-Agulhas Fracture Zone by about 825 km (LaBrecque and Hayes, 1979). As both the Meteor Rise and Islas Orcadas Rise parallel the Mid-Atlantic Ridge and are flanked by lower Eocene oceanic crust, it is likely that they formed as a result of excessive volcanism along the locus of the new spreading center and were later separated by seafloor spreading. Seamounts reaching 1100 mbsl on Meteor Rise and several flat-topped guyotlike seamounts at 1800 mbsl on Islas Orcadas Rise must have been at or near sea level at the ridge crest. The presence of the rises at the ridge crest represents a major shallowing of the Mid-Atlantic Ridge segment abutting the southern side of the Falkland-Agulhas Fracture Zone, and these topographic elements constituted major obstacles to deep and intermediate oceanic circulation, particularly during the early Paleogene. Subsequent seafloor spreading and thermal relaxation of the oceanic crust opened a gateway for deep oceanic communication between antarctic water masses and the South Atlantic.

The Meteor Rise has a more rugged basement topography than the Islas Orcadas Rise, and the seismic data show a depositional environment strongly influenced by bottom currents (Figs. 3 and 4). The pelagic sediments infill topographic lows or occur as sediment drifts near major seamounts or basement ridges. Four distinct seismic-stratigraphic units are apparent in the reflection data. An upper 0–100-ms-thick unit with acoustic stratification unconformably overlies a 150–300-ms-thick highly reflective unit above the main sequence, which may be up to 500 ms thick and exhibits weak internal acoustic lamination. In some places a basal seismic sequence (150 ms thick) is highly reflective and partly masks basement in the seismic records.

Site 703 is located at 47°03.04′S, 07°53.7′E, in a water depth of 1796.1 m. This location is between the present position of the Subtropical Convergence and the ACZ. The northern edge of the ACZ is presently about 2.5° south of Site 703 and is, in this region, characterized by a drop in surface temperature of 1.5°–2°C over a distance of 126 km (Lutjeharms and Valentine, 1984). Approximately 5° to the north (42°S) is the Subtropical Convergence, the region where subantarctic surface water subducts northward beneath subtropical surface water to form South Atlantic Central Water. Site 703 is positioned near the mean position of the polar front, which is expressed as a subsurface tem-

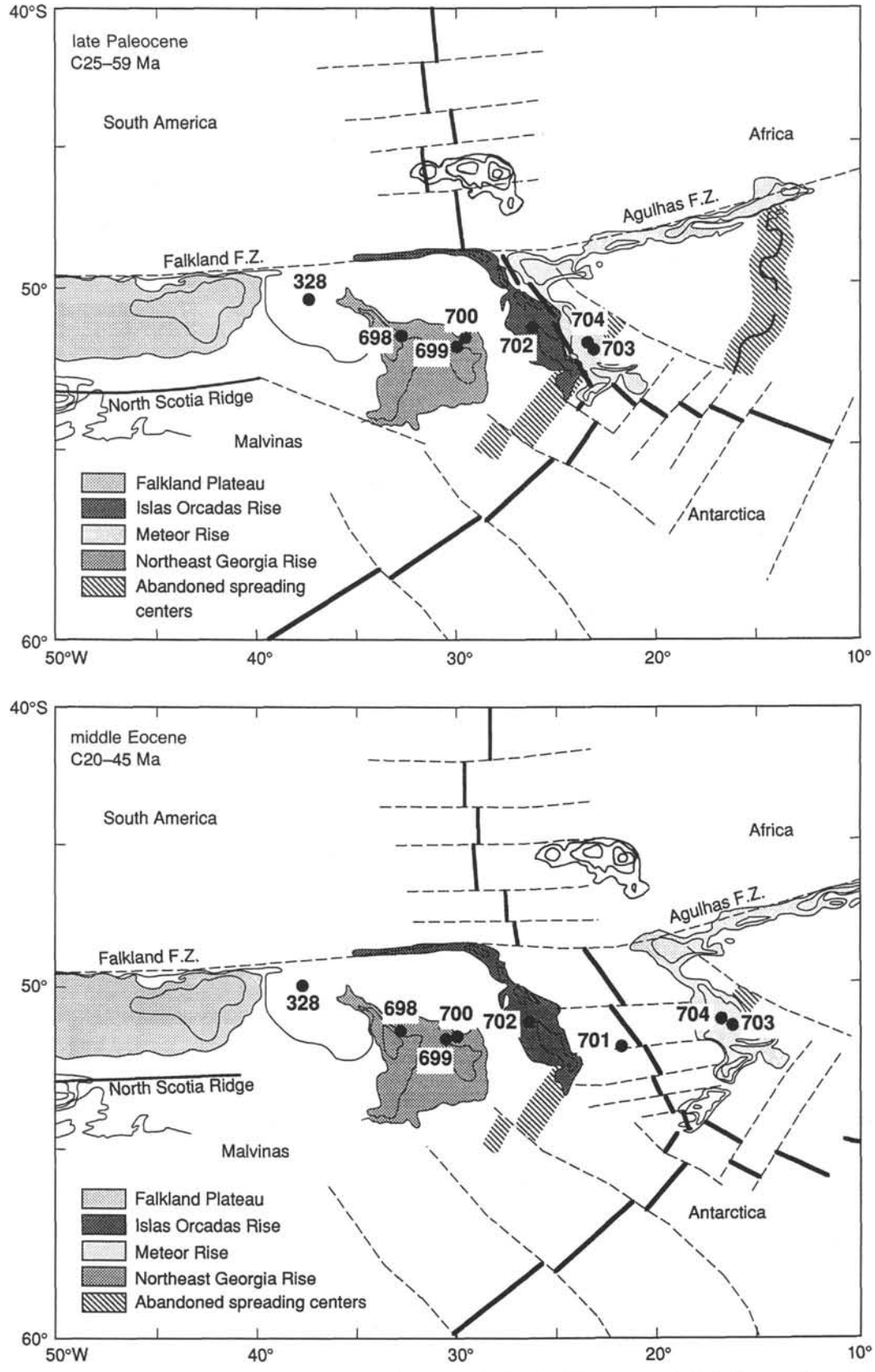

Figure 2. Reconstruction of the subantarctic sites of Leg 114 for the late Paleocene and middle Eocene. Spreading-center location is based on magnetic anomaly locations. Supporting data from OMD Region 13 synthesis (LaBrecque, 1986).

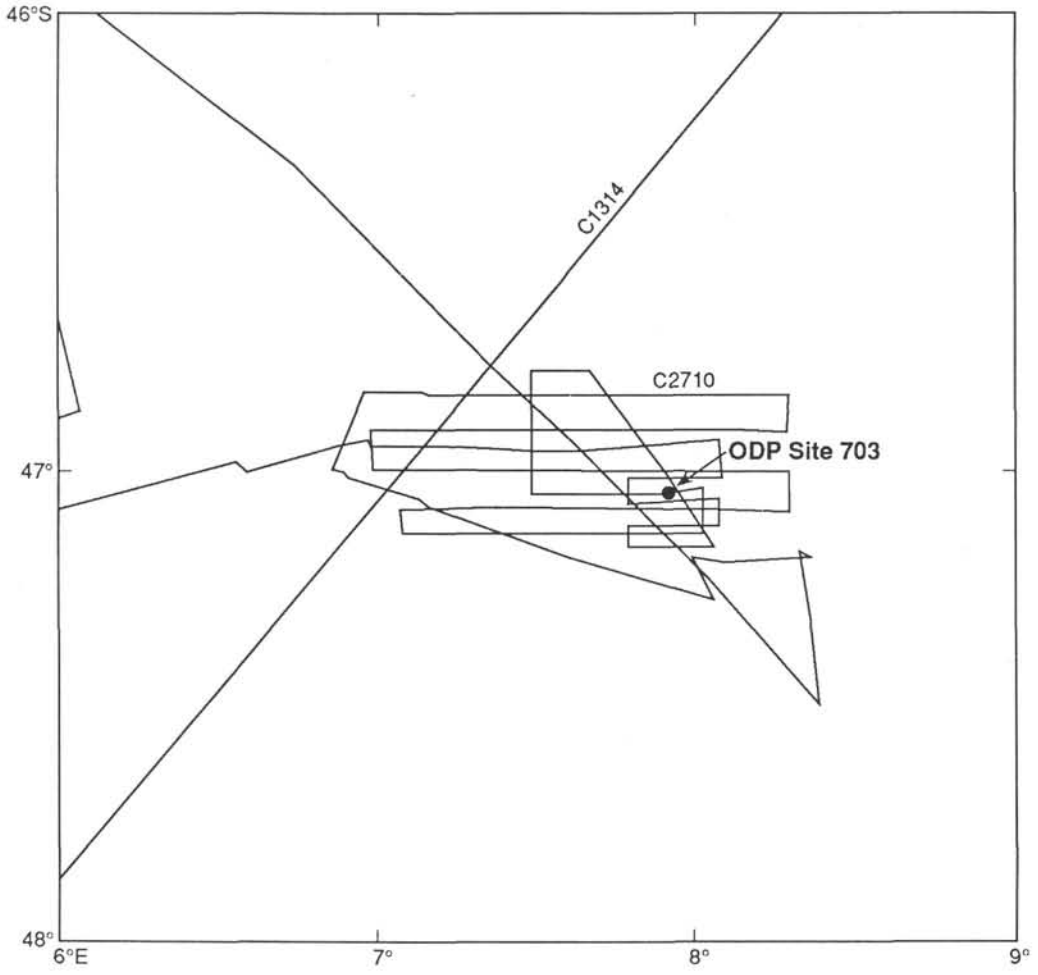

Figure 3. Site survey data for Meteor Rise, with location of Site 703.

perature gradient between 3° and 5°C. Present-day sea surface temperatures over the Meteor Rise average 6° to 7°C.

The rationale for drilling Site 703 on the Meteor Rise was to test models for its origin in a plate tectonic framework and to investigate its influence on paleocirculation. The specific objectives were:

1. to determine the nature, age, and subsidence history of the rise;
2. to interpret the influence of the shallow Paleogene Meteor Rise, Islas Orcadas Rise, and the adjacent fracture zones on oceanic communication between the high and temperate latitudes of the South Atlantic;
3. to interpret the vertical temperature structure of Paleogene water masses;
4. to evaluate the geochemistry of aseismic ridges;
5. to integrate biostratigraphic zonal schemes of high and temperate latitudes;
6. to calibrate subantarctic biostratigraphy to the GPTS;
7. to document the evolutionary history of high-latitude biota.

The original drilling plan for Meteor Rise called for a single site with deep penetration (800 m) to meet all objectives. To minimize the risk of not achieving the deep objectives because of hole instability, as experienced at previous sites, two sites (703 and 704) were selected for drilling. Site 703 focused on obtaining the oldest sediments and basement penetration in an area where the sediment thickness is 300–400 m.

OPERATIONS

Heavy seas and strong winds that hampered the survey of Site 703 also prevented an expeditious return to the beacon. Nevertheless, within 3 hr of dropping the beacon, the vessel was operating in dynamic positioning mode. Because the Navidrill coring system was to be deployed again at this site, the landing/saver sub and head sub with a double window latch sleeve were replaced with those that had already been checked. Replacement core barrels, made up during the transit, were checked for proper space-out. Prior to running in the hole, a Navidrill flow test was conducted at the rig floor. As a result of the test, a bearing sub on the mud motor was found to be oversized, causing the tool to jam and preventing the seals from seating properly. The sub was ground down on the rig floor and the test continued. The main outer core barrel assembly was held above the rotary table, and tension was held on the sand line to prevent scoping of the Navidrill core barrel (NCB). Circulation through the motor initiated rotation of the diamond NCB bit, and the tool appeared to be functioning properly. The test was rigged down, the top drive set back, and the pipe was run in the hole.

At 1955 hr, Hole 703A was spudded in 1796.1 m of water (Table 1). Coring continued with the APC until the NR2 (short) sand line broke at the rope socket during retrieval of Core

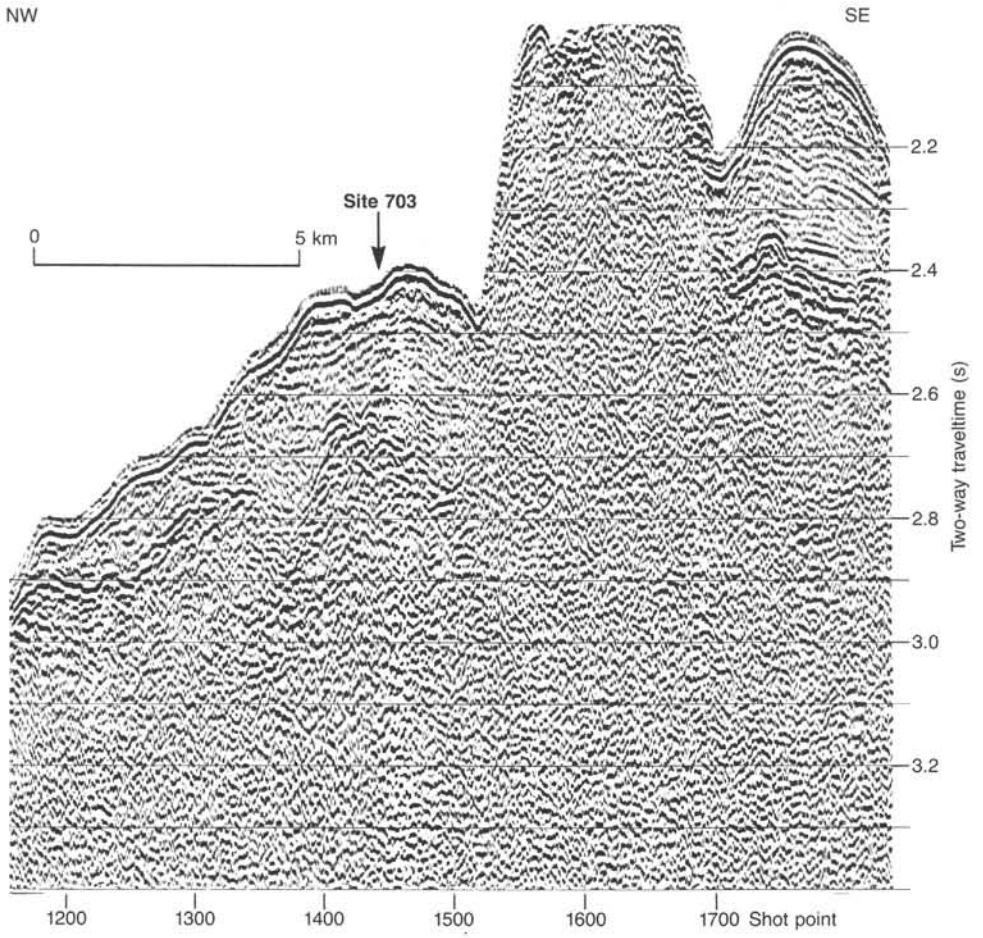

Figure 4. Single-channel seismic-reflection profile (*Conrad* cruise 2710) with general location of Site 703. Location of line shown in Figure 3.

114-703A-9H. Because this line was quite brittle and in bad shape, it had not been used during the leg, except as a backup to the NR1 sand line. Coring resumed until 0530 hr, when the weather forced coring operations to cease. The pipe was pulled off the bottom by several stands, and a stand of wear-knotted drill pipe was picked up and placed in the horn. We spent 12.5 hr waiting on weather while the seas built. Winds gusted to 63 kt, and the vessel rolled 10°–15°. By now, all aboard were quite accustomed to these "little blows," and little attention was given to the weather until a large wave broke over the bow. Caught somewhat unaware, the mate and dynamic positioning system operators instinctively ducked while the wooden ice observer station, secured forward on the bridge deck, was completely demolished. By 1830 hr the weather was still not good, but it had improved enough so that it was safe for operations to resume. Coring with the APC was halted after the core barrel bent and sanded up. Heavy circulation eventually freed the barrel, and coring operations with the XCB system were initiated. We cored continuously, with 15-bbl mud pills spotted every third core to aid in maintaining good hole condition.

The multiple chert and sand layers were worrisome; however, they seemed to affect core recovery more than hole stability. Recovery was affected tremendously by a very soft foraminifer ooze that was extremely water sensitive. All known coring techniques were tried. Circulation rates, weight on bit, and revolutions per minute were all varied in an attempt to improve recovery but without success. We even tried laying down the core barrel immediately upon arrival rather than placing it in the handling shuck. This seemed to help in some instances when the heavy surging in the moon pool was removing what little core was recovered. We were reluctant to return to use of the APC because it was judged to be too risky, in consideration of the previously encountered chert and sand layers. Operations continued until the overshot 2-lug quick release disengaged while cutting Core 114-703A-40X. A fishing attempt was made with a standard Bowen spear and grapple with no success. It was determined that the nut terminating the spear had to be reduced in length because of the shallow depth of the Q/R bore. While the spear was being modified, the pipe became stuck and the bit plugged. One half hour later the pipe was freed, the bit unplugged, and the second fishing attempt was made. This time the barrel, containing approximately 1.5 m of basalt core, was recovered without incident. The hole was swept with a mud pill, and one final core was cut with the XCB system, with negligible recovery, while readying the NCB for deployment.

Several modifications were made to the NCB prior to this site: the tool was equipped with a solid landing shoulder to allow downhole free-fall, the O-ring spring pack was replaced with a solid metal spacer, and no latching system was used. The main XCB bit was set on bottom prior to landing so that no tensile load would be transmitted through the male spline. The tool was redressed with nonjamming, steel torque segments that were fabricated aboard ship. Standpipe pressures were normal upon landing. Coring pressures were abnormally low, and no pressure spike (indicating full stroke) was evident after coring for approximately 30 min. The tool was retrieved without any problem,

Table 1. Coring summary, Site 703.

Core no.	Date (Apr. 1987)	Local time (hr)	Depths (mbsf)	Cored (m)	Recovered (m)	Recovery (%)
Hole 703A						
1H	21	2002	0.0–4.9	4.9	4.93	100.0
2H	21	2035	4.9–14.4	9.5	9.96	105.0
3H	21	2100	14.4–23.9	9.5	9.33	98.2
4H	21	2135	23.9–33.4	9.5	9.65	101.0
5H	21	2158	33.4–42.9	9.5	9.93	104.0
6H	21	2225	42.9–52.4	9.5	10.00	105.2
7H	21	2300	52.4–61.9	9.5	7.82	82.3
8H	21	2323	61.9–71.4	9.5	8.95	94.2
9H	22	0125	71.4–80.9	9.5	10.11	106.4
10H	22	0215	80.9–90.4	9.5	9.84	103.0
11H	22	0320	90.4–99.9	9.5	10.01	105.3
12H	22	0415	99.9–109.4	9.5	9.92	104.0
13H	22	0505	109.4–118.9	9.5	6.40	67.3
14H	22	2050	118.9–128.4	9.5	8.76	92.2
15H	22	2315	128.4–137.9	9.5	8.77	92.3
16X	23	0030	137.9–143.4	5.5	1.90	34.5
17X	23	0120	143.4–152.9	9.5	4.24	44.6
18X	23	0200	152.9–162.4	9.5	6.48	68.2
19X	23	0315	162.4–171.9	9.5	0.14	1.5
20X	23	0410	171.9–181.4	9.5	7.79	82.0
21X	23	0515	181.4–190.9	9.5	8.01	84.3
22X	23	0600	190.9–200.4	9.5	3.53	37.1
23X	23	0725	200.4–209.9	9.5	1.14	12.0
24X	23	0815	209.9–219.4	9.5	0.04	0.4
25X	23	0900	219.4–228.9	9.5	0.00	0.0
26X	23	1020	228.9–238.4	9.5	7.27	76.5
27X	23	1115	283.4–247.9	9.5	0.29	3.1
28X	23	1140	247.9–257.4	9.5	0.05	0.5
29X	23	1245	257.4–266.9	9.5	0.00	0.0
30X	23	1315	266.9–276.4	9.5	5.66	59.6
31X	23	1550	276.4–285.9	9.5	0.01	0.1
32X	23	2010	285.9–295.4	9.5	0.00	0.0
33X	23	2115	295.4–304.9	9.5	0.16	1.7
34X	23	2210	304.9–314.4	9.5	7.04	74.1
35X	23	2255	314.4–323.9	9.5	0.00	0.0
36X	23	2345	323.9–333.4	9.5	0.20	2.1
37X	24	0045	333.4–342.9	9.5	0.00	0.0
38X	24	0125	342.9–352.4	9.5	0.01	0.1
39X	24	0215	352.4–361.9	9.5	0.04	0.4
40X	24	0645	361.9–371.4	9.5	3.76	39.6
41X	24	1035	371.4–377.4	6.0	0.15	2.5
				377.4	192.29	

and the barrel did not stick like on earlier runs. Inspection of the landing shoulder and torque segments indicated that the barrel had landed and latched properly. The diamond bit was somewhat damaged, most likely as a result of impact with the actuation balls in the lockable float-valve (LFV) assembly. There was no evidence that any rotation of the bit had taken place, and we believe that the mud motor stalled, resulting in no rotation.

The top drive was set back, and the drill pipe was pulled to a logging depth of 1910 m. The suite of logging tools to be deployed would not accommodate the actuation bull plug for the LFV assembly, so an expendable actuation go-devil was deployed at 60 strokes per minute. There was no indication that the flapper was locked open, so an XCB system core barrel was deployed to ensure that the go-devil had indeed gone through the LFV. As we feared might happen, the "expendable" go-devil was recovered with the XCB core catcher engaging the pulling neck. The logging suite was changed to one with an actuating bull nose and was run in the hole. Logging with the DIT-D, BHC, MCD, and SGT tools was conducted to 2121 mbsl. Upon reaching the bottom-hole assembly (BHA) with the logging tools, an overpull was experienced, and the tools would not enter the drill string. Indications were that the lockable flapper had not locked open and was preventing the tools from being retrieved any further. Eventually the tools were recovered by pumping the flapper open with 40 strokes/min while simultaneously retrieving the logging cable. This was done with great care so as not to cause the weak point of the cable head to fail, which would result in tool loss. Once the tools were started into the BHA, we ceased pumping and brought the tools to the surface. After rigging down the logging sheaves, the hole was displaced with heavy mud, and the drill string was pulled out of the hole. The pipe cleared the seafloor at 0320 hr, and the bit cleared the rotary at 0715 hr, terminating Hole 703A. As suspected, when the LFV assembly was inspected we found it to be sanded-up with sand and coarse gravel, preventing the mechanism from functioning.

LITHOSTRATIGRAPHY

Site 703 consists of a single hole drilled on the slope of a basement peak on the Meteor Rise in a water depth of 1796.1 m. The hole was drilled to a depth of 377.4 mbsf. Core recovery in the upper 190 m was very good with an average recovery of 84.6%. However, below this depth recovery was exceptionally poor, reaching only 15.7% (Fig. 5). Thus, the average recovery for the whole site is 50%.

The Quaternary to lower middle Eocene sediments recovered consist of a single lithofacies (Unit I) of calcareous ooze and

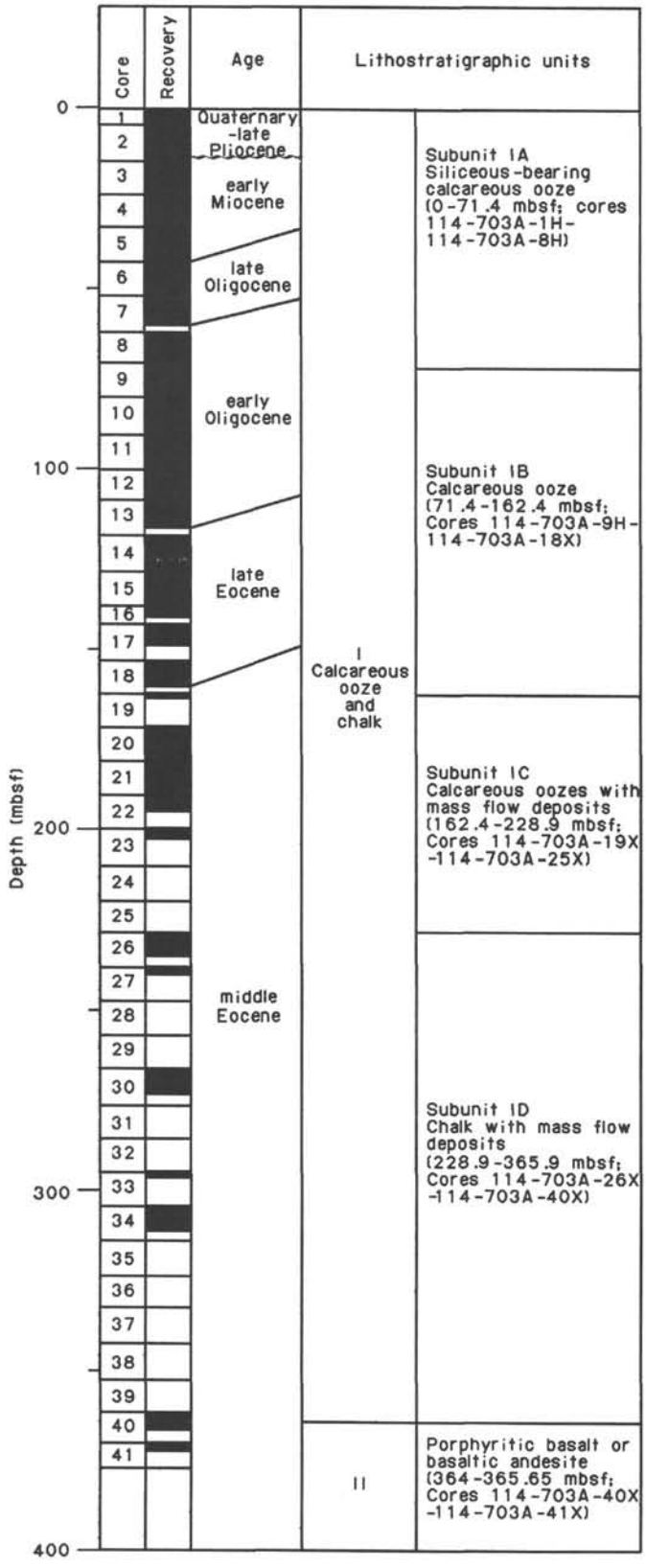

Figure 5. Core recovery and lithostratigraphic units, Site 703.

chalk, which has been subdivided into four subunits on the basis of slight changes in the lithology and diagenesis (Fig. 5 and Table 2). Additional information from downhole logging results was also used in determining the subunit boundaries, especially below 190 m where core recovery was poor.

Subunit IA: siliceous- and foraminifer-bearing nannofossil ooze of latest early Oligocene to Quaternary age, 0–71.4 mbsf;

Subunit IB: foraminifer-bearing nannofossil ooze of latest middle Eocene to latest early Oligocene age, 71.4–162.4 mbsf;

Subunit IC: nannofossil ooze containing mass flow deposits of clay, foraminifer ooze, and a gravelly sand, middle middle Eocene to latest middle Eocene in age, 162.4–228.9 mbsf.

Subunit ID: nannofossil chalk containing mass flow deposits of gravel (the downhole log also suggests mass flow deposits in this subunit) of middle Eocene age, 228.9–371.9 mbsf.

A second lithofacies (Unit II, 364–365.65 mbsf) consists of porphyritic and holocrystalline basalt or basaltic andesite with lithic (dacitic to rhyolitic) tuff.

Unit I: Cores 114-703A-1H to 114-703A-40X; Depth: 0–365.9 mbsf; Age: Eocene to Quaternary.

Subunit IA: Cores 114-703A-1H to 114-703A-8H; Depth: 0–71.4 mbsf; Age: latest early Oligocene to Quaternary.

A number of cores in this subunit were disturbed during drilling, resulting in soupy or biscuited sediments (Cores 114-703A-1H, 114-703A-2H, 114-703A-4H, 114-703A-5H, and 114-703A-7H).

The lithology varies depending on the composition of the minor constituents (Fig. 6). There is a trend in the minor constituents from volcanic ash, nannofossils, and siliceous organisms to foraminifers with depth. In detail, the sediment grades from white (10YR 8/1) foraminifer ooze and volcanic-ash- and nannofossil-bearing foraminifer ooze and white (no color code) to pinkish white (7.5YR 8/2) foraminifer nannofossil ooze and foraminifer-bearing nannofossil ooze at the top of the hole through pinkish white (5YR 8/2) siliceous- and foraminifer-bearing nannofossil ooze to light gray (10YR 7/1) foraminifer-bearing nannofossil ooze at the base of the subunit.

Minor lithologies include light gray (10YR 7/1) volcanic-ash- and diatom-bearing foraminifer ooze (Cores 114-703A-1H and 114-703A-2H), pinkish white (5YR 8/2) siliceous foraminifer nannofossil ooze (Core 114-703A-8H), and a 1-cm-thick ash layer at 75 cm in Core 114-703A-3H. Sparsely disseminated, fine lithic fragments occur in Cores 114-703A-5H to 114-703A-8H. A gravel horizon at 28–39 cm in Section 114-703A-1H-3 and a pebble in Section 114-703-2H-4 at 58 cm may represent ice-rafted debris. However, mixed gravel and sediment at the top

Table 2. Lithostratigraphic units at Site 703.

Unit/ subunit	Lithology	Depth	Age
IA	Siliceous foraminifer-bearing nannofossil ooze	0–71.4	latest early Oligocene–Quaternary
IB	Foraminifer-bearing nannofossil ooze	71.4–162.4	latest middle Eocene–latest early Oligocene
IC	Nannofossil ooze with mass flow deposits	162.4–228.9	middle Eocene
ID	Nannofossil chalk with mass flow deposits	228.9–365.9	middle Eocene(?)–Eocene
II	Porphyritic basalt or basaltic andesite	364–365.65	?

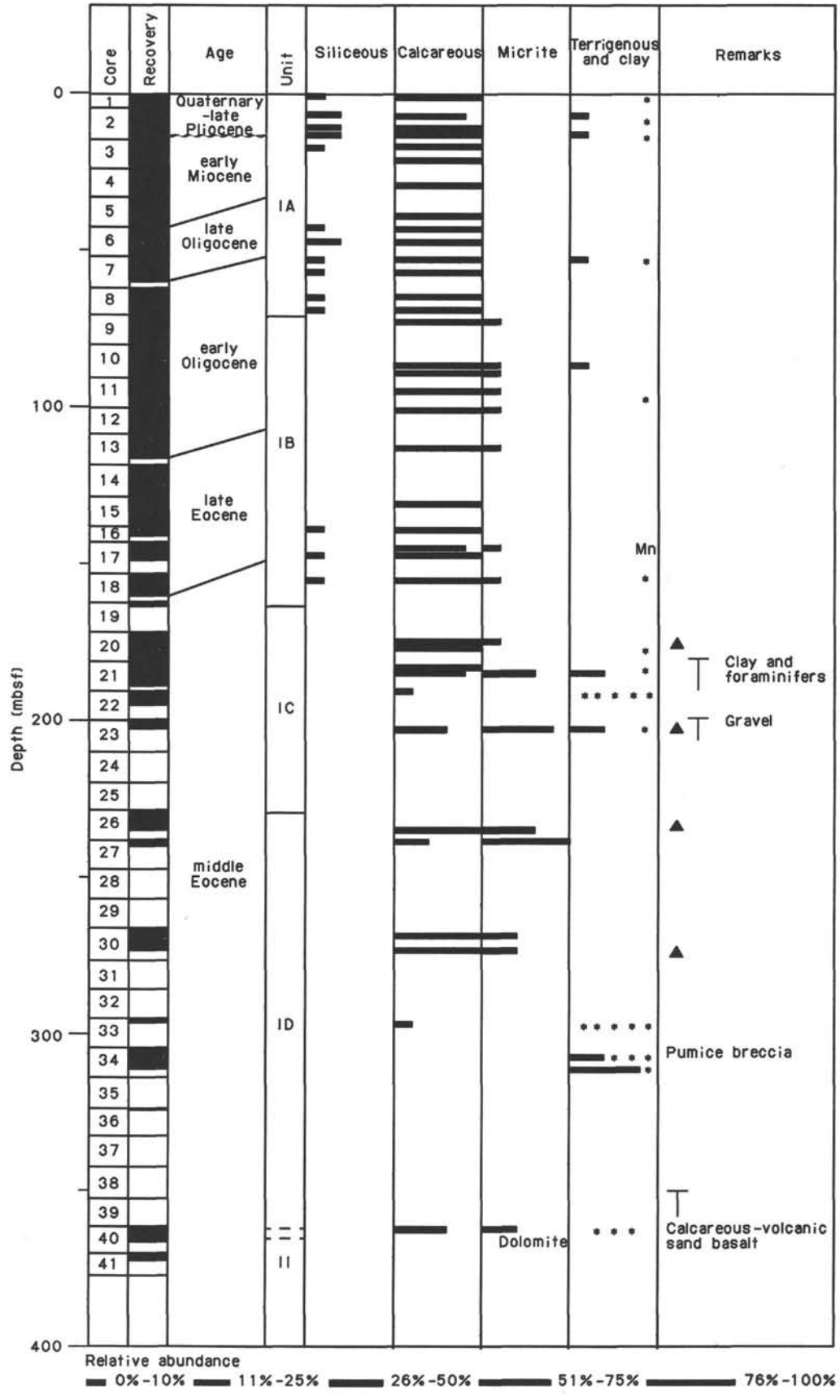

Figure 6. Smear slide analysis, Site 703. Volcanic ash = *; turbidite = T ; chert = solid triangle.

of Cores 114-703A-3H to 114-703A-8H probably represent downhole contamination.

The sediments in this subunit exhibit almost no structures. Minor mottling resulting from bioturbation was observed below Core 114-703A-6H.

The carbonate content is high, averaging over 90% (Fig. 7). Fluctuations of up to 7% reflect the presence of noncarbonate components such as volcanic ash and siliceous organisms.

Subunit IB: Cores 114-703A-9H to 114-703A-18X; Depth: 71.4–162.4 mbsf; Age: latest middle Eocene to latest early Oligocene.

Drilling disturbance in these cores is manifested as soupy sediment at the tops of the cores and within Sections 114-703A-12H-2 and 114-703A-3. Core 114-703A-14H consists entirely of soupy sediment. Gravel, found also at the tops of the cores, is believed to be downhole contamination.

Homogenous, white (no color code) foraminifer-bearing and micrite- and foraminifer-bearing nannofossil oozes characterize this subunit (Fig. 6). Minor manganese staining is observed in most of the cores, with Mn-stained layers occurring in Cores 114-703A-17X and 114-703A-18X. The sediment is structureless, apart from minor mottling in Cores 114-703A-9H, 114-703A-11H, and 114-703A-15H.

The average carbonate content remains above 90%, but there is less fluctuation than within Subunit IA (Fig. 7). Lower values of 79%–82% between 102 and 108 mbsf do not appear to be related to any visible lithological change. These values correlate with other changes in the physical properties and magnetic susceptibility (see "Paleomagnetics" and "Physical Properties" sections, this chapter).

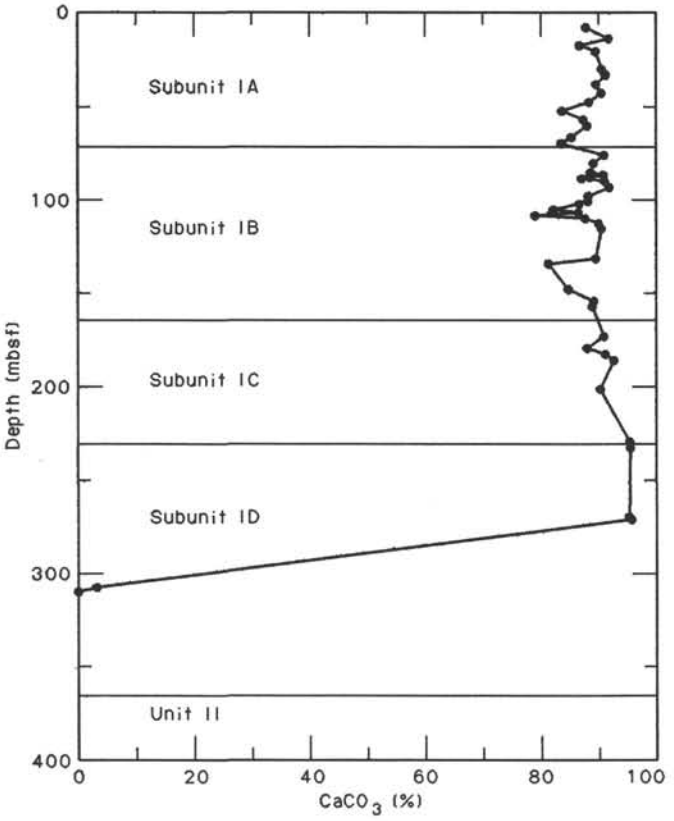

Figure 7. Calcium carbonate content, Hole 703A.

Subunit IC: Cores 114-703A-19X to 114-703A-25X; Depth: 162.4–228.9 mbsf; Age: middle Eocene.

Subunit IC is characterized by poor recovery. The downhole log data suggest that the cause may be mass flow deposits of sand and other sediment, such as foraminifer oozes, that are easily washed out during the drilling process (see "Logging" section, this chapter). The stiff calcareous oozes that were recovered show no disturbance other than minor cracks.

The lithology in this subunit is mixed (Fig. 6). The calcareous sediments consist of light greenish gray (5GY 7/1) foraminifer-bearing nannofossil ooze (Core 114-703A-19X), white (no color code) nannofossil ooze with common Mn staining (Cores 114-703A-20X and 114-703A-21X), and white (no color code) clay- and nannofossil-bearing micritic chalk (Core 114-703A-23X). Minor lithologies associated with the calcareous sediments include chert nodules in Cores 114-703A-20X and 114-703A-23X, a 13-cm-thick, pale yellow (5Y 8/3) ash layer at 35 cm in Section 114-703A-21X-5, and a number of more indurated horizons in Core 114-703A-21X that consist of two layers of pinkish white (7.5YR 8/2) clay-bearing nannofossil ooze at 34–44 and 93–102 cm, as well as two additional layers of sharp-based, normally graded, white (2.5Y 8/2) nannofossil foraminifer chalk at 54–67 (Fig. 8) and 91–120 cm. These indurated horizons are interpreted as mass flow deposits, probably turbidites.

A 3.5-m interval of gravelly volcanic sand was recovered in Core 114-703A-22X and consists of glass shards, pumice, volcanic rock fragments, chert fragments, and granite(?), with an admixture of nannofossil ooze. Primary structures are not visible, but this may be the result of washing of the sediment during core recovery. The sand is also interpreted as a mass flow deposit.

Because of poor recovery below Core 114-703A-22X, the downhole log was used to define the lower boundary of this subunit. The log exhibits a marked change in sonic velocity at about 230 m, which is interpreted as reflecting a change in the induration of the sediment. We have therefore placed the nannofossil ooze/chalk boundary at this depth (below Core 114-703A-25X), despite the fact that the sediments in Core 114-703A-23X have also been described as chalk.

Subunit ID: Cores 114-703A-26X to 114-703A-40X; Depth: 228.9–365.9 mbsf; Age: middle Eocene.

As in the overlying subunit, the core recovery was very poor. Soupy sediments occurred in Cores 114-703A-26X and 114-703A-29X. Indurated sediments in Core 114-703A-34X appear to be extremely broken up.

Lithologies in this subunit are also variable. White (no color code) micritic nannofossil chalk and light gray (5Y 7/1) micrite- and foraminifer-bearing nannofossil chalk occur in the upper part of the subunit (Cores 114-703A-26X and 114-703A-30X). The chalk appears to be structureless apart from faint mottling in Cores 114-703A-26X and 114-703A-30X. The only obviously recognizable bioturbation structure seen at this site is a *Zoophycos* burrow at 113 cm in Section 114-703A-26X-1. Chert nodules occur in Core 114-703A-26X, Section 114-703A-27X, CC, and Core 114-703A-30X.

Core 114-703A-33X consists of a gravelly volcanic sand containing fragments of chert, basalt and basaltic andesite, rhyolitic tuff, and granodiorite. The fragments are probably not in place but are downhole contamination, because they were found only in the core catcher.

A volcanic breccia was recovered in Core 114-703A-34X. The yellow (5Y 8/6) to olive yellow (5Y 6/6) sediment consists of pumice and volcanic glass shards that have been partly cemented by a noncalcareous, white substance (zeolitic?). The sediment

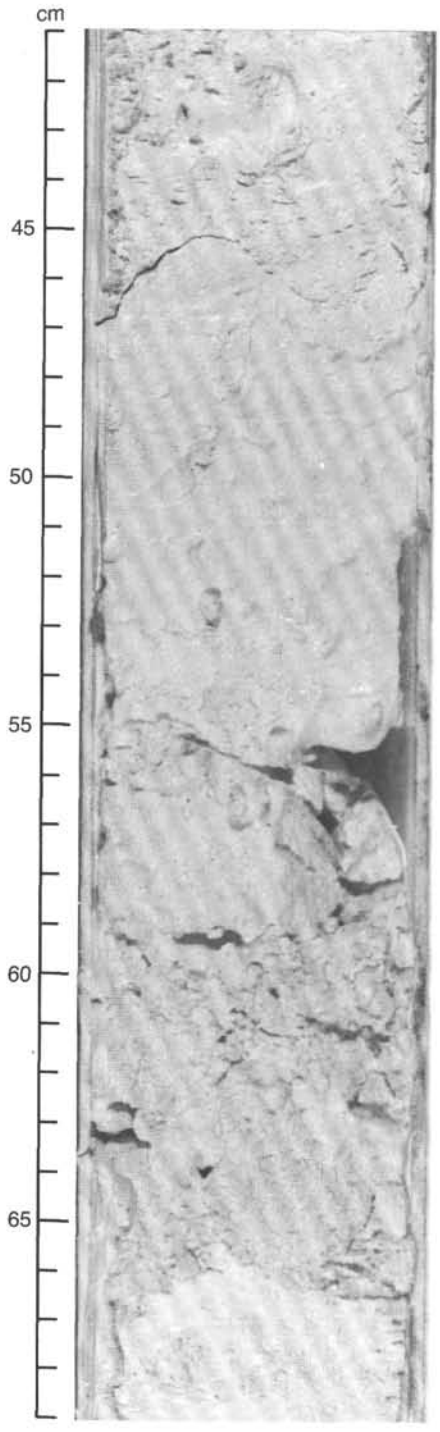

Figure 8. Nannofossil-bearing foraminifer chalk interval (Sample 114-703A-21X-2, 41–69 cm). Note the sharp base and normal grading suggestive of turbiditic origin.

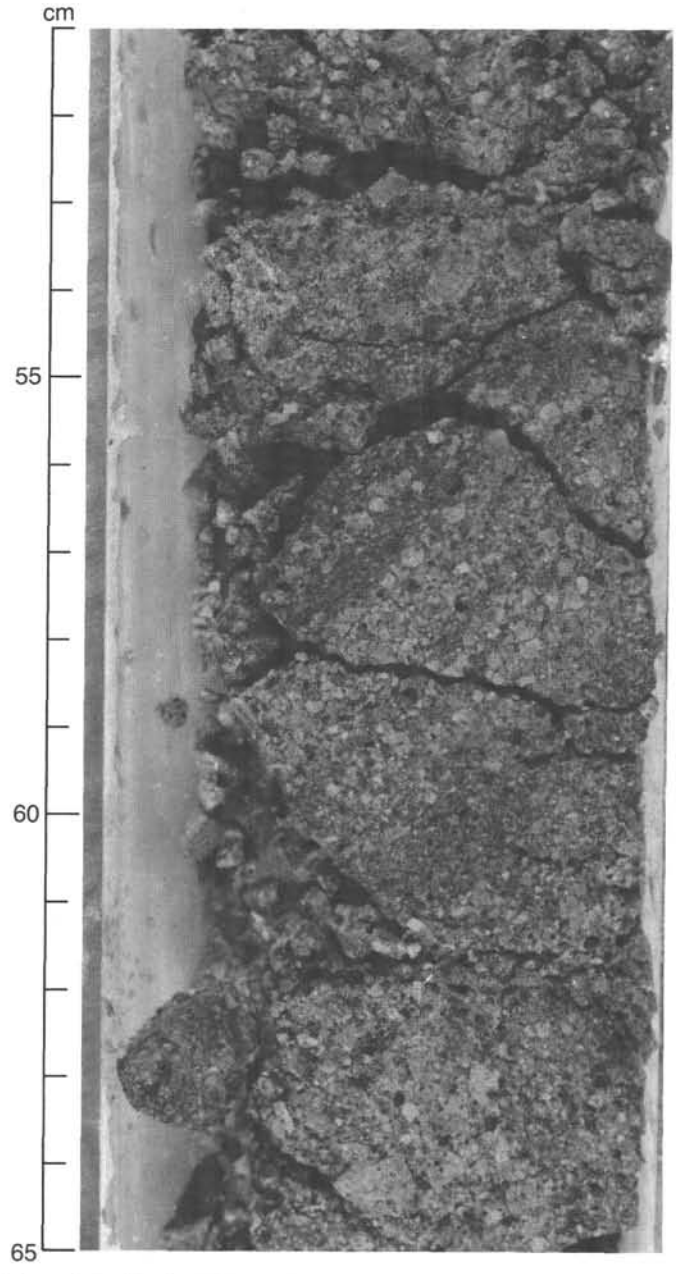

Figure 9. Inclined bedding in the volcanic breccia horizon (Sample 114-703A-34X-3, 51–65 cm). Coarse-grained pumice layers (5–20 mm thick) alternate with finer-grained layers (2–3 mm thick).

was indurated but was extensively broken up by drilling. A few undisturbed clasts exhibit inclined bedding (although not in the same direction), in which 5–20-mm-thick layers of coarse pumice alternate with fine-grained layers (2–3 mm thick) at intervals of about 1–2 cm (Fig. 9).

The lowermost lithology in Subunit ID is a white (2.5Y 8/2) to light olive brown (2.5Y 5/4), dolomite-bearing volcanic ash calcareous sand in Core 114-703A-40X. There appears to be a gradation in grain size from coarser particles at the bottom to finer grain sizes at the top, but this may be a drilling disturbance artifact, especially as the sand is intermixed with pieces of amygdaloidal basalt below 2.5 m in the core. The mixed lithology together with the presence of dolomite (forming within foraminifer chambers), as well as microfossils that have been transported from shallower depths (see "Biostratigraphy" section, this chapter) indicate that the sand is a mass flow deposit or series of deposits.

Downhole logging data for Subunit ID are available to a depth of 320 mbsf and suggest that this subunit consists of interbedded lithologies, which are probably turbidites. The lower limit of this subunit is difficult to define because of poor recovery and the lack of logging data below 320 mbsf. There was no recovery below the hard sediments in Core 114-703A-34X and the volcanic sand in Core 114-703A-40X. The drillers reported,

however, that the sediment below Core 114-703A-34X was probably soft and may have been washed away during drilling, suggesting that a lithology similar to that above Core 114-703A-34X may have been present. On this basis, it was decided to include the volcanic sand in Core 114-703A-40X within Subunit ID.

There is also an overlap in the boundary between Units I and II because Unit II occurs as fragments intermixed with the volcanic sand of Core 114-703A-40X. This is probably an artifact of the drilling process.

Unit II: Cores 114-703A-40X and 114-703A-41X; Depth: 364–365.65 mbsf; Age: indeterminate.

Unit II consists of 1.65 m of slightly altered porphyritic basalt or andesitic basalt occurring as pieces intermixed with the volcanic carbonate sand in Core 114-703A-40X and as fragments retrieved in the core catcher of Core 144-703A-41X. The basalt is dark brown (10YR 4/3) and contains phenocrysts of feldspar and altered pyroxene. The mixed lithology in this core is a result of drilling disturbance.

Discussion

The very high carbonate content (Fig. 7) and preservation of even fragile calcareous microfossils indicate that deposition of these sediments occurred above the lysocline at Site 703. The dominance of calcareous over siliceous organisms in the upper Neogene and Quaternary sediments (Fig. 6) contrasts strongly with the other, more southerly, Leg 114 sites. Site 703 lies within the calcareous biozone to the north of the present position of the polar front. Fluctuations in the siliceous content of the upper Neogene and Quaternary sediments (Fig. 6; see also "Biostratigraphy" section) are probably related to northward excursions of the polar front during periods of climatic cooling, with more siliceous sediments deposited during cold periods when the polar front had a more northerly position.

In contrast to the other Leg 114 sites, there is no dramatic increase in the siliceous content within the upper Neogene and Quaternary. At the other sites, this event was interpreted to be a response to the northward migration of the biosiliceous province associated with the polar front during the early Miocene. The absence of a marked change in the siliceous content at Site 703 is probably because of its position about 350 km north of the front. The only indication of a progressively cooling paleoenvironment comes from changes in the species of individual microfossil groups (see "Biostratigraphy" section).

The sedimentary sequence at Site 703 is characterized by reworking of the microfossils (from Cores 114-703A-40X to 114-703A-7H; lower middle Eocene to upper Oligocene–lower Miocene) as well as by mass flow deposits in the lower part of the sequence (middle Eocene). These sediments were deposited on the lee slope of a basement peak. Reworking could therefore be explained either by bottom-current redistribution or by mass flow transport. The existence of steeper slopes during the early part of the depositional history of this site would have caused the apparent preponderance of mass flow deposits up to the Eocene.

Basalt and tuff were found intermixed with sediments in the lowermost two cores (114-703A-40X and 114-703A-41X). It is not possible, therefore, to determine whether it represents basement sensu stricto.

Conclusions

1. A 365.9-m-thick section of calcareous sediment ranging in age from early middle Eocene to Quaternary was recovered at this site. The underlying (and interbedded?) lithology is basalt and tuff, of which 1.65 m were recovered. The sediment sequence has been subdivided into four subunits: siliceous- and foraminifer-bearing nannofossil ooze (Cores 114-703A-1H to 114-703A-8H; latest early Oligocene to Quaternary age), foraminifer-bearing nannofossil ooze (Cores 114-703A-9H to 114-703A-18X; latest middle Eocene to latest early Oligocene age), nannofossil ooze with mass flow deposits (Cores 114-703A-19X to 114-703A-25X; middle Eocene age), and nannofossil chalk with mass flow deposits (Cores 114-703A-26X to 114-703A-40X; middle Eocene age).

2. The sediments have been deposited above the lysocline throughout the history of sedimentation at this site. Minor but persistent reworking of microfossils up to the upper Oligocene may be due to bottom-current transport and/or mass flow effects. Mass flow deposits are characteristic of the lower sedimentary sequence within the Eocene. Fluctuations in the biosiliceous content in Subunit IA may be related to migrations of the polar front.

BIOSTRATIGRAPHY

Biostratigraphy and Paleoenvironment Synthesis

At Site 703, on the eastern slope of the Meteor Rise, we recovered 377 m of Tertiary and Quaternary biosiliceous and biocalcareous sediments. Because of the relatively shallow water depth (1796.1 m at present) this site never subsided below the carbonate compensation depth (CCD). Paleodepth estimates based on benthic foraminifer analyses indicate a lower bathyal to abyssal depth (>1000 m) for the early Oligocene, and a middle bathyal to abyssal depth (>600 m) for the Eocene. Therefore, the entire Tertiary and Quaternary sediment sequence consists of calcareous oozes grading downward into chalks.

The Quaternary sediments are composed of volcanic ash- and nannofossil-bearing foraminifer ooze, dominated by the planktonic foraminifer *Neogloboquadrina pachyderma*. In the older Tertiary sediments, calcareous nannofossils are the dominant microfossil group. The zonal and age assignments of planktonic microfossils are shown in Figure 10, and the age-depth relationships of the biostratigraphic and magnetostratigraphic datums are given in Table 3 and plotted in Figure 11.

Although the calcareous nannofossils are poorly preserved, showing calcite overgrowth throughout, planktonic foraminifers are well preserved in the Quaternary and Neogene. In the Eocene the nannofossils are also recrystallized and show signs of dissolution. In spite of poor nannofossil preservation, the nannofossil age determinations have a resolution equal to those based on planktonic foraminifers (Fig. 10).

Siliceous microfossils are abundant and well preserved only in the upper Pliocene and Quaternary. In the underlying Tertiary sediments, their abundance is reduced to common or even few (Fig. 12). Dissolution has affected the diatoms in particular, whereas silicoflagellates remain abundant and are sufficiently well preserved to allow assignment to the zones established by Ciesielski (1975) and Shaw and Ciesielski (1983). No siliceous microfossils were found below Core 114-703A-23X.

Planktonic foraminifers and diatoms indicate relatively warm-water conditions at Site 703 for the middle to late Eocene. The warm-water planktonic *Acarinina* species are present, and they disappear within the middle Eocene. The diatom assemblage contains several warm-water and cosmopolitan species, such as *Skeletonema barbadiense*, *Melosira architecturalis*, and *Asterolampra vulgaris*. A few warm-water specimens still occur in the lowermost Oligocene. In the younger sediments the assemblages exhibit an increasingly cooler water affinity until the characteristic endemic subantarctic-antarctic assemblages appear in the Pliocene. Compared to the subantarctic assemblages recovered at the other Leg 114 sites farther west, several characteristic species, such as *Coscinodiscus elliptipora* and *Rhizosolenia barboi*, are missing at Site 703. This, together with the relatively low abundance of diatoms, might mean that this site was on the margin of the high-productivity belt surrounding Antarctica.

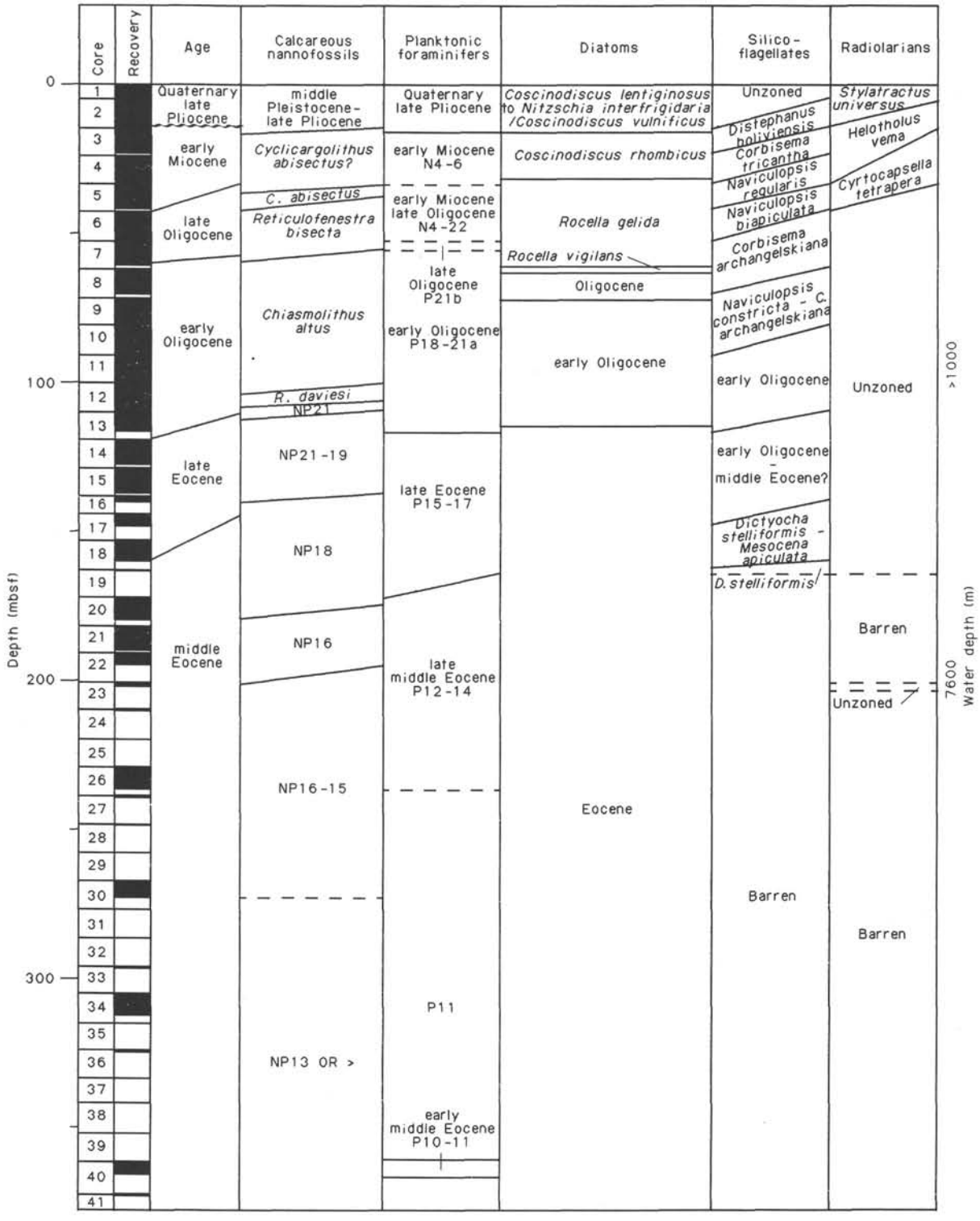

Figure 10. Zonal and age assignments from planktonic microfossils in Hole 703A. Water-depth estimates are derived from the analysis of benthic foraminifers.

Calcareous nannofossils at the more westerly Leg 114 sites exhibit an analogous change from relatively warm-water assemblages in the Eocene, containing discoasters and sphenoliths, to cooler assemblages in the Oligocene and Neogene. Such an assemblage change was not noted at this site. Instead, sporadic occurrences of single discoasters are found through the Eocene and Oligocene at Site 703 (Fig. 12), as well as a peak in abundance in the lower Miocene. In addition, the presence of the radiolarian species *Cyrtocapsella tetrapera* and orosphaerid fragments, as well as the common presence of the silicoflagellate species *Corbisema triacantha*, indicate a period of warm-water influence during the early Miocene. The lower Miocene species indicating warm water occur in a comparable stratigraphic position to those found in Holes 699A and 701C.

Table 3. Microfossil and magnetostratigraphic datums identified at Site 703. Multiple disconformities exist in the Neogene portion of the sequence. Precise determination of the number and extent of the hiatuses in the condensed section will be presented in the *Scientific Results*.

Microfossil and paleomagnetic datums[a]	Age (Ma)	Reference[b]	Bracketing samples	Depth range[c] (mbsf)	Mean position (mbsf)
1. LAD *Hemidiscus karstenii* (D)	+0.195	19	1H, 0 cm, to 1H, 1 cm	0.00–0.01	
2. *LAD *Actinocyclus ingens* (D)	+0.60	10	1H, 98 cm to 1H, CC	0.98–4.90	(2.94)
3. *LAD *Coscinodiscus vulnificus* (D)	+2.22	10	2H-2, 90 cm to 2H-5, 20 cm	7.30–11.10	(9.20)
4. LAD *Nitzschia interfrigidaria* (D)	+2.81	10	2H-5, 20 cm to 2H, CC	11.10–14.40	(15.50)
5. *Base *N. interfrigidaria/ C. vulnificus* (D)	+3.10	10	2H, CC, to 3H-2, 70 cm	14.40–16.60	(15.50)
Hiatus Maximum range = 20 m.y. Minimum range = 18.5 m.y.		(~3.0–23.2 Ma) (3.0–21.5 Ma)	2H, CC, to 3H-2, 70 cm	14.40–16.60	
6. LAD *Rocella gelida* (D)	21.50	16	3H, CC to 4H, CC	23.90–33.40	(28.65)
7. Top *Cyclicargolithus abisectus* Zone (N)	23.2–23.7	1, 4	4H, CC, to 5H-2, 20 cm	33.40–35.10	(34.25)
8. Top *Reticulofenestra bisecta* Zone (N)	23.70	1, 4	5H-2, 21 cm, to 5H, CC	35.11–42.90	(39.01)
Hiatus duration ~5 m.y. (~25–30 Ma), depth uncertain				(~50–60 mbsf)	
9. *Top P21b Zone (F)	28.10	4	7H-1, 124 cm, to 6H, CC	52.40–53.64	(53.02)
10. *Top *Chiasmolithus altus* Zone (N)	23.7–28.1	2, 4	7H-2, 11 cm, to 7H-5, 10 cm	54.00–58.50	(56.25)
11. *Base P21b Zone (F)	30.00	4	7H-3, 126 cm, to 7H-4, 124 cm	56.66–58.14	(57.40)
12. *FAD *R. gelida* (D)	26.00	16, 17	7H-2, 90 cm, to 7H, CC	54.80–61.90	(58.35)
13. Chron C10N/C10R	30.33	4, 5	8H-3, 95 cm, to 8H-3, 104 cm	65.85–65.94	(65.89)
14. Chron C10R/C11N	31.23	4, 5	9H-5, 85 cm, to 9H-5, 104 cm	78.25–78.44	(78.34)
15. Chron C11N/C11R	32.06	4, 5	9H-7, 75 cm, to 10H-5, 15 cm	80.90–87.05	(83.98)
16. Chron C11R/C12N	32.46	4, 5	11H-2, 5 cm, to 11H-2, 45 cm	91.95–92.35	(92.15)
17. Chron C12N/C12R	32.90	4, 5	11H-4, 65 cm, to 11H-4, 85 cm	95.55–95.75	(95.65)
18. LAD *Reticulofenestra umbilicus* (N)	34.60	4	12H-2, 22 cm, to 11H, CC	99.90–101.62	(100.76)
19. Top *Clausicoccus subdistichus* acme (N)	35.10	3	12H-4, 25 cm, to 12H-6, 21 cm	104.65–107.61	(106.13)
20. Chron C12R/C13N	35.29	4, 5	13H-3, 5 cm, to 13H-3, 35 cm	112.45–112.75	(112.60)
21. Base P18 Zone (F)	36.30	6	13H, CC, to 14H, CC	118.90–128.40	(123.65)
22. Top NP18 Zone (N)	37.80	4	15H, CC, to 16X-1, 20 cm	137.90–138.10	(138.00)
23. Base P16 Zone (F)	38.00	7	16X-1, 92 cm, to 16X, CC	138.82–143.40	(141.11)
24. Base P15 Zone (F)	41.30	7	18X, CC, to 19X, CC	162.40–171.90	(167.15)
25. Top NP16 Zone (N)	42.30	4	20X, CC, to 20X-2, 31 cm	173.71–181.40	(177.55)
26. Base NP15 Zone (N)	49.80	4	30X, CC, to 33X, CC	276.40–304.90	(290.65)
27. NP13–14 Zone (B)	50.0–53.7	4	33X, CC	309.40	
28. P11–P10 Zones (F)	48.0?–52.0	7	40X-1, 120 cm, to 40X, CC	363.10–371.40	

[a] D = diatom; N = calcareous nannofossil; F = planktonic foraminifer; + = direct correlation to paleomagnetic stratigraphy; # = absolute age date; * = probable truncation of datum by hiatus

[b] 1. Wise (1983); 2. Martini and Müller (1986); 3. Perch-Nielsen (1985); 4. Berggren et al. (1985); 5. Kent and Gradstein (1985); 6. Jenkins (1985); 7. McGowran (1986); 8. Paleomagnetic correlation at Hole 702B; 9. Burckle et al. (1978); 10. Ciesielski (1983); 11. Chen (1975); 12. Weaver (1983); 13. L. H. Burckle pers. comm. to Barron (1985); 14. Barron et al. (1985), Ciesielski (1985); 15. Ciesielski (1985); 16. Gombos (1983); 17. Fenner (1984); 18. Weaver and Gombos (1981); 19. Hays and Shackleton (1976); 20. Barron (1985).

[c] Core-catcher depths in this table were calculated by assuming the core-catcher sample was obtained from the bottom of the cored interval.

Despite the paleoenvironmental differences with the previously described more westerly Leg 114 sites, the relatively poor preservation, a relatively low diversity, and the absence of some stratigraphical marker species, the following biostratigraphic divisions were identified in Hole 703A:

Age	Interval	Depth (mbsf)
Quaternary	1H-1, 1 cm, to 2H-2, 90 cm	0.01–0.73
late Pliocene	2H-5, 20 cm, to 2H, CC	11.1–14.4
early Miocene	3H-2, 70 cm, to 4H, CC	16.6–33.4
late Oligocene	5H, CC, to 7H-3, 120 cm	42.9–56.66
early Oligocene	7H-4, 130 cm, to 12H, CC	58.14–109.4
late Eocene	13H, CC, to 18X, CC	118.9–162.4*
middle Eocene	19X, CC, to 30X, CC	171.9–238.4
early middle Eocene	40X, CC	371.4

(*late/middle Eocene boundary from foraminifer data).

The top of the lower Oligocene is placed by planktonic foraminifers at the last occurrence (LO) of *Chiloguembelina* spp., whereas it is placed further down by all other microfossil groups (in the upper part of the *Chiasmolithus altus* Zone, below the *Rocella vigilans* Zone, and below the *Corbisema archangelskiana* Zone). Detailed shore-based study and correlation of the microfossil datums with the paleomagnetic results from this leg should resolve this conflict.

In addition to the hiatus in the Oligocene indicated by diatom biostratigraphy in Core 114-703A-7H, a Neogene hiatus, recognized in all microfossil groups, exists between Section 114-703A-2H, CC, and Sample 114-703A-3H-2, 70 cm. This latter hiatus separates upper Pliocene from lower Miocene sediments (approximately 20 to 18.5 m.y. missing; see Table 3).

Throughout the Eocene and lower Oligocene section, large, heavily ornamented ostracodes and echinoderm spines occur sporadically in the sand fraction, indicating downslope transport of shallow-water material (Fig. 12). Also, the presence throughout the section of calcareous nannofossil *Zygrhablithus bijugatus*, which is indicative of relatively shallow water (<1000 m), and the common occurrence of shallow-water diatoms in Section 114-703A-19X, CC, suggest that a shallow-water environment existed upslope from Site 703. Site 703 is on the foot of a 15° slope of a seamount that presently reaches 1300 mbsl. These depths are consistent with islands existing in this area up to the end of the early Oligocene. Because reworked planktonic foraminifers are found in the samples along with downslope-transported material, their origin probably lies upslope also, rather than upcurrent.

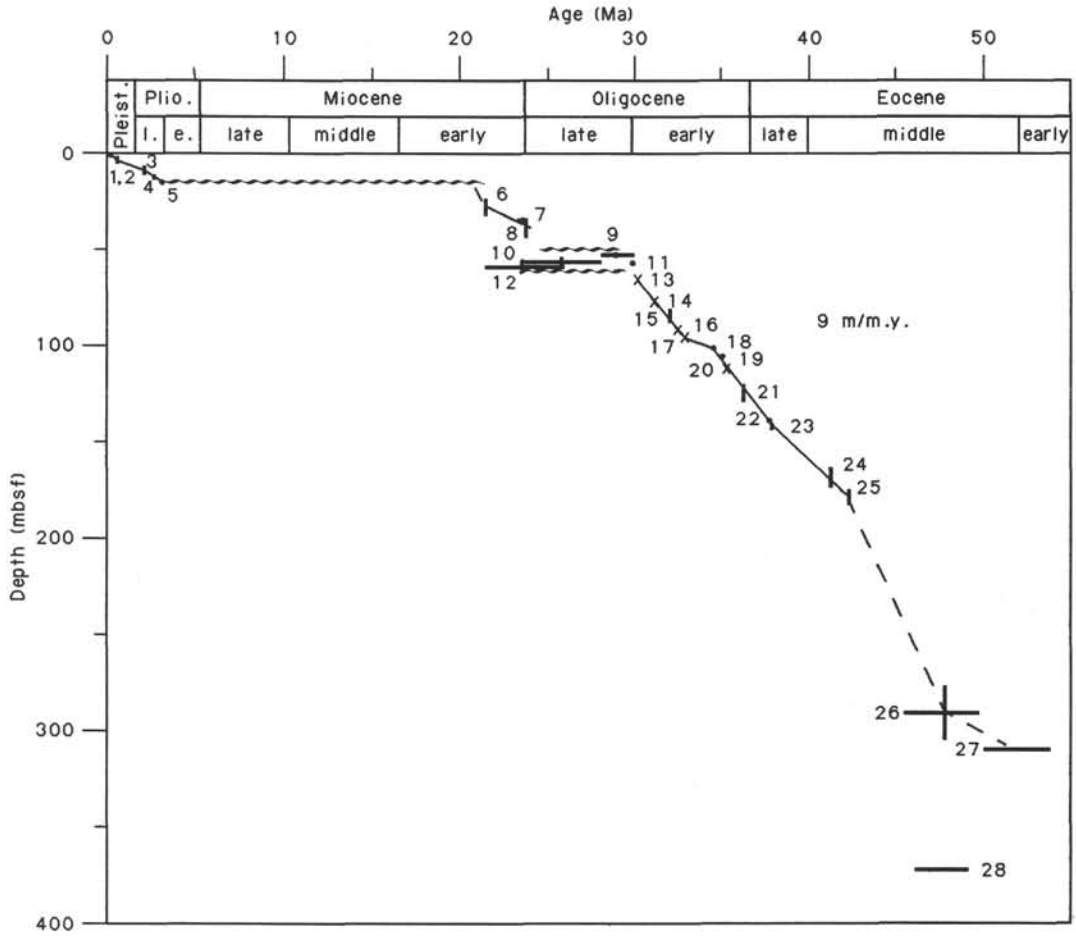

Figure 11. Age-depth curve and resulting sedimentation rates for Hole 703A based on biostratigraphic and magnetostratigraphic datums listed in Table 3.

Calcareous Nannofossils

Twenty-eight core-catcher and 17 core samples from Hole 703A were examined for nannofossils. All samples are fossiliferous. The nannofossil floras found are assigned to the zones of Wise (1983) and Martini (1971), as described in the "Explanatory Notes" chapter, this volume.

Biostratigraphy

Sample 114-703A-1H-1, 1–2 cm, to Section 114-703A-2H, CC, contain sparse nannofossil floras, including *Pseudoemiliana lacunosa* and *Gephyrocapsa* spp. The co-occurrence of these taxa indicates the presence of middle Pleistocene to upper Pliocene strata.

A stratigraphic break lies between Section 114-703A-2H, CC, and Sample 114-703A-3H-2, 134–135 cm, with most of the Miocene and Pliocene absent. The nannofossil floras recovered from the interval between Sample 114-703A-3H-2, 134–135 cm, and Section 114-703A-4H, CC, are dominated by *Cyclicargolithus floridanus*; also present are rare *Cyclicargolithus abisectus* and *Chiasmolithus altus*. This may belong to the *C. abisectus* Zone or may represent the reworking of *C. abisectus* and *C. altus* into younger Miocene strata. The presence of *C. floridanus* is taken to indicate a middle Miocene or older age.

The abundant occurrence of *C. abisectus* in Sample 114-703A-5H-2, 20–21 cm, indicates the presence of definite *C. abisectus* Zone strata (lower Miocene–upper Oligocene). The interval between Section 114-703A-5H, CC, and Sample 114-703A-7H-2, 10–11 cm, is assigned to the *Reticulofenestra bisecta* Zone (upper Oligocene), as the nominate taxon occurs in all samples from this interval. The first downhole occurrence of common *C. altus* in Sample 114-703A-7H-5, 10–11 cm, indicates the presence of the *C. altus* Zone (upper to lower Oligocene), which extends down to Section 114-703A-11H, CC. The interval from Samples 114-703A-12H-2, 22–23 cm, to 114-703A-12H-4, 24–25 cm, is assigned to the *Reticulofenestra umbilicus*. The presence of NP21 (lower Oligocene–upper Eocene) between Sample 114-703A-12H-6, 21–22 cm, and Section 114-703A-12H, CC, is inferred from the presence of abundant *Clausicoccus subdistichus*. The last appearance datums (LADs) of the species *Ericsonia formosa* and *Discoaster saipanensis* define the top and base of this zone, respectively, but they occur much lower in Hole 703A.

Below the abundant occurrence of *C. subdistichus* and down to the first appearance datum (FAD) of *Isthmolithus recurvus* (Sample 114-703A-13H-2, 74–75 cm, to Section 114-703A-15H, CC), the presence of undifferentiated NP21–19 (lower Oligocene–upper Eocene) is inferred. The presence of *Reticulofenestra oamaruensis* between Samples 114-703A-13H-2, 74–75 cm, and 114-703A-15H-2, 95–96 cm, supports the zonal assignment. The interval between the FAD of *I. recurvus* and the FAD of *Chiasmolithus oamaruensis* defines NP18 (upper Eocene) and is present between Samples 114-703A-16X-1, 20–21 cm, and 114-703A-20X-2, 30–31 cm. A possible stratigraphic break occurs between the base of this zone and the top of the underlying NP16 at Section 114-703A-20X, CC, with NP17 absent. This

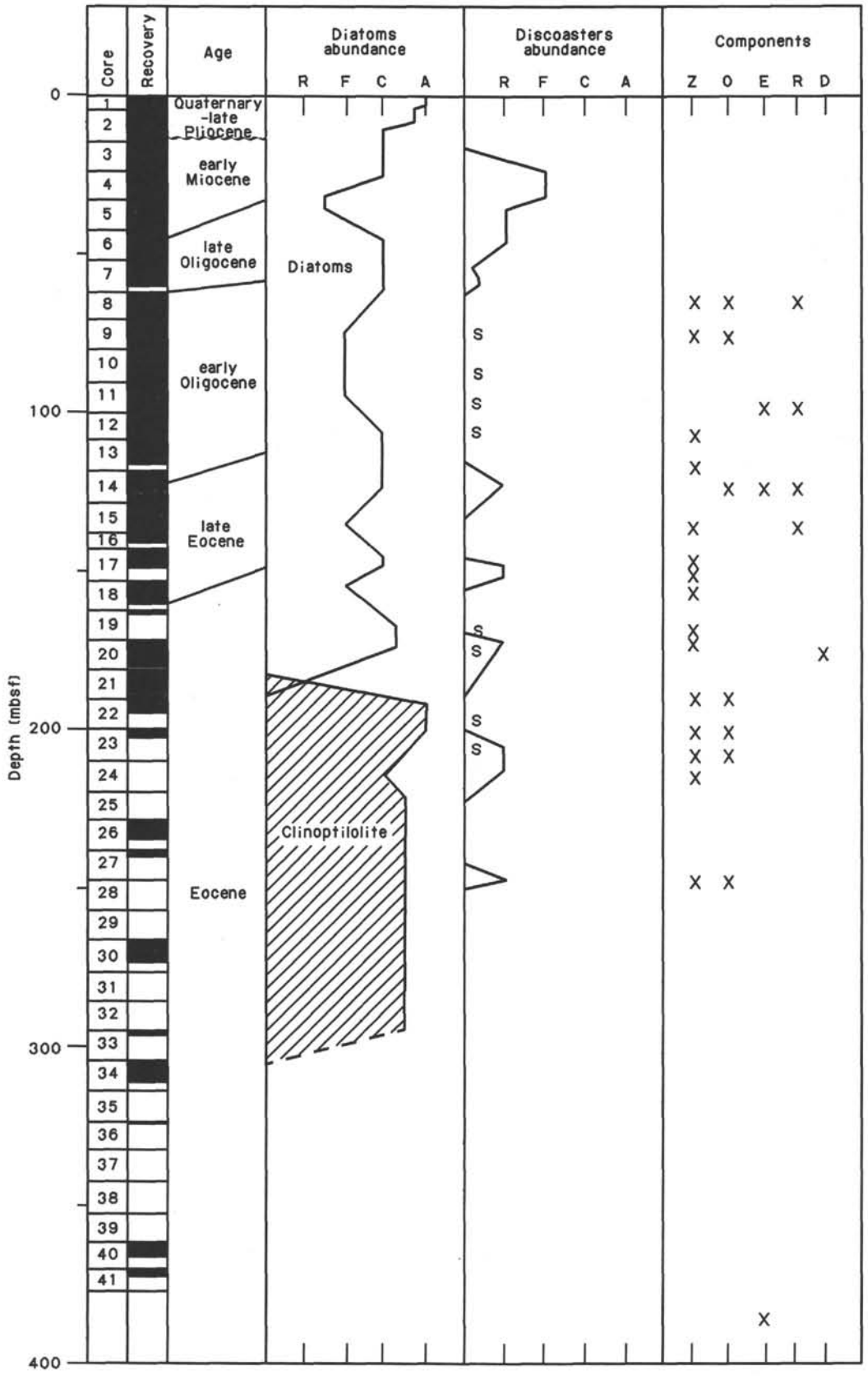

Figure 12. Comparison of the relative abundance of diatoms and clinoptilolite in the HCl-insoluble residue, the relative abundance of discoasters and presence of small sphenoliths (s) in the sediment, and the presence of reworked planktonic foraminifers (R) and shallow-water components: diatoms (D), *Zygrhablithus bijugatus* (Z), large, heavily ornamented ostracodes (O), and echinoderm spines (E).

apparent break is possibly not real, but simply caused by the extended ranges of *C. oamaruensis* and/or *Chiasmolithus solitus*, which define the base of NP18 and the top of NP16, respectively.

NP16 is definitely present between Sections 114-703A-20X, CC, and 114-703A-22X, CC, as indicated by the co-occurrence of *C. solitus* and *R. bisecta*. The base of NP16 cannot be defined in this area because of the absence of *Rhabdosphaera gladius*. In this study, the FAD of *R. bisecta* is used to define the base of definite NP16, with an underlying interval between Sample 114-703A-23X-1, 20–21 cm, and Section 114-703A-30X, CC. Supporting evidence for this zonal assignment is provided by the occurrence of *Sphenolithus furcatolithoides* in Sample 114-703A-30X-2, 30–32 cm, whereas its base is defined by the occurrence of *Nannotetrina fulgens* at Section 114-703A-30X, CC.

The only sample available for study in the lower part of the hole is Section 114-703A-33X, CC. It contains *R. umbilicus*, the FAD of which lies within NP14–13.

Paleoenvironment

Deposition at Site 703 was above the CCD during the Pleistocene to Pliocene and the early Miocene to Eocene. The presence of *Zygrhablithus bijugatus* throughout the Oligocene to middle Eocene section is in contrast to Site 699, where this species was absent above the lower Eocene. This possibly indicates a shallower paleowater depth for Site 703, as this species is thought to have a preference for shallow water (less than 1000 m).

The nannofossil floras from the Oligocene to middle Eocene section are of low diversity, which is probably the result of poor preservation as well as their high-latitude origin.

Preservation

The Pleistocene to Pliocene nannofossil floras are composed of slightly etched fossils. The Miocene to middle Eocene nannofossils are overgrown with secondary calcite deposition, which increases downhole.

Planktonic Foraminifers

Planktonic foraminifers are abundant and are the dominant microfossil in the washed residue of the examined samples. Radiolarians and siliceous sponge spicules are common to abundant from the top of the hole to Section 114-703A-19X, CC, below which they disappear. Thus, calcareous and siliceous plankton coexist over a stratigraphic thickness of approximately 171 m.

In some samples there is evidence of reworking of older planktonic foraminifers; their ages are not older than early or middle Eocene. Reworking is evidenced between Sections 114-703A-7H, CC, and 114-703A-14H, CC. The upper section, from the top of the hole to Section 114-703A-2H, CC, can be assigned to the Quaternary–upper Pliocene and from Sections 114-703A-3H, CC, to 114-703A-4H, CC, to the lower Miocene. Between Sections 114-703A-4H, CC, and 114-703A-6H, CC, the age is uncertain, and this interval can be tentatively assigned to lower Miocene–upper Oligocene. The underlying section spans the Oligocene to lower middle Eocene.

An unconformity is evident between Sections 114-703A-2H, CC, and 114-703A-3H, CC, because middle Miocene to lower Pliocene sediments are missing. Jenkins' (1985) biozonation is difficult to employ in this hole because of the paucity or absence of the marker species, the different range, and discontinuous core recovery, as well as because of reworking and poor preservation in some samples. It is easier to attribute the stratigraphic subdivisions to the P zones of the standard zonation on the basis of magnetostratigraphic control and by finding some of the important marker species such as *Globorotalia opima opima*. Some events, such as the LAD of chiloguembelininds and *Catapsydrax dissimilis*, common both to midlatitudes and to this region, are very useful for biostratigraphic resolution.

Biostratigraphy

The age of the examined samples is summarized as follows:

114-703A-1H, 0 cm: early Pleistocene (N22) to Recent;
114-703A-1H, CC, and 114-703A-2H, CC: early Pleistocene–late Pliocene;
114-703A-3H, CC, to 114-703A-4H, CC: early Miocene (N6–4);
114-703A-5H-1, 34–36 cm, to 114-703A-6H, CC: early Miocene–late Oligocene (N4–P22);
114-703A-7H-1, 124–126 cm, to 114-703A-7H-3, 124–126 cm: late Oligocene (P21b);
114-703A-7H-4, 124-126 cm, to 114-703A-9H, CC: early Oligocene (P21a–20);
114-703A-10H-3, 68–70 cm, to 114-703A-13H, CC: early Oligocene (P20–18);
114-703A-14H, CC, to 114-703A-18X, CC: late Eocene;
114-703A-19X, CC, to 114-703A-26X, CC: late middle Eocene, *Globigerinatheka index* Zone (P14–12/11);
114-703A-34X, CC, and 114-703A-35X, CC: barren;
114-703A-40X-1, 120–122 cm: early middle Eocene, *Acarinina primitiva* Zone, with major downhole contamination.

The P zones are approximate and, as yet, not well calibrated with the GPTS for the Oligocene interval. Reworking is evident in the following samples:

114-703A-7H, CC: middle Eocene species reworked;
114-703A-13H, CC: lower middle Eocene species reworked;
114-703A-14H, CC: middle Eocene species reworked.

At the top of the hole, the Pleistocene marker species, *Globorotalia truncatulinoides* (N22 of the standard zonation), was recognized.

In the stratigraphic interval assigned to the upper Pliocene–lower Pleistocene, the assemblage consists mainly of sinistral *Neogloboquadrina pachyderma* (the most abundant species at >50%), *Globorotalia inflata*, *Globorotalia crassaformis* group, and *Globigerina bulloides*.

In the lower Miocene there are species characteristic of low- to midlatitude assemblages, such as *Catapsydrax dissimilis ciperoensis*, *Globoquadrina dehiscens*, and *Globorotalia praescitula*, and southern hemisphere species such as *Globorotalia zealandica*, which has a range within the lower Miocene. During this period the high-latitude character of the assemblage is illustrated by the almost total absence of *Globigerinoides*, which is a warm-water taxon extensively distributed in tropical to temperate regions.

The Oligocene/Miocene boundary is not definable at the present because the FAD of *G. dehiscens* is not clear. The LO of this species is recognized to be the most useful worldwide indicator of the Oligocene/Miocene boundary. Another event, such as the FAD of *Globigerinita incrusta*, may be used if the paleomagnetic data can confirm the correspondence of the Oligocene/Miocene boundary position.

The lower and upper Oligocene stratigraphic interval can be subdivided on the basis of the LAD of *Chiloguembelina cubensis* and the other chiloguembelinids that occur in Sample 114-703A-7H-4, 124–126 cm. This event has been used by Berggren et al. (1985) for subdividing Zone P21 in two, with the boundary between P21a and P21b occurring between lower and upper Oligocene. In the upper Oligocene (the stratigraphic interval above the LAD of *C. cubensis*) the assemblages contain *Globigerina euapertura*, *Globigerina praebulloides*, *Globigerina juvenilis*, *Globigerina ciperoensis*, "*Globigerina*" *labiacrassata*, and rare *Globigerina woodi woodi* in the upper part. The upper boundary of P21b Zone is placed at the LAD of *G. opima opima*.

It must be noted that 9 m below the chiloguembelinids extinction, in P21a Zone, there are a few occurrences of *Cassigerinella* and *Guembelitria*; some specimens of the last genus are referable to *Jenkinsina samwelli*. This horizon has been found at Site 704 at the same stratigraphic position.

The lower Oligocene stratigraphic interval is characterized by the occurrence of large (>150 μm) *C. cubensis*, which is associated with *G. praebulloides*, *Globorotaloides suteri*, *C. dissimilis*, *Globigerina venezuelana*, and "*G.*" *labiacrassata*. In the older part (below Section 114-704A-9H, CC), *Subbotina angiporoides* and *Subbotina linaperta* are very abundant and indicate that this stratigraphic interval is not younger than Zone P19/20.

Globigerina brevis (Jenkins' (1985) zonal marker for the Eocene/Oligocene boundary) is very rare and its occurrence is sporadic. This species was found associated with *Globigerinatheka index*. According to the paleomagnetic data, the Eocene/Oligocene boundary, as it is considered here, falls below Chron C13N—in agreement with Berggren et al. (1985)—at 117 mbsf. Section 114-703A-13H, CC, is just above the boundary as extrapolated by paleomagnetic data and is considered lower Oligocene because of the FAD of *Catapsydrax dissimilis dissimilis* and absence of *G. index*.

The upper and middle Eocene assemblages are similar to those at Site 702. However, Jenkins' (1985) zones are not applicable. The *Globigerina linaperta* Zone, defined as the stratigraphic interval from the LAD of *Acarinina aculeata* to the FAD of *G. brevis*, cannot be identified because the two species are found together. This may be due to reworking or downhole contamination. The boundary between *Acarinina primitiva* Zone and *G. index* Zone below Section 114-703A-26, CC, is not present because of the poor recovery below this depth.

At the bottom of the section, Core 114-703A-40X can be assigned to lower middle Eocene, P11 (lower part), on the basis of assemblages represented by *Planorotalites*, *Pseudohastigerina danvillensis*, *Guembelitria*, and *Cassigerinella* sp. 1. Species limited to the lower Eocene are absent. Abundant downhole contamination, as previously mentioned, results in the presence and abundance of the characteristic forms that occur in Hole 702B between the LAD of *Planorotalites* and the FAD of *G. index* such as *Globorotaloides* species, which are not yet classified.

Paleoenvironment

At this site, as at the other Leg 114 sites, the middle Eocene to late Eocene cooling trend is marked by the disappearance of acarininids and the enrichment of cold-water species. The rarity of Oligocene low- to midlatitude marker species and of *Globigerinoides* taxon in the Miocene allows us to consider this region as a cool South Atlantic bioprovince for this time period, without excluding some warm event, particularly in the P21b Zone.

Deposition was above the foraminifer lysocline, as indicated by the continuous occurrence of delicate planktonic foraminifer forms. Mass flow in the lower part of the section and reworking in the Oligocene upper part indicate a certain instability of the seafloor in this area.

Preservation

In the Neogene section the planktonic foraminifers are well preserved. Within the Paleogene section they are recrystallized, with some signs of dissolution, which has not been strong enough to dissolve the most delicate forms, such as tenuitellids.

Benthic Foraminifers

Core-catcher samples from Site 703 contain well-preserved and generally diverse benthic foraminifer assemblages down to Section 114-703A-26X, CC. The Neogene samples (the top of Section 114-703A-1H, CC, to Section 114-703A-2H, CC) are slightly less diverse than the older assemblages recovered from Hole 703A. They include several species of *Cibicidoides*, *Uvigerina*, and *Pullenia*, and several occurrences of *Globocassidulina subglobosa*, *Cassidulina crassa*, *Laticarinina pauperata*, *Melonis barleeanus*, *Sphaeroidina bulloides*, and *Valvulineria laevigata*.

Nonion havanensis, *Pullenia bulloides*, *Pullenia eocaenica*, and *Pullenia quinqueloba* are common to abundant throughout Hole 703A. *Cibicidoides mundulus* is abundant in the Neogene and Oligocene. In the lower Oligocene, there is a transition between *C. mundulus* and its predecessor, *Cibicidoides praemundulus*. Other *Cibicidoides* species are common throughout Hole 703A and include *Cibicidoides bradyi*, *Cibicidoides cicatricosus*, *Cibicidoides dickersoni*, *Cibicidoides eocaena*, *Cibicidoides havanensis*, and *Cibicidoides laurisae*. The occurrence of *Nuttallides umbonifera* is common to sparse in the Oligocene (Sections 114-703A-3H, CC, to 114-703A-12H, CC), whereas *Nuttallides truempyi* is fairly common from Sections 114-703A-16H, CC, to 114-703A-26X, CC. *Uvigerina* species are common to abundant in the Oligocene and Neogene, but are rare in the Eocene. They include *Uvigerina havanensis*, *Uvigerina spinulosa*, and *Uvigerina* sp. 17. *Astrononion pusillum*, *C. crassa*, *C. havanensis*, and *L. pauperata* are common to abundant in and above Section 114-703A-9H, CC, whereas *Cibicides* sp. and *Cibicidina* sp. are rare to common in several samples in the same interval. The buliminids are common to abundant in and below this sample, and include *Turrilina alsatica*, *Bulimina macilenta*, *Bulimina semicostata*, *Bulimina trinitatensis*, and *Bulimina tuxpomensis*. *Anomalinoides captitatus*, *Anomalinoides semicribratus*, *Cibicidoides micrus*, and *Osangularia mexicana* are common to abundant in some Eocene samples. Rare miliolids are scattered in the hole. Rare to few agglutinated benthic foraminifers are present in the core-catcher samples, dominated by *Karreriella chapapotensis*, *Karreriella subglabra*, and *Vulvulina spinosa*.

Paleobathymetric estimates for Hole 703A are based on van Morkhoven et al. (1986). The Oligocene benthic foraminifer assemblage lies within the lower bathyal to abyssal zone (>1000 m). The Eocene fauna indicates a paleodepth in the middle bathyal to abyssal realm (>600 m).

Diatoms

Diatoms are present from Cores 114-703A-1H to 114-703A-19X (Quaternary to middle Eocene; NP16). They are abundant and well preserved only in the Quaternary. In the pre-Quaternary cores their abundance varies from few to common, and their preservation is poor to moderate. In Cores 114-703A-20X to 114-703A-21X and 114-703A-23X to 114-703A-26X, diatoms have been completely dissolved, and clinoptilolite is found in the silt fraction. Cores 114-703A-27X to 114-703A-40X recovered volcanic rocks (clastic sediments and basalt). The abundance of diatoms in the HCl-insoluble residue is shown in Figure 12.

In the first core, the *Coscinodiscus lentiginosus* Zone McCollum (1975) was identified in Samples 114-703A-1H-1, 1 cm, to 114-703A-1H-1, 98 cm. The uppermost part of the Quaternary seems to be missing because *Hemidiscus karstenii* was found in the sample at the top of the core. Section 114-703A-1H, CC, to Sample 114-703A-2H-2, 90 cm, belong in the *Coscinodiscus elliptipora–Actinocyclus ingens* to *Rhizosolenia barboi–Nitzschia kerguelensis* Zones Weaver and Gombos (1981). This interval was identified using the LADs of *A. ingens* and *Coscinodiscus kolbei*. *C. elliptipora* and *R. barboi*, which are characteristically present at subantarctic sites for this age interval, were not found in the sediments recovered at Site 703. Sample 114-703A-2H-5,

20 cm, was assigned to the *Coscinodiscus vulnificus* Zone because of the presence of the nominate species and the absence of slightly older stratigraphic marker species such as *Cosmiodiscus insignis* and *Nitzschia weaveri*. In Section 114-703A-2H, CC, *C. insignis*, *C. vulnificus*, *Nitzschia interfrigidaria*, *Nitzschia praeinterfrigidaria*, and *N. weaveri* co-occur, which places this sample in the *N. interfrigidaria–C. vulnificus* Zone of Ciesielski (1983).

Sample 114-703A-3H-2, 70 cm, and Section 114-703A-3H, CC, belong in the lower Miocene *Coscinodiscus rhombicus* Zone of Gombos and Ciesielski (1983) on the basis of the presence of the nominate species together with *Synedra miocenica*. In Section 114-703A-4H, CC, the LAD of *Rossiella symmetrica* is found, and in Section 114-703A-6H, CC, is that of *Rocella gelida*. The first occurrence of the latter species is recorded from Sample 114-703A-7H-2, 90 cm, placing the interval from this sample to Section 114-703A-4H, CC, in the *R. gelida* Zone of Gombos and Ciesielski (1983). In Section 114-703A-7H, CC, *R. gelida* is absent, but *Rocella vigilans* is present. The occurrence of nannofossils *C. altus* and *Chiloguembelina* spp. in this sample indicates that a hiatus is present in the upper part of Core 114-703A-7H (compare Fig. 11 and Table 3).

Preservation of diatoms in Sample 114-703A-8H-2, 80 cm, to Section 114-703A-9H, CC, is poor, and their abundance is few; therefore, no detailed age assignment is possible based upon the diatom assemblage other than that these samples are of Oligocene age. Lower Oligocene diatom assemblages are found from Sample 114-703A-10H-3, 80 cm, to Section 114-703A-12H, CC.

Sections 114-703A-13H, CC, to 114-703A-19X, CC, have characteristic Eocene species present. However, no zonation exists for the Eocene, and this together with the low diversity of the diatom assemblage prevents more precise age determination.

Below Core 114-703A-19X diatoms have been completely dissolved.

Based on diatom datums, a long hiatus separates upper Pliocene and lower Miocene sediments. A second, shorter hiatus is probably present in the upper Oligocene. Sedimentation rates and the duration of these two hiatuses are shown in Table 3 and Figure 11.

The Neogene diatom assemblages at this site are dominated by subantarctic species. However, the diversity is low compared to that found at the other Leg 114 sites (e.g., species such as *R. barboi* and *C. elliptipora* are not present). Their absence may result from the fact that during much of the Neogene this site was north of the high-productivity circum-antarctic belt.

The Eocene-Oligocene diatom assemblages are poorly preserved. The presence of warm-water and cosmopolitan species in the Eocene and their disappearance in the lower Oligocene correlates with the our findings at the other Leg 114 sites and is interpreted as reflecting the northward expansion of the circum-antarctic province.

In Section 114-703A-19X, CC, a high abundance of neritic diatoms was found, indicating that an island, with shallower water around it, must have been present upslope from this site during the middle Eocene. For a discussion of this strong neritic influence in connection with the results of the other microfossil groups, see the biostratigraphy synthesis in the "Summary and Conclusions" section, this chapter.

Strong reworking of diatoms was found in the upper Pliocene Section 114-703A-1H, CC.

Radiolarians

Common to abundant and moderately well-preserved radiolarians were observed in core-catcher samples from Sections 114-703A-1H, CC, to 114-703A-19X, CC, and 114-703A-23X, CC. The remaining samples were barren. Among the biostratigraphic zones of Hays and Opdyke (1967) and Chen (1975), the following were recognized:

114-703A-1H, CC: *Stylatractus universus* (Quaternary; 0.49-0.7 Ma; ψ zone; Brunhes);

114-703A-2H, CC: *Helotholus vema* (early Pliocene; 2.43-4.25 Ma; γ and τ zones; Gauss-Gilbert);

114-703A-3H, CC, and 114-703A-4H, CC: *Cyrtocapsella tetrapera* (early Miocene);

114-703A-5H, CC, to 114-703A-19X, CC, and 114-703A-23X, CC: unzoned (Oligocene-Eocene).

The presence of *Stylatractus universus* in the top of Core 114-703A-1H suggests that at the least, sediments of the last 0.5 Ma are missing from this site.

Section 114-703A-23X, CC, contains abundant *Lychnocanoma amphitrite* together with *Lophoconus titanothericeraos* and *Lophocyrtis biaurita* and thus may correlate with the interval from Sections 114-702B-10X, CC, to 114-702B-12X, CC, of Site 702.

Silicoflagellates

Core-catcher samples from this site yielded a more diversified silicoflagellate assemblage than that of any previous site drilled during Leg 114. Adopting the Ciesielski (1975) and Shaw and Ciesielski (1983) zonal scheme, the following zones are recognized:

114-703A-1H, CC: unzoned (Quaternary);

114-703A-2H, CC: *Distephanus boliviensis* (early Pliocene);

114-703A-3H, CC: *Corbisema triacantha* (middle to early Miocene);

114-703A-4H, CC: *Naviculopsis regularis* (early Miocene);

114-703A-5H, CC: *Naviculopsis biapiculata* (late Oligocene);

114-703A-6H, CC, and 114-703A-7H, CC: *Corbisema archangelskiana* (late Oligocene);

114-703A-8H, CC, and 114-703A-9H, CC: [*Naviculopsis constricta–C. archangelskiana*] (late to early Oligocene);

114-703A-10H, CC–114-703A-12H, CC: [*N. constricta/Dictyocha deflandrei*]–*Naviculopsis trispinosa* (early Oligocene);

114-703A-13H, CC–114-703A-16X, CC: *Mesocena occidentalis–Mesocena apiculata* (subzone) (early Oligocene–middle Eocene?);

114-703A-17X, CC, and 114-703A-18X, CC: *Dictyocha stelliformis–M. apiculata* (subzone) (middle Eocene);

114-703A-19X, CC: *D. stelliformis* (subzone) (middle Eocene).

In this summary, the two bracketed Oligocene zones are tentative, mainly because of the absence of an index species, *Dictyocha deflandrei*, in the examined samples.

Furthermore, it is somewhat puzzling that no specimens of *Dictyocha grandis* were encountered from Site 703 sediments, although other co-occurring enigmatic species, that is, *Dictyocha stelliformis* and *Dictyocha challengeri*, were observed. The top of the *D. stelliformis* subzone is slightly older than Chron C19N (~44.1 Ma) (Shaw and Ciesielski, 1983).

Ebridians

Ebridians are rare to few but occur more consistently in the core-catcher samples of Site 703 than in any of the previous sites drilled during Leg 114. They were recovered from the following samples with the indicated species:

114-703A-2H, CC: *Ebriopsis antiqua antiqua*;

114-703A-10H, CC–114-703A-19X, CC: *Ebriopsis crenulata*;

114-703A-13H, CC–114-703A-19X, CC: *Ammodochium ampulla*, *Micromarsupium anceps*, *Parebriopsis fallax*.

Many *Ammodochium ampulla* possess a lorica like those of *Ebriopsis crenulata* observed from Site 702.

Paleoenvironment

The results of examination of core-catcher samples from the Miocene-Quaternary interval, Sections 114-703A-3H, CC, to 114-703A-1H, CC, indicate that middle Miocene sediments were deposited under the influence of warm water (low to middle latitudes), as inferred from the presence of *C. tetrapera* and orosphaerid fragments (radiolarians), and *C. triacantha* (silicoflagellate). A much colder environment existed in the early Pliocene but changed back to slightly warmer (north of the polar front) conditions during the Quaternary, as indicated by the presence of *Euchitonia* (radiolarian) species.

GEOCHEMISTRY

A pore-water sample was squeezed at ambient temperature from each of eleven 5-cm-long whole-round samples taken at about 30-m intervals from Hole 703A. Most deep intervals recovered contained broken biscuits of doubtful formational integrity, so we suspect that the data from this hole are of dubious value. The results of the pore-water chemistry are reported in Table 4 and in Figure 13. Fourteen headspace samples were analyzed for volatile hydrocarbon gases (Table 5), and both organic carbon and carbonate were determined throughout the recovered section (Table 6).

Salinity and Chloride

Salinity and chloride values throughout the sediment column are indistinguishable from those in the overlying seawater.

Calcium and Magnesium

Calcium concentrations increase slightly downhole from a bottom-water concentration of 10 mmol/L to a maximum of about 14 mmol/L at 270 mbsf, decreasing abruptly from that depth to 11.8 mmol/L near the bottom of the hole (311 mbsf) (Fig. 13). Magnesium concentrations decrease erratically downhole from a bottom-water concentration of 55 mmol/L to a minimum concentration of about 50 mmol/L in the interval between 79 and 270 mbsf. The bottommost magnesium value increases to 53.5 mmol/L. The magnesium/calcium ratio decreases downhole from seawater values of 5.2 to about 3.6. The ratio rises again in the bottommost sample to 4.5. A plot of calcium vs. magnesium demonstrates that the Mg/Ca covariation observed in Hole 703 is a weak trend that reflects silicic ash alteration in the apparent absence of contemporaneous basalt basement reactions (Fig. 14). The concentration gradients of calcium and magnesium are very weak, suggesting either the absence of contemporaneous reactions or some recent event (slump?) that has effectively erased the pore-water signatures. One possibility is that the sand layer at the bottom of the sediment column above basement is acting as a submarine aquifer, injecting bottom water into the basal portion of the sediment column. An alternate explanation that we prefer is that surface seawater penetrated and diluted the formation interstitial waters during drilling operations.

pH and Alkalinity

The pH values are fairly constant at 7.6–7.7. Alkalinity values are very near that of bottom water, between 2.5 and 2.9 mmol/L. The sharp decrease at the bottom of the hole to near surface seawater values (about 2.0) reinforces the supposition raised by the calcium and magnesium data that surface seawater has displaced the initial interstitial waters during coring or by submarine aquifer discharge at the bottom of the hole.

Fluoride, Silica, and Sulfate

Fluoride concentrations decrease downhole slightly from bottom water values of 70 μmol/L to a minimum of about 57 μmol/L between 100 and 160 mbsf. Values below 190 mbsf are again near those of seawater.

Dissolved silica increases downhole from bottom-water concentrations to a maximum concentration of about 870 μmol/L at 134 mbsf. Below this depth, dissolved silica concentrations decrease almost linearly to a minimum concentration of 137 μmol/L at the bottom of the hole. This concentration is only slightly above that of bottom water. The profile almost certainly reflects dilution of interstitial waters with surface or bottom waters below 130 mbsf.

Sulfate decreases very slightly from bottom-water concentrations of 28.9 mmol/L to a minimum of 27 mmol/L at 187 mbsf, with an increase to seawater values at the bottom of the hole. This sulfate profile reflects the virtual absence of organic matter reactivity in these sediments (Table 6); thus, only trace microbial sulfate reduction occurred in addition to flushing of the bottom of the sediment column with either bottom water or surface seawater during drilling disturbance.

Volatile Hydrocarbon Gases

Methane (C1) and ethane (C2) are both very low, at detection limits. There is no methanogenesis in these sediments.

Sedimentary Organic and Inorganic Carbon

Sedimentary organic carbon and calcium carbonate concentrations in Hole 703A are discussed elsewhere in this chapter (see "Lithostratigraphy" and "Biostratigraphy" sections). Organic carbon values are statistically not different from zero (0.0 ± 0.1 $\%C_{org}$). The negative values reflect statistical uncertainty in the difference-on-combustion technique.

PALEOMAGNETICS

A single hole was drilled at Site 703 using the APC to a depth of 137.9 mbsf, followed by the XCB system to basement at a depth of 377.4 mbsf. Recovery averaged 97% in the upper 15 cores but progressively deteriorated below this depth. Few

Table 4. Interstitial-water chemistry data from Hole 703A.

Sample (cm)	Depth (mbsf)	Volume (mL)	pH	Alkalinity (mmol/L)	Salinity (g/kg)	Magnesium (mmol/L)	Calcium (mmol/L)	Chloride (mmol/L)	Sulfate (mmol/L)	Fluoride (μmol/L)	Silica (μmol/L)	Mg/Ca
2H-5, 145–150	12.35	40	7.65	2.88	35.0	52.96	11.53	558.00	28.61	73.80	701	4.59
3H-5, 145–150	21.85	40	7.59	2.90	35.0	52.48	11.77	559.00	28.86	73.20	720	4.46
6H-5, 145–150	50.35	50	7.62	2.98	35.0	51.37	12.88	564.00	28.20	73.50	786	3.99
9H-5, 145–150	78.85	33	7.72	3.08	35.5	50.03	13.18	563.00	27.68	61.90	850	3.80
12H-4, 145–150	105.85	46	7.73	2.97	34.6	50.36	13.41	561.00	27.72	57.20	857	3.76
15H-4, 145–150	134.35	40	7.63	2.69	35.0	50.09	13.76	562.00	27.64	57.00	867	3.64
18X-3, 145–150	157.35	31	7.63	2.79	34.8	49.82	13.71	559.00	27.58	57.40	810	3.63
21X-4, 145–150	187.35	32	7.62	2.47	34.8	50.34	13.67	563.00	27.05	69.50	592	3.68
26X-2, 145–150	231.85	35	7.78	3.17	34.8	51.32	13.65	561.00	27.91	69.20	474	3.76
30X-2, 145–150	269.85	28	7.66	2.97	34.8	50.30	14.11	562.00	28.09	73.20	290	3.56
34X-4, 145–150	310.85	18	7.77	1.97	35.0	53.49	11.80	556.00	28.24	59.00	137	4.53

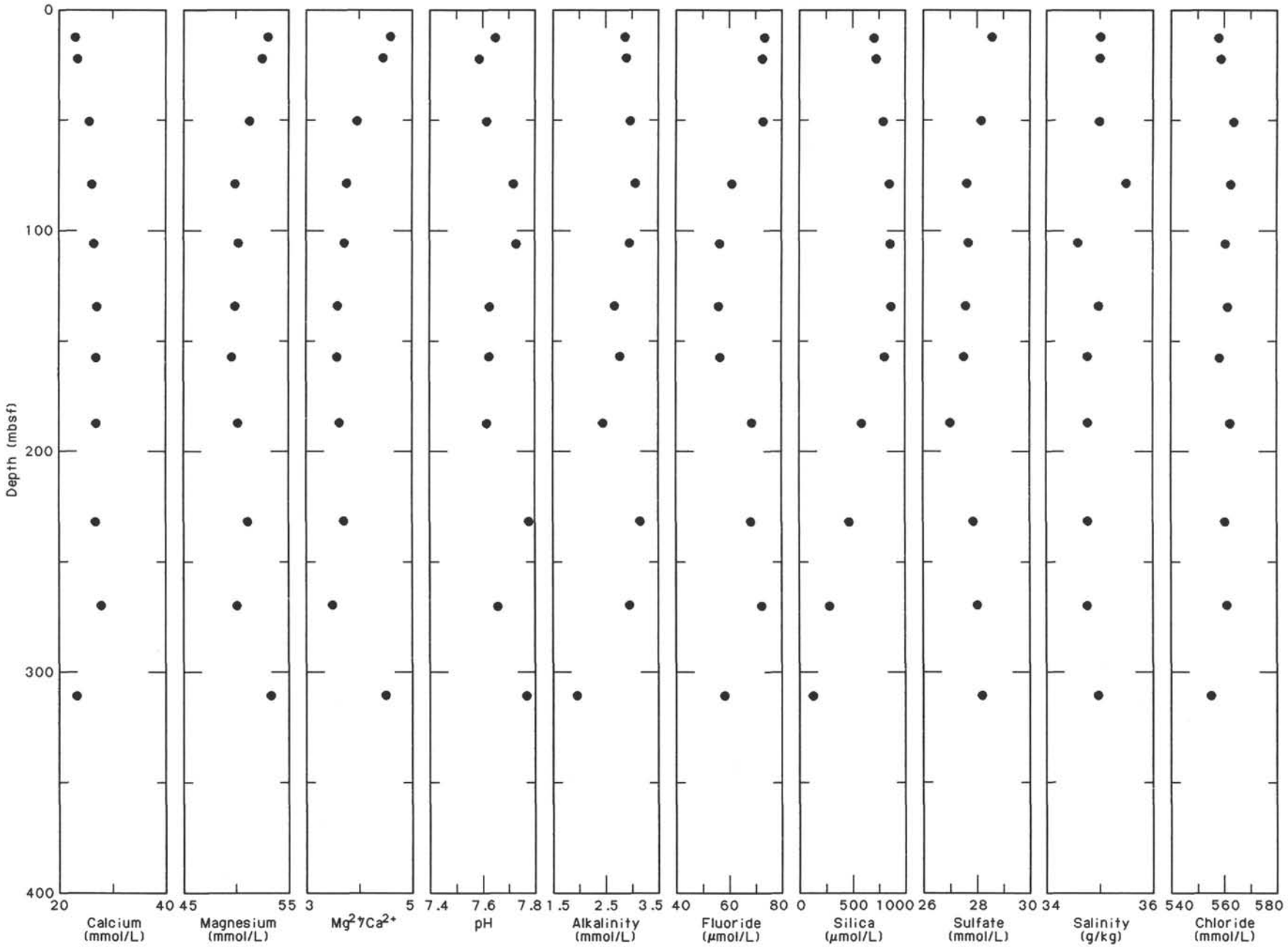

Figure 13. Pore-water calcium, magnesium, Mg/Ca ratio, pH, titration alkalinity, fluoride, dissolved silica, sulfate, salinity, and chloride profiles, Hole 703A.

Table 5. Volatile hydrocarbons (methane and ethane) from headspace samples, Hole 703A.

Sample (cm)	Depth (mbsf)	C_1 (ppm)	C_2 (ppm)
2H-6, 0–5	12.40	1.1	0.0
3H-6, 0–5	21.90	1.7	0.0
5H-6, 0–5	40.90	1.6	0.5
6H-6, 0–5	50.40	1.9	0.4
8H-6, 0–5	69.40	1.2	0.0
9H-3, 0–5	74.40	2.5	1.1
10H-3, 0–5	83.90	1.9	0.0
12H-5, 0–5	105.90	2.1	0.9
15H-5, 0–5	134.40	2.1	1.3
18X-3, 0–5	155.90	2.5	0.5
21X-3, 0–5	184.40	2.3	0.0
26X-3, 0–5	231.90	2.0	0.0
30X-3, 0–5	269.90	1.9	0.0
34X-4, 140–145	310.80	1.4	1.6

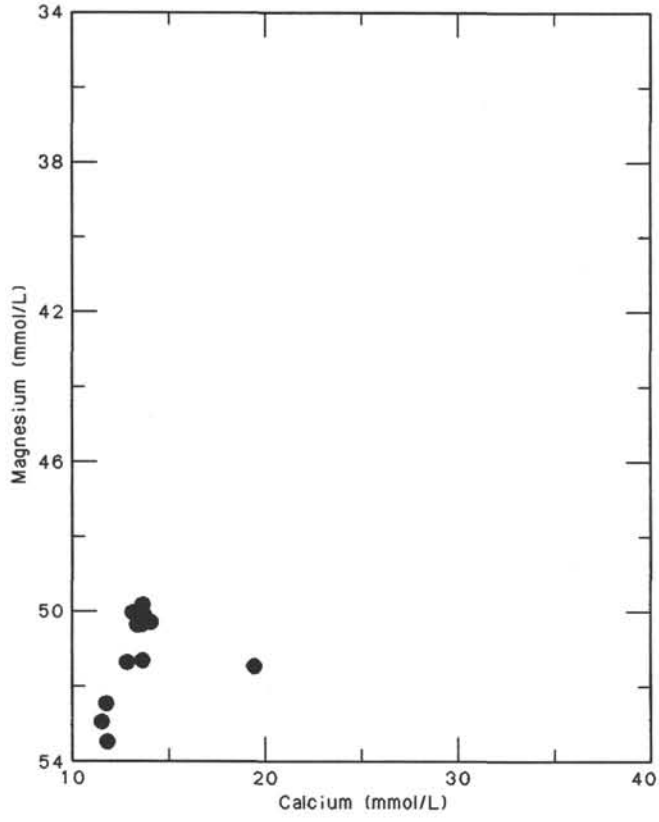

Figure 14. Pore-water calcium vs. magnesium in Hole 703A.

cores yielded any significant sediment recovery beneath about 200 mbsf. The cored sequence is dominated by nannofossil-foraminifer oozes. A short Pliocene to Quaternary section in the first 2 cores overlies a thick Eocene-Oligocene section. Because of the poor sediment recovery beneath 140 mbsf, shipboard paleomagnetic investigations were restricted to the upper Eocene–lower Miocene section recovered in Cores 114-703A-3H to 114-703A-13H. These investigations included whole-core susceptibility and half-core paleomagnetic determinations on all sediment recovered from this interval.

Magnetic Susceptibility

The variation of susceptibility with depth for the interval from 15 to 110 mbsf is shown in Figure 15. Large susceptibility

Table 6. Sedimentary organic carbon and calcium carbonate, Hole 703A.

Sample (cm)	Depth (mbsf)	C_{org} (%)	$CaCO_3$ (%)
2H-2, 100–102	7.40	−0.06	87.82
2H-6, 100–102	13.40		91.74
3H-2, 100–102	16.90	−0.11	86.74
3H-4, 100–102	19.90		89.49
4H-4, 100–102	29.40	0.13	90.57
4H-6, 100–102	32.40		91.32
5H-3, 100–102	37.40	0.17	89.49
5H-6, 100–102	41.90		90.49
6H-3, 100–102	46.90	−0.07	88.32
6H-6, 100–102	51.40		83.73
7H-3, 100–102	56.40	−0.21	87.40
7H-5, 100–102	59.40		88.07
8H-3, 100–102	65.90	−0.02	85.32
8H-5, 100–102	68.90		83.65
9H-3, 100–102	75.40	−0.26	90.99
9H-6, 100–102	79.90		89.15
10H-3, 80–82	84.70	−0.09	88.57
10H-4, 100–102	86.40		90.91
10H-5, 71–73	87.61		88.49
10H-5, 100–102	87.90		87.15
10H-6, 100–102	89.40		91.16
11H-2, 100–102	92.90	−0.11	91.91
11H-5, 100–102	97.40		88.32
12H-1, 50–52	100.40		88.15
12H-2, 50–52	101.90	−0.28	86.74
12H-4, 50–52	104.90		82.32
12H-5, 50–52	106.40		86.57
12H-6, 60–62	108.00		79.15
12H-7, 60–62	109.50		87.74
13H-2, 100–102	111.90	−0.10	89.99
13H-4, 90–92	114.80		90.57
15H-2, 100–102	130.90	−0.22	89.57
15H-4, 100–102	133.90		81.48
17X-3, 100–102	147.40	−0.11	84.98
18X-1, 100–102	153.90	0.01	89.24
18X-3, 100–102	156.90		88.99
20X-1, 100–102	172.90	−0.02	90.99
20X-5, 100–102	178.90		88.07
21X-1, 100–102	182.40	−0.08	91.32
21X-3, 100–102	185.40		92.74
23X-1, 90–92	201.30	−0.02	90.41
26X-1, 42–44	229.32	−0.18	95.41
26X-3, 82–84	232.72		95.49
30X-2, 93–95	269.33	−0.13	95.24
30X-3, 100–102	270.90		95.58
34X-2, 122–124	307.62	0.02	3.25
34X-4, 60–62	310.00		0.17

spikes occur near the tops of most cores as a result of downhole contamination (see "Paleomagnetics" section, "Site 701" chapter, this volume). Data from these intervals have been edited from the downhole plot.

A significant feature of this plot is the occurrence of "pulses" of relatively high and low susceptibility values. These susceptibility pulses have a typical amplitude of 10^{-10} SI units and wavelengths of ~15 to 20 m. They extend through lithostratigraphic Subunit IA and at least the upper part of Subunit IB. Some layers containing indications of volcanic ash and/or terrigenous clay were identified from smear slides (see "Lithostratigraphy" section). The positions of these layers are shown in Figure 15. They do not appear to be associated with significant perturbations of the susceptibility record. This may be a result of strong dilution of the volcanic and/or terrigenous material in these layers by the nonmagnetic carbonate and silica components. Because the susceptibility meter averages over ~5-cm intervals, susceptibility signals from individual thin layers may not be detectable unless they are particularly strong.

The susceptibility pulses evident in Figure 15 may result from small but significant fluctuations in the overall terrigenous content of the sediment, which are not readily identifiable in smear slides. Alternatively, the pulses may relate to episodes of re-

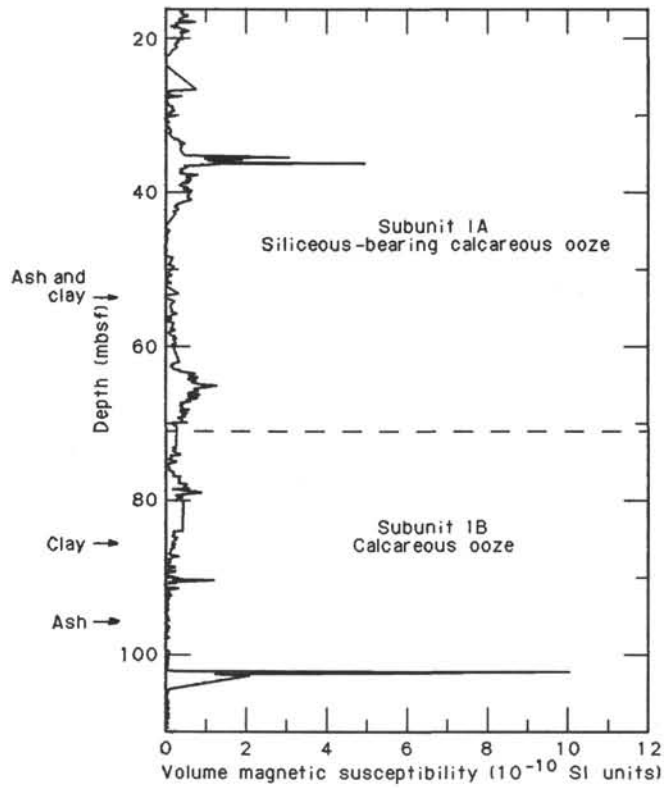

Figure 15. Downhole variation of magnetic susceptibility in the upper 110 m of Hole 703A. Anomalous spikes resulting from downhole contaminants at core tops have been removed. Positions of the ash and clay units identified from smear slides are shown at left.

working of older sediments containing higher concentrations of magnetite derived from basement erosion. More detailed post-cruise mineralogical studies of closely spaced samples will be necessary to confirm the origin of these distinctive susceptibility features.

A large peak in susceptibility values at 102 to 103 mbsf does not appear to result from downhole contamination. Dramatic changes in physical properties are observed in this same interval (see "Physical Properties" section), suggesting that the variation in magnetic susceptibility results from a notable (but as yet unexplained) change in the nature of the sediment across this interval.

A pumice breccia composed of angular fragments of basaltic material was encountered in the lower part of lithostratigraphic Subunit ID, within Core 114-703-34X. The deepest core in this hole, Core 114-703A-40X, contains massive altered basalt and medium- to coarse-grained sand. Mean susceptibility values for these materials are listed in Table 7, together with the mean value for a typical core of calcareous ooze (Core 114-703A-7H) for comparison. The susceptibility values for the altered basalt and associated sands are closely similar, indicating that the sand was probably derived from erosion of the basalt.

Paleomagnetism

The variation of paleomagnetic inclination with depth in Hole 703A, after alternating field (AF) demagnetization at 5 mT, is shown in Figure 16. These results were obtained from pass-through measurements of the archive core halves. Discrete paleomagnetic samples were taken at regular intervals (usually two per core section).

Magnetic intensity values obtained from the pass-through measurements are typically in the range 0.1 to 1.0 mA/m. For

Table 7. Mean susceptibility values for different lithologies, Hole 703A.

Interval	Lithology	Susceptibility ($\times 10^{-6}$ cgs units)
7H-2 to 7H-5	Calcareous ooze	1.3 ± 0.1
34X-1 to 34X-5	Pumice breccia	228.6 ± 44.4
40X-1	Fine sand	52.0 ± 23.0
40X-3	Coarse sand	72.8 ± 14.2
40X-2	Altered basalt	25.9 ± 22.2

much of the cored interval the paleomagnetic inclinations show a regular downhole alternation between values of about +70° and −70°; however, a number of intervals (e.g., 113 to 114.5 mbsf) are characterized by anomalously low inclination values. Within individual cores the change in sign of the inclination usually is accompanied by a change in declination of about 180°, as illustrated in Figure 17 by a comparison to the paleomagnetic data from Core 114-703A-8H.

Polarity Stratigraphy

The succession of normal and reverse polarity magnetozones identified within the depth interval from 15 to 115 mbsf in Hole 703A is shown in Figure 18. Biostratigraphic control on the magnetozone boundaries is very poor at this site. Therefore, correlation of these boundaries with the GPTS of Berggren et al. (1985) is equivocal for much of the interval.

Available nannofossil data indicate a late Eocene to early Oligocene age, within the range NP21 to NP19, for the base of Core 114-703A-13H, and NP22 to NP21 for Core 114-703A-12H (see "Biostratigraphy" section). The overlying interval from Core 114-703A-11H to Section 114-703A-7H-5 has been assigned to the lower Oligocene *Chiasmolithus altus* Zone (approximately lower NP25 to upper NP22). Thus, nannofossil data suggest that the Eocene/Oligocene boundary probably lies in the vicinity of Core 114-703A-13H. On this basis, the long reverse interval in Core 114-703A-12H and the lower part of Core 114-703A-11H can be assigned to the distinctive, long reverse polarity Chron C12R. The short normal polarity magnetozone at about 110 mbsf then can be correlated with the upper part of Chron C13N, and the position of the Eocene/Oligocene boundary can be extrapolated from the GPTS of Berggren et al. (1985) to lie in the lower half of Core 114-703A-13H (Fig. 18).

In the upper part of the interval represented in Figure 18, the base of Core 114-703A-3H and Section 114-703A-5H-2 have been tentatively assigned to the *Cyclicargolithus abisectus* nannofossil Zone, of early Miocene age, whereas Section 114-703A-5H, CC, has been assigned to the *Reticulofenestra bisecta* Zone of late Oligocene (~NP25) age (see "Biostratigraphy" section). Thus, nannofossil data indicate that the Oligocene/Miocene boundary lies within Core 114-703A-5H. The normal polarity magnetozone in the lower part of Core 114-703A-5H and the upper part of Core 114-703A-6H therefore can be assigned to Chron C6CN (which straddles the Oligocene/Miocene boundary) and the underlying reverse polarity magnetozone in Core 114-703A-6H to Chron C6CR.

Biostratigraphic control is currently inadequate to permit a confident correlation of the polarity zones in Cores 114-703A-7H to 114-703A-10H with the GPTS. An important tie-point within this sequence is the P21a/21b foraminifer zonal boundary, marking the early/late Oligocene boundary. This boundary has been established within Core 114-703A-7H, at a depth of about 57.5 mbsf. The datum indicates that the upper Oligocene section in Hole 703A is very short in comparison with the lower Oligocene section and requires either a dramatic reduction in sedimenta-

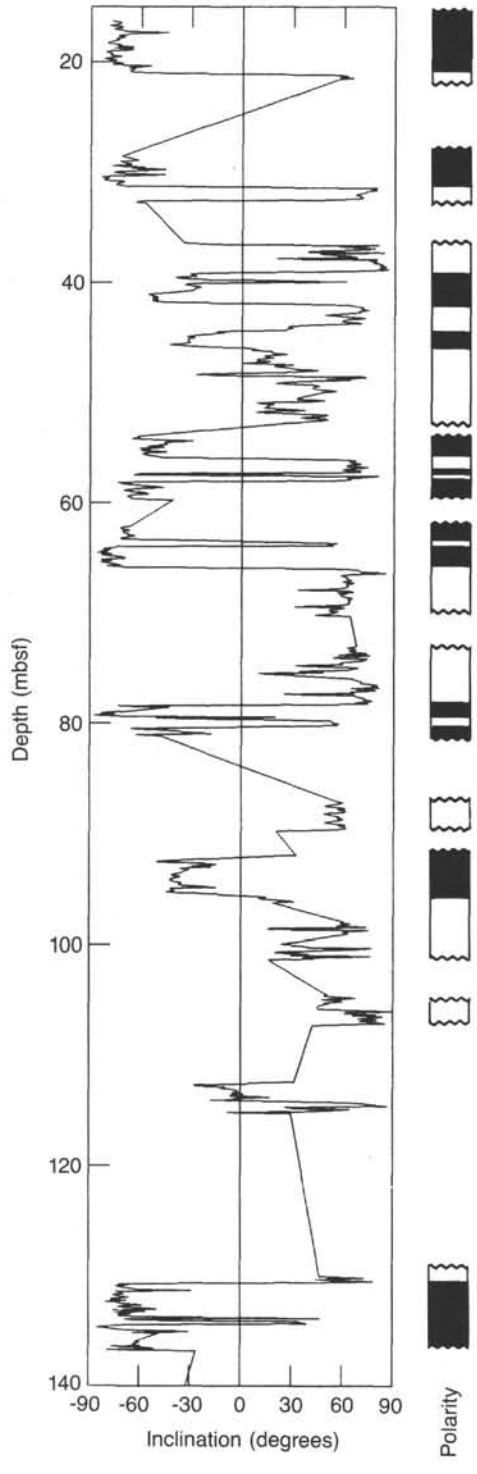

Figure 16. Downhole variation of paleomagnetic inclination after AF demagnetization at 5 mT for the upper 140 m of Hole 703A, with interpreted magnetic polarity zonations. These data were obtained from pass-through measurements of the archive core halves.

tion rate or the existence of a stratigraphic hiatus in the lower part of the upper Oligocene section. The latter interpretation appears to be most compatible with available nannofossil, foraminifer, and magnetostratigraphic data and is shown in Figure 18. However, it must be emphasized that this interpretation is tentative and may require revision in the light of further post-cruise paleomagnetic and biostratigraphic (especially diatom) investigation.

PHYSICAL PROPERTIES

Physical-property measurements were carried out at Site 703 to examine the effects of reworking, slumping, and mass flow on the physical properties. The physical-property measurements have been described in the "Explanatory Notes" chapter. Four sets of measurements were obtained on selected samples of APC and XCB sediment core sections at Site 703 (Cores 114-703A-1H to 114-703A-15H, and 114-703A-16X to 114-703A-41X, respectively): (1) index properties (wet-bulk density, dry-bulk density, porosity, water content, and grain density), (2) compressional (*P*-wave) velocity, (3) vane shear strength, and (4) thermal conductivity. The carbonate content (from "Geochemistry" section, this chapter) is shown for comparison with the physical-property data. All of the data presented are unfiltered for any bad data points.

Physical-Property Summary and Lithostratigraphic Correlation

The index properties, carbonate contents, *P*-wave velocities, thermal conductivities, and shear strengths are listed in Tables 8 through 12. Downcore profiles of wet-bulk density, porosity, water content, grain density, carbonate content, *P*-wave velocity, thermal conductivity, and shear strength are presented in Figure 19. The section is divided into two units, calcareous ooze and chalk with mass flow deposits and basaltic basement. The physical properties are summarized as follows: lithostratigraphic Unit I (0–363.9 mbsf; middle Eocene to Quaternary) is composed primarily of calcareous ooze and chalk. Wet-bulk density and thermal conductivity gradually increase, porosity and water content gradually decrease, and grain density and shear strength are variable with sub-bottom depth. Unit I is divided into four subunits: Subunit IA (0–71.4 mbsf) is a siliceous- and foraminifer-bearing nannofossil ooze, Subunit IB (71.4–162.4 mbsf) is a foraminifer-bearing nannofossil ooze, Subunit IC (162.4–228.9 mbsf) is a nannofossil ooze with mass flow deposits, and Subunit ID (228.9–363.9) is a nannofossil chalk with mass flow deposits. Two main features are apparent in the physical properties of Unit I. Within Subunit IA, the grain density is highly variable but generally decreases toward the Eocene/Oligocene boundary (see "Biostratigraphy" section) at about 110 mbsf. Below that depth the grain density increases slightly. All of the physical properties have distinct minima or maxima near 100 mbsf (Fig. 19). This zone, for example, has high water and low carbonate content and may correspond to a clay-bearing zone, which shows up as a low-resistivity layer in the resistivity log (see "Logging" section). The high velocity in Subunit ID, 5108 m/s (Fig. 19 and Table 10), corresponds to chert at 233.75 mbsf (Sample 114-703A-26X-4, 35–37 cm). This erratic value was excluded from the calculation of the means for Subunit ID because it was so much higher than any other velocities obtained for that subunit. The high velocities and the low carbonate content near the base of Subunit ID are representative of an altered volcanic breccia in Core 114-703A-34X.

Unit I (0–363.9 mbsf, middle Eocene to Quaternary)

Subunit IA (0-71.4 mbsf, uppermost lower Oligocene to Quaternary)

		Mean	Maximum	Minimum
Wet-bulk density	(g/cm^3)	1.69	1.53	1.82
Dry-bulk density	(g/cm^3)	0.99	0.74	1.18
Grain density	(g/cm^3)	2.83	2.67	3.07
Porosity	(%)	66.56	74.70	60.40
Water content	(%)	41.76	51.52	35.08
Carbonate content	(%)	88.15	91.74	83.65
Thermal conductivity	(W/m/K)	1.3548	1.2130	1.5850
Shear strength	(kPa)	41.31	86.1	14.0

Subunit IB (71.4–162.4 mbsf, uppermost middle Eocene to uppermost lower Oligocene)

		Mean	Maximum	Minimum
Wet-bulk density	(g/cm^3)	1.75	1.61	1.88
Dry-bulk density	(g/cm^3)	1.11	1.23	0.92
Grain density	(g/cm^3)	2.77	2.96	2.65
Porosity	(%)	61.39	67.00	56.92
Water content	(%)	36.84	43.08	32.44
Carbonate content	(%)	87.82	91.91	79.15
Thermal conductivity	(W/m/K)	1.3274	1.4720	1.1640
Shear strength	(kPa)	50.39	137.3	9.3
P-wave velocity	(m/s)	1598	1630	1572

Subunit IC (162.4–228.9 mbsf, middle Eocene)

		Mean	Maximum	Minimum
Wet-bulk density	(g/cm^3)	1.85	2.04	1.78
Dry-bulk density	(g/cm^3)	1.23	1.46	1.15
Grain density	(g/cm^3)	2.84	2.90	2.79
Porosity	(%)	58.48	61.66	52.24
Water content	(%)	33.57	36.09	28.45
Carbonate content	(%)	90.71	92.74	88.07
Thermal conductivity	(W/m/K)	1.5450	1.5670	1.5230
Shear strength	(kPa)	57.37	79.1	46.5
P-wave velocity	(m/s)	1979		

Subunit ID (228.9–363.9 mbsf, middle Eocene)

		Mean	Maximum	Minimum
Wet-bulk density	(g/cm^3)	1.89	2.07	1.77
Dry-bulk density	(g/cm^3)	1.30	1.53	1.15
Grain density	(g/cm^3)	2.86	2.98	2.64
Porosity	(%)	55.99	61.84	50.36
Water content	(%)	31.23	36.00	25.84
Carbonate content (breccia included)	(%)	64.19	95.58	0.17
Carbonate content (breccia excluded)	(%)	95.43	95.58	95.24
Thermal conductivity	(W/m/K)	1.5055	1.5770	1.4340
Shear strength	(kPa)	6.20	34.9	17.5
P-wave velocity (breccia included, chert excluded)	(m/s)	2035	2541	1571
P-wave velocity (breccia and chert excluded)	(m/s)	1631	1671	1571

Lithostratigraphic Unit II (363.9–377.4 mbsf; middle Eocene) consists of altered porphyritic basalt or basaltic andesite. The exact boundary of the unit is difficult to define. We have used an upper boundary of 363.9 mbsf to correspond with the first basalt sampled for physical properties. The basalt is weathered and altered to varying degrees, as is evident from the porosity and velocity (Fig. 19). Porosities range from 2.55% to 10.55%, and velocities are as low as 3961 m/s. The maximum velocity is 5260 m/s. The velocity was measured at adjacent locations, once on the split core half and again on a discrete sample. The difference between the respective velocity measurements is only 5 m/s.

Unit II (363.9–377.4 mbsf, Eocene)

		Mean	Maximum	Minimum
Wet-bulk density	(g/cm^3)	2.89	3.02	2.73
Dry-bulk density	(g/cm^3)	2.80	2.90	2.71
Grain density	(g/cm^3)	2.89	3.01	2.74
Porosity	(%)	8.07	10.55	2.55
Water content	(%)	2.99	3.84	0.99
P-wave velocity	(m/s)	4826	5260	3961

Discussion

The physical properties of the sediments at Site 703 display no direct manifestation of mass flow or reworking, in spite of lithostratigraphic and biostratigraphic evidence. However, closer examination may reveal subtle effects (Fig. 19). The porosity, for example, decreases gradually, with only a few excursions, with increasing sub-bottom depth, in spite of the presence of mass flows. This pattern continues even through the volcanic breccia, where markedly higher velocities occur. The bulk density, water content, and thermal conductivity all change gradually with depth. The grain density, which is initially quite variable, first generally decreases with depth and then gradually increases toward basement. The carbonate content is quite high, but has small variations that seem to correlate with changes in the grain density, as well as in the other physical properties.

SEISMIC STRATIGRAPHY

Site 703 was intended as a complement to Site 704 with the specific objective of obtaining the oldest sediment and penetrating basement. Although the area has good site survey coverage, the rapid lateral changes in sediment thickness and basement elevation made it difficult to occupy an optimum site location with an attenuated section on the basis of transit satellite navigation (Figs. 21 and 22). *JOIDES Resolution* started seismic profiling on approach to the crest area in heavy seas (sea state 8) but was blown off course. Another pass was made with the same result, and we decided to drop the beacon on a ledge about 450 m deeper than the top of the ridge. After completing Site 703, the site was resurveyed (Fig. 20).

The sediments at Site 703 consist of calcareous ooze and chalk with increasing contributions of clay, foraminifer ooze, sand, and gravel by mass flow below 162.4 mbsf. Altered porphyritic basalt encountered at 364–365.65 mbsf may represent basement or a sill (Fig. 21). Wet-bulk densities show fluctuations superimposed on a linear increase with depth, which corresponds to small variations in the high carbonate content (around 90%). *P*-wave velocity is nearly constant (~1600 m/s) down to about 200 mbsf, where *in-situ* velocities increase to 2000–2100 m/s with the occurrence of several mass flows. At about 230 mbsf there is a drop in porosity with no concomitant change in velocity, suggesting a carbonate section with no foreign material. Samples from the volcanic breccia at 307 mbsf yield a velocity of about 2500 m/s. The altered basalt has a seismic velocity in the range of 3900–5300 m/s.

A major hiatus that separates lower Miocene from upper Pliocene sediments (~15 m.y. duration) is associated with a distinct reflection in the 3.5-kHz record (Fig. 22). The transition from the upper siliceous foraminifer-bearing ooze to the underlying foraminifer-bearing nannofossil ooze around 71.4 mbsf is accompanied by a gradual 5%–10% reduction in porosity and a similar increase in wet-bulk density, which appear to generate a reflection event (Fig. 21). Other reflections associated with fluctuations in the carbonate content are on the order of 10% and are observed at 100–110 and 130–150 mbsf. At about 170 mbsf the Schlumberger logs (see "Logging" section) show well-defined minima in resistivity and velocity, which are indicative of ~5-m thick turbidite, but representation in the relatively noisy reflection record is not clear. The quality of the record also concerns the acoustic expression of the ooze/chalk transition that, because of the lack of core recovery, has been tentatively positioned at 230 mbsf in correlation with the drop in resistivity at this interval (see "Lithostratigraphy" section). Reflection events corresponding to the ooze/chalk transition have not been observed at other Leg 114 sites. The basal volcanic breccia below 300 mbsf has a 20% higher seismic velocity and a slight increase in wet-bulk density with respect to the chalk, and these properties give rise to a discernable reflection. Basement level or any possible sill at the bottom of the hole has a relatively weak acoustic expression.

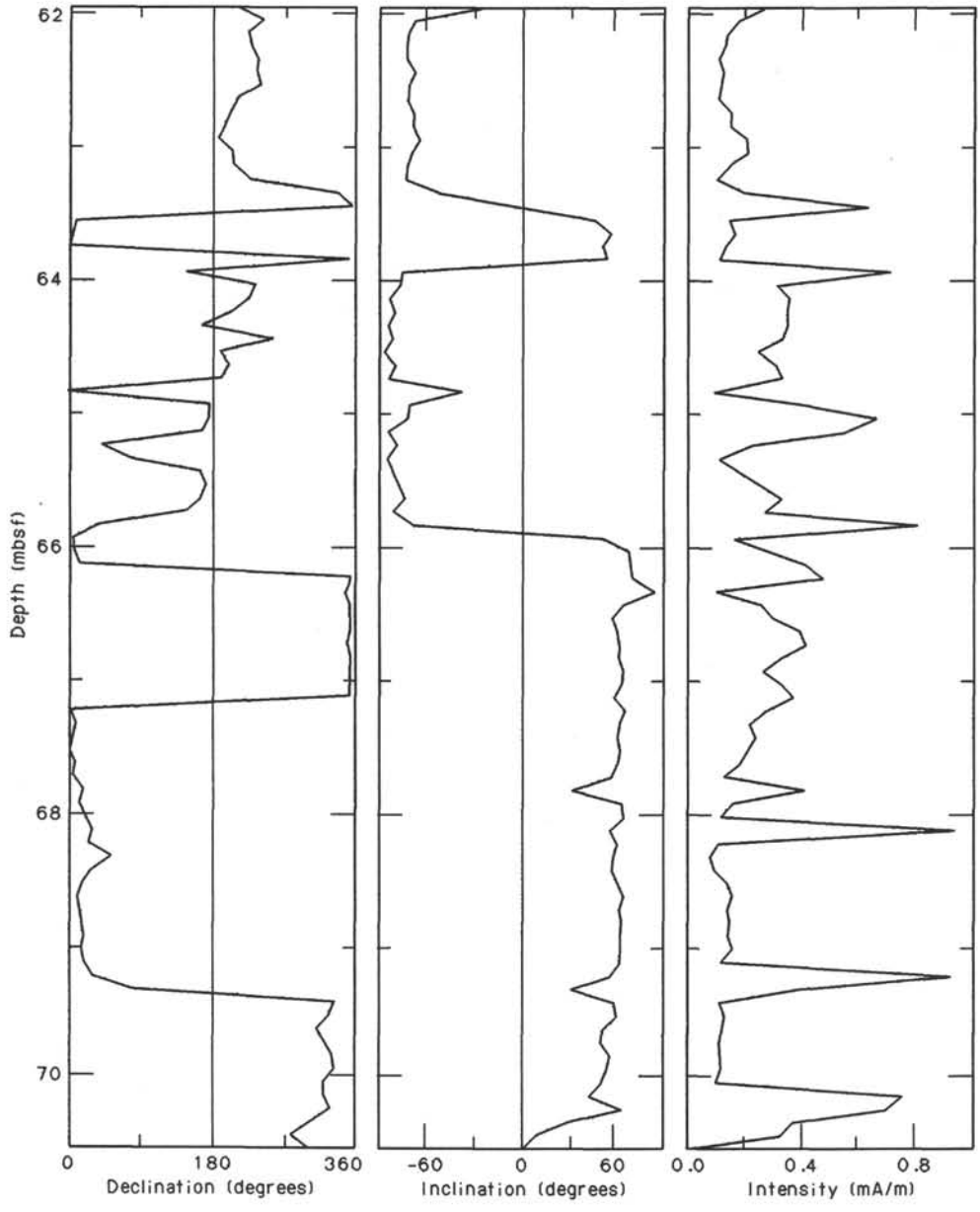

Figure 17. Variation of paleomagnetic declination, inclination, and intensity after AF demagnetization at 5 mT in Core 114-703A-8H, measured using the pass-through cryogenic magnetometer. Note how changes in sign of inclination are accompanied by changes of nearly 180° in declination.

Because Site 703 is only about 2 km from the foot of a seamount with a 500 m higher elevation and a slope of 15°, it is not optimally located to minimize the potential effect of mass flow in the section. However, the rugged basement topography, lack of sufficient navigational control, and severe weather conditions made any attempts to reach preset locations very difficult. The southern part of Meteor Rise sampled here appears from the site survey data and other bathymetric information (LaBrecque, 1986) to have a particularly high relief, with some seamounts reaching 1300 mbsl, which may represent a younger volcanic event than formation of the plateau proper. The oldest sediments of middle Eocene age contain redeposited microfossils that are no older than Eocene. On the conjugate structure, the Islas Orcadas Rise, Late Cretaceous age microfossils are reworked in the upper Paleocene, suggesting a minimum Late Cretaceous age for the Islas Orcadas Rise.

LOGGING

One logging run was made in Hole 703A. The main objective was to provide a continuous geophysical record of the hole to tie with the lithostratigraphy and to aid in the interpretation of sections with poor or no core recovery.

Logging Operations

Hole 703A was fairly stable, except for one or two areas of turbiditic sand deposition, where the recovery was poor and the borehole wall could potentially cave in. The lithodensity, neutron porosity, and natural gamma-ray spectrometry string (LDT-CNL-NGT combination) was originally planned, because it is the best string that can be be run for lithologic identification purposes. However, we could not use this string because no bull nose section was present at the bottom of the tool assembly. The

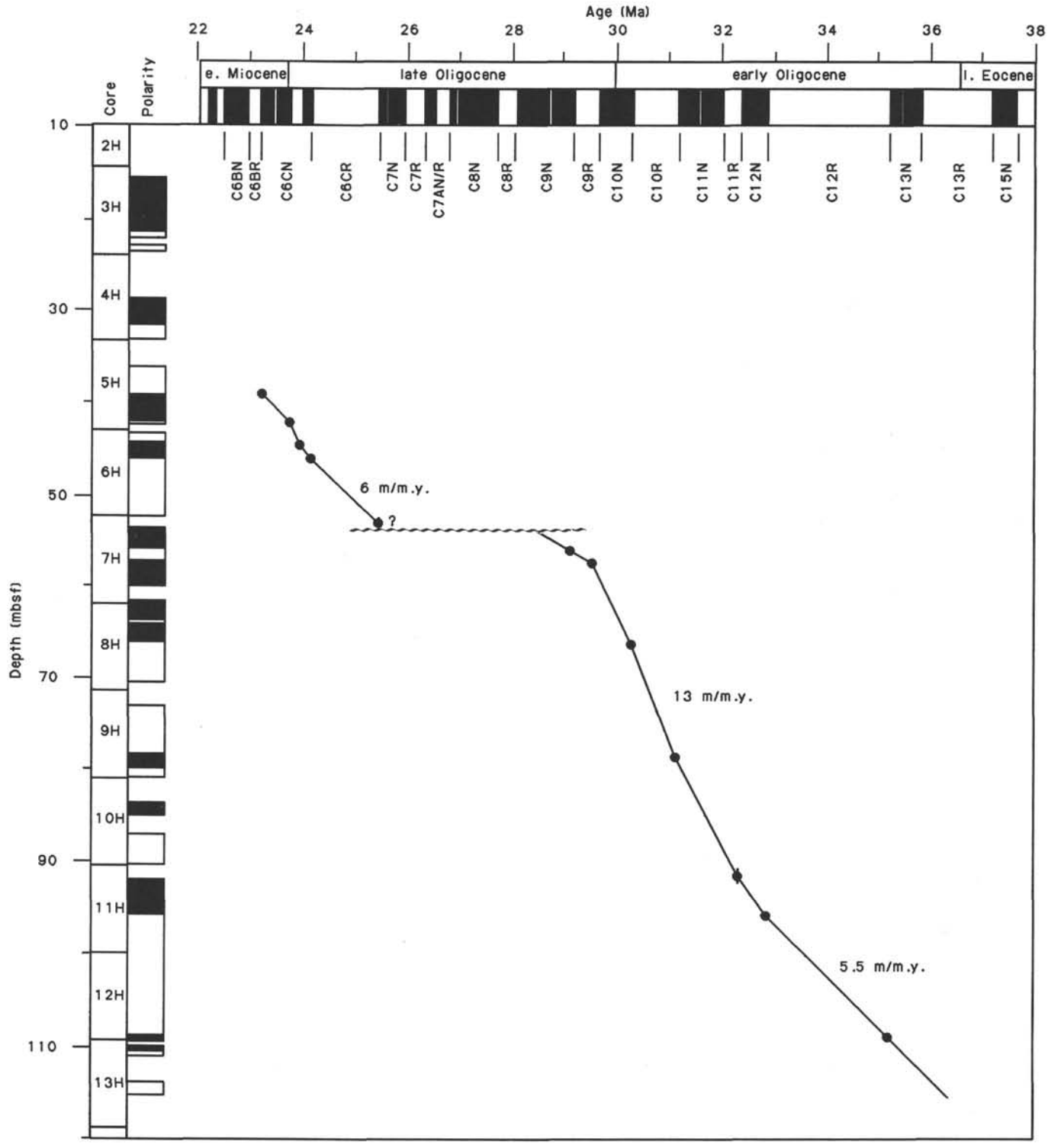

Figure 18. Tentative correlation of magnetic polarity zones (vertical axis) in Hole 703A with the GPTS of Berggren et al. (1985) (horizontal axis). Normal polarity is represented by black, reverse polarity by white. This correlation is based on preliminary shipboard biostratigraphic data.

bull nose is normally used to open a flapper inside the pipe near the drill bit. We elected to bypass the bull nose operation by sending down a go-devil, which would automatically open the flapper. The two go-devils sent did not open the flapper, and we decided to change tool strings. The seismic-stratigraphic combination, consisting of a borehole-compensated sonic (BHC) log, three resistivity logs (SFLU, ILM, ILD), a total count gamma-ray (GR) log, and a caliper (CALI) was chosen.

Use of the side entry sub was not necessary because few bridging problems were encountered while drilling soft sediments. The drill pipe was raised to a level of approximately 110 mbsf, and all logging measurements were acquired below this depth.

Table 8. Index properties, Hole 703A.

Sample (cm)	Depth (mbsf)	Water content (%)	Porosity (%)	Densities		
				Wet bulk (g/cm³)	Dry bulk (g/cm³)	Grain (g/cm³)
2H-2, 100–102	7.40	51.52	74.70	1.53	0.74	2.81
2H-6, 100–102	13.40	44.00	68.54	1.59	0.89	2.81
3H-1, 100–102	15.40	40.57	65.67	1.76	1.04	2.84
3H-2, 100–102	16.90	45.08	70.46	1.61	0.88	2.94
3H-3, 100–102	18.40	41.30	67.82	1.69	0.99	3.03
3H-4, 100–102	19.90	42.21	66.88	1.69	0.98	2.80
4H-4, 100–102	29.40	44.65	68.25	1.62	0.90	2.69
4H-5, 100–102	30.90	41.03	65.71	1.68	0.99	2.79
4H-6, 100–102	32.40	38.51	63.78	1.76	1.08	2.85
5H-3, 100–102	37.40	40.78	67.57	1.76	1.04	3.07
5H-4, 100–102	38.90	35.08	60.40	1.82	1.18	2.86
5H-5, 100–102	40.40	42.98	66.76	1.61	0.92	2.70
5H-6, 100–102	41.90	41.57	67.55	1.68	0.98	2.96
6H-3, 100–102	46.90	43.49	67.87	1.64	0.93	2.78
6H-4, 100–102	48.40	44.23	68.94	1.86	1.04	2.83
6H-5, 100–102	49.90	42.52	66.80	1.64	0.94	2.75
6H-6, 100–102	51.40	44.01	68.56	1.63	0.92	2.81
7H-3, 100–102	56.40	42.08	66.75	1.66	0.96	2.80
7H-4, 100–102	57.90	41.32	66.04	1.67	0.98	2.80
7H-5, 100–102	59.40	41.21	66.20	1.68	0.98	2.83
8H-3, 100–102	65.90	38.37	62.16	1.77	1.09	2.67
8H-4, 100–102	67.40	37.17	62.23	1.80	1.13	2.82
8H-5, 100–102	68.90	36.70	61.16	1.75	1.11	2.75
9H-3, 100–102	75.40	36.40	62.08	1.74	1.11	2.90
9H-4, 100–102	76.90	37.12	61.76	1.71	1.08	2.77
9H-5, 100–102	78.40	33.48	57.61	1.77	1.18	2.74
9H-6, 100–102	79.90	33.57	57.46	1.80	1.20	2.71
10H-3, 80–82	84.70	37.36	61.98	1.73	1.08	2.77
10H-4, 100–102	86.40	35.75	59.34	1.76	1.13	2.66
10H-5, 71–73	87.61	37.03	61.35	1.75	1.11	2.73
10H-5, 100–102	87.90	35.99	60.36	1.74	1.12	2.74
10H-6, 100–102	89.40	32.44	56.92	1.81	1.23	2.79
11H-2, 100–102	92.90	33.78	58.78	1.82	1.20	2.83
11H-3, 100–102	94.40	33.59	57.50	1.78	1.18	2.71
11H-4, 100–102	95.90	40.26	64.95	1.70	1.02	2.78
11H-5, 100–102	97.40	37.58	62.09	1.68	1.05	2.75
11H-6, 100–102	98.90	36.29	60.66	1.71	1.09	2.74
12H-1, 50–52	100.40	40.86	65.50	1.65	0.98	2.78
12H-2, 50–52	101.90	43.08	67.00	1.61	0.92	2.71
12H-4, 50–52	104.90	42.24	66.03	1.62	0.93	2.69
12H-5, 50–52	106.40	39.68	64.09	1.66	1.00	2.75
12H-6, 60–62	108.00	39.81	63.37	1.64	0.99	2.65
12H-7, 60–62	109.50	39.30	63.31	1.67	1.01	2.70
13H-2, 100–102	111.90	36.51	60.70	1.74	1.11	2.72
13H-4, 90–92	114.80	37.08	61.03	1.74	1.09	2.69
15H-2, 100–102	130.90	34.72	58.70	1.80	1.18	2.71
15H-3, 100–102	132.40	37.12	62.89	1.84	1.15	2.91
15H-4, 100–102	133.90	34.35	60.44	1.85	1.22	2.96
15H-5, 100–102	135.40	34.97	60.02	1.80	1.17	2.83
17X-3, 100–102	147.40	39.06	63.45	1.68	1.02	2.74
18X-1, 100–102	153.90	35.86	60.73	1.88	1.21	2.80
18X-2, 100–102	155.40	36.15	61.48	1.83	1.17	2.86
18X-3, 100–102	156.90	35.76	60.90	1.82	1.17	2.84
18X-4, 100–102	158.40	34.87	60.50	1.82	1.19	2.90
20X-1, 100–102	172.90	36.05	61.66	1.82	1.17	2.89
20X-3, 100–102	175.90	33.57	58.19	1.78	1.19	2.79
20X-5, 100–102	178.90	32.38	57.24	1.87	1.26	2.83
21X-1, 100–102	182.40	36.09	61.05	1.79	1.15	2.81
21X-2, 100–102	183.90	32.55	57.95	1.86	1.25	2.90
21X-3, 100–102	185.40	35.38	60.89	1.80	1.16	2.88
21X-4, 100–102	186.90	34.05	58.65	1.82	1.20	2.79
23X-1, 90–92	201.30	28.45	52.24	2.04	1.46	2.79
26X-1, 42–44	229.32	36.00	61.84	1.81	1.16	2.92
26X-2, 100–102	231.40	35.08	58.53	1.77	1.15	2.64
26X-3, 82–84	232.72	32.37	57.06	1.86	1.26	2.81
26X-5, 71–73	235.61	32.87	57.17	1.84	1.23	2.76
30X-2, 93–95	269.33	32.38	58.44	1.89	1.28	2.98
30X-3, 100–102	270.90	31.98	56.87	1.84	1.25	2.84
34X-2, 122–124	307.62	26.28	50.36	2.07	1.53	2.89
34X-3, 100–102	308.90	25.84	50.49	2.01	1.49	2.97
34X-4, 60–62	310.00	28.28	53.13	1.94	1.39	2.92
40X-2, 60–62	364.00	3.84	10.55	2.90	2.79	3.01
40X-2, 127–129	364.67	0.96	2.55	2.73	2.71	2.74
40X-3, 90–92	365.80	3.39	8.93	2.91	2.81	2.84
40X-3, 102–105	365.92	3.75	10.24	3.02	2.90	2.98

Table 9. Calcium carbonate content, Hole 703A.

Sample (cm)	Depth (mbsf)	Carbonate content (%)
2H-2, 100–102	7.40	87.82
2H-6, 100–102	13.40	91.74
3H-2, 100–102	16.90	86.74
3H-4, 100–102	19.90	89.49
4H-4, 100–102	29.40	90.57
4H-6, 100–102	32.40	91.32
5H-3, 100–102	37.40	89.49
5H-6, 100–102	41.90	90.49
6H-3, 100–102	46.90	88.32
6H-6, 100–102	51.40	83.73
7H-3, 100–102	56.40	87.40
7H-5, 100–102	59.40	88.07
8H-3, 100–102	65.90	85.32
8H-5, 100–102	68.90	83.65
9H-3, 100–102	75.40	90.99
9H-6, 100–102	79.90	89.15
10H-3, 80–82	84.70	88.57
10H-4, 100–102	86.40	90.91
10H-5, 71–73	87.61	88.49
10H-5, 100–102	87.90	87.15
10H-6, 100–102	89.40	91.16
11H-2, 100–102	92.90	91.91
11H-5, 100–102	97.40	88.32
12H-1, 50–52	100.40	88.15
12H-2, 50–52	101.90	86.74
12H-4, 50–52	104.90	82.32
12H-5, 50–52	106.40	86.57
12H-6, 60–62	108.00	79.15
12H-7, 60–62	109.50	87.74
13H-2, 100–102	111.90	89.99
13H-4, 90–92	114.80	90.57
15H-2, 100–102	130.90	89.57
15H-4, 100–102	133.90	81.48
17X-3, 100–102	147.40	84.98
18X-1, 100–102	153.90	89.24
18X-3, 100–102	156.90	88.99
20X-1, 100–102	172.90	90.99
20X-5, 100–102	178.90	88.07
21X-1, 100–102	182.40	91.32
21X-3, 100–102	185.40	92.74
23X-1, 90–92	201.30	90.41
26X-1, 42–44	229.32	95.41
26X-3, 82–84	232.72	95.49
30X-2, 93–95	269.33	95.24
30X-3, 100–102	270.90	95.58
34X-2, 122–124	307.62	3.25
34X-4, 60–62	310.00	0.17

An additional 28 m of data was recorded by raising the entire drill string at the end of the run, which is standard procedure. The hole was drilled to a depth of approximately 377 mbsf, but as a result of either bridging or cave-in, logs were acquired only to a depth of approximately 310 mbsf.

Seismic-stratigraphic combination data were first acquired on a downhole run from 145 to 312 mbsf and subsequently on an uphole run from 315 to 82 mbsf. The failure of the heave compensator mechanism created an additional problem. However, the logs from the two runs appear to be fairly repeatable. One way to monitor the motion resulting from the ship's heave is to observe the caliper or, preferably, the cable tension. A logging speed of approximately 1800 ft/hr was deliberately chosen to try and minimize the loss of vertical resolution caused by heave. Measurements were made at 15-cm intervals. All logs are referenced to zero depth at the seafloor, which was determined from the drilling information and should agree fairly well with the depths from the cores. The water depth (determined by measurement of the drill pipe from sea level) was 1796.1 m. All of the logs were provided by Schlumberger logging services.

Table 10. *P*-wave velocity, Hole 703A.

Sample (cm)	Depth (mbsf)	Direction[a]	Velocity (m/s)
10H-3, 80–82	84.70	C	1607.2
10H-5, 69–71	87.59	C	1572.4
10H-5, 100–102	87.90	C	1598.9
11H-2, 100–102	92.90	C	1591.2
11H-4, 100–102	95.90	C	1607.0
11H-6, 100–102	98.90	C	1621.0
12H-1, 50–52	100.40	C	1511.8
12H-5, 50–52	106.40	C	1629.8
12H-7, 60–62	109.50	C	1616.7
13H-2, 100–102	111.90	C	1622.8
13H-4, 90–92	114.80	C	1598.8
23X-1, 90–92	201.30	C	1979.4
26X-1, 40–42	229.30	C	1570.8
26X-3, 80–82	232.70	C	1665.3
26X-4, 35–37	233.75		5107.7
26X-5, 70–72	235.60	C	1611.3
30X-2, 95–97	269.35	C	1670.6
30X-3, 100–102	270.90	C	1637.9
34X-2, 122–124	307.62	C	2540.7
34X-3, 100–102	308.90	A	2422.5
34X-4, 60–62	310.00	A	2443.2
34X-4, 60–62	310.00	B	2457.5
34X-5, 11–13	311.01		2324.7
40X-2, 60–62	364.00	C	4828.2
40X-2, 127–129	364.67	C	3961.1
40X-3, 88–90	365.78		5260.4
40X-3, 90–92	365.80	C	5255.0

[a] A = perpendicular to split-core surface; B = parallel to split-core surface; C = axial.

Table 11. Thermal conductivity, Hole 703A.

Sample (cm)	Depth (mbsf)	Thermal conductivity (W/m/K)
4H-3, 100–100	27.90	1.2760
4H-4, 100–100	29.40	1.2400
5H-3, 100–100	37.40	1.3690
5H-6, 100–100	41.90	1.4490
6H-2, 100–100	45.40	1.2300
6H-4, 100–100	48.40	1.5410
7H-2, 100–100	54.90	1.2130
7H-3, 100–100	56.40	1.3340
8H-2, 100–100	64.40	1.3110
8H-4, 100–100	67.40	1.5850
9H-2, 100–100	73.90	1.2980
9H-3, 100–100	75.40	1.3700
10H-3, 100–100	84.90	1.4080
10H-4, 100–100	86.40	1.3070
11H-2, 100–100	92.00	1.2950
11H-4, 100–100	95.90	1.3120
11H-6, 100–100	98.90	1.3600
12H-2, 100–100	102.40	1.2410
12H-4, 100–100	105.40	1.1640
12H-6, 100–100	108.40	1.3400
15H-2, 100–100	130.90	1.4720
15H-4, 100–100	133.90	1.3620
20X-5, 100–100	178.90	1.5230
21X-3, 95–95	185.35	1.5670
26X-3, 100–100	232.90	1.4340
30X-3, 100–100	270.90	1.5770

Logging Measurements

An analog string tool combination was used, as opposed to the digital strings used in Hole 700B. However, the caliper, tension, and three resistivity measurements are comparable to those discussed in the "Logging" section of the "Site 700" chapter, this volume. The gamma-ray tool provides only a GR log. The GR log corresponds to the SGR log of the natural gamma-ray spectrometry tool but does not differentiate between the U, Th, and K components.

Sonic measurements were made with the BHC tool, which consists of two acoustic sources of several kilohertz and two receivers that are geometrically arranged to compensate for tool tilt and borehole radius variations. The full-waveform train is recorded at each receiver (as shown in Fig. 23). The *P*-wave arrival is detected by a threshold/expected arrival time algorithm. An interval transit time is then calculated for the difference in arrival time between the two receivers, which are 0.61 m apart. This is a measurement of the *in-situ* compressional-wave velocity. Further analysis of these logs will be conducted at a later date.

Table 12. Vane shear strength, Hole 703A.

Sample (cm)	Depth (mbsf)	Shear strength (kPa)
3H-1, 100–102	15.40	27.9
3H-5, 100–102	21.40	18.6
4H-4, 100–102	29.40	14.0
4H-6, 100–102	32.40	23.3
5H-6, 100–102	41.90	32.6
6H-4, 100–102	48.40	65.2
7H-5, 100–102	59.40	62.8
8H-3, 100–102	65.90	86.1
9H-4, 100–102	76.90	100.1
10H-3, 80–82	84.70	9.3
10H-5, 100–102	87.90	30.3
11H-2, 100–102	92.90	16.8
11H-4, 100–102	95.90	18.6
11H-6, 100–102	98.90	32.6
12H-1, 50–52	100.40	36.1
12H-5, 50–52	106.40	48.9
12H-7, 60–62	109.50	37.2
13H-2, 100–102	111.90	20.9
13H-4, 90–92	114.80	25.6
15H-2, 100–102	130.90	44.2
15H-4, 100–102	133.90	137.3
15H-5, 100–102	135.40	65.2
18X-1, 100–102	153.90	69.8
18X-2, 100–102	155.40	41.9
18X-3, 100–102	156.90	53.5
18X-4, 100–102	158.40	118.7
20X-1, 100–102	172.90	46.5
20X-5, 100–102	178.90	79.1
21X-1, 100–102	182.40	46.5
26X-1, 40–42	229.30	34.9
30X-3, 100–102	270.90	17.5

Interpretation of Results

Figures 24 and 25 show the logs obtained during the downhole and uphole runs, respectively. A record of the downhole run is usually not discussed, and it is presented here to show repeatability of the data. Data include the CALI, GR, the three SFLU, ILM, and ILD resistivities, which are displayed as conductivities, and interval transit times (DT), displayed as compressional velocity. Cable tension was also recorded. Overall trends reveal a fairly homogeneous section. Both tension and caliper indicate that the tool string was constantly moving up and down at a fairly high frequency because of the ship's heave. The heave compensator is rated to compensate heaves of less than 3.05 m, with a frequency range between 0.01 and 0.25 Hz. Observed heave during logging operations was frequently greater than 3.05 m and, therefore, could not be sufficiently compensated. A comparison between downhole and uphole logging runs shows good repeatability in spite of the failure of heave compensation. The caliper indicates stable hole conditions, and this could also be an indirect indication of a fairly uniform lithology overall.

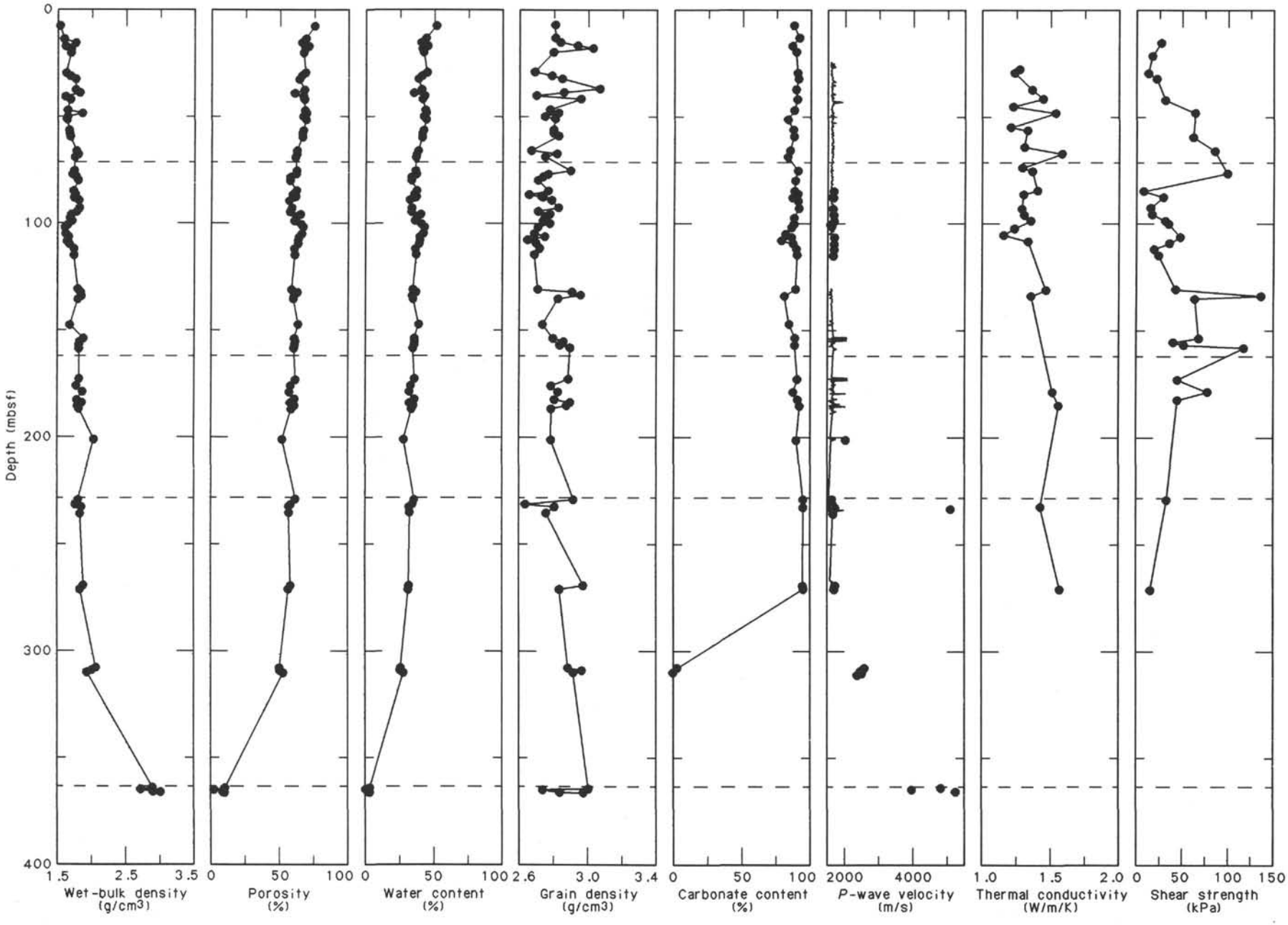

Figure 19. Wet-bulk density, porosity, water content, grain density, calcium carbonate content, *P*-wave velocity, thermal conductivity, and shear strength profiles, Hole 703A. The subunits of Unit I are delineated by short-dashed lines.

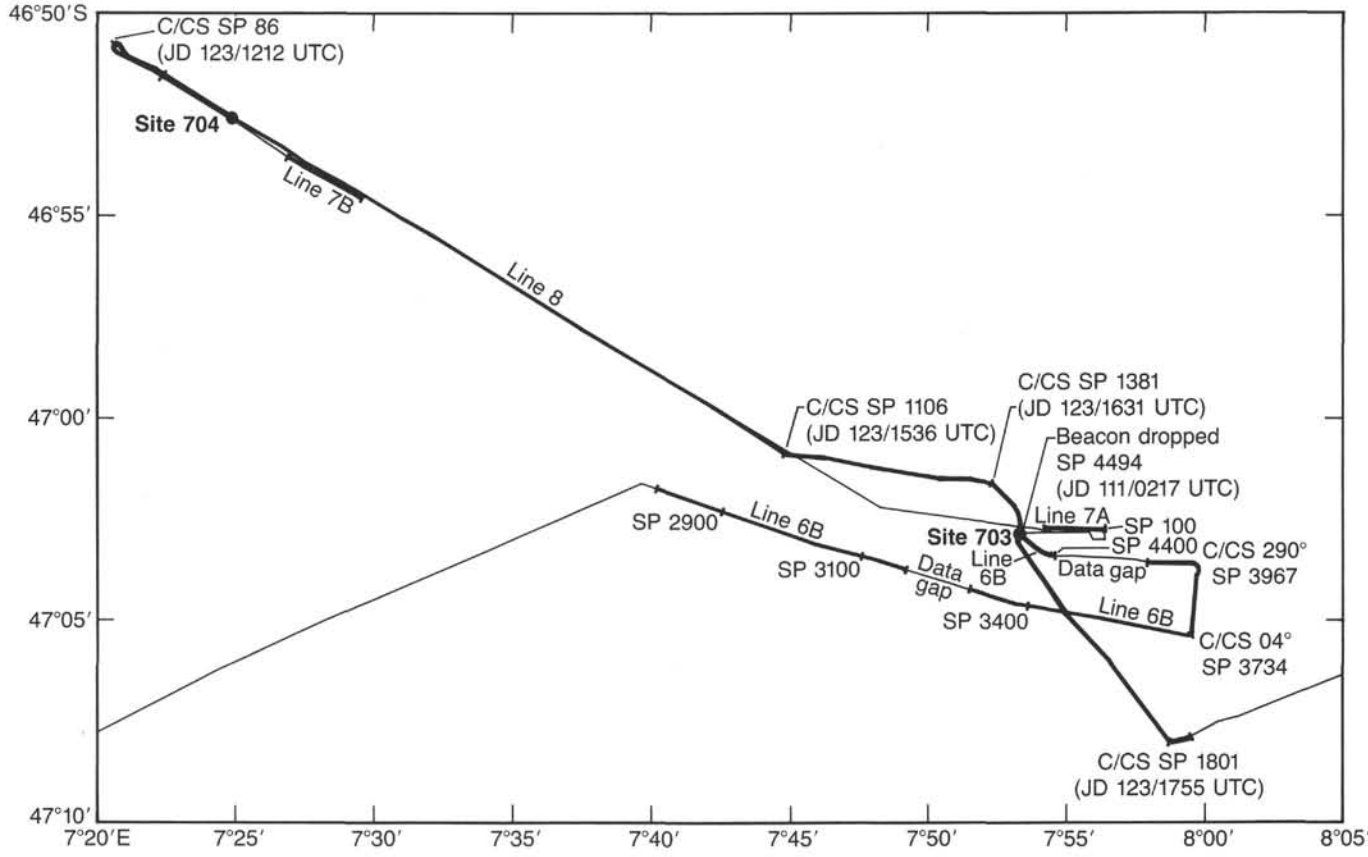

Figure 20. Track of *JOIDES Resolution* on approach and departure from Site 703. Seismic profile shown in Figure 21 is indicated by the bold line.

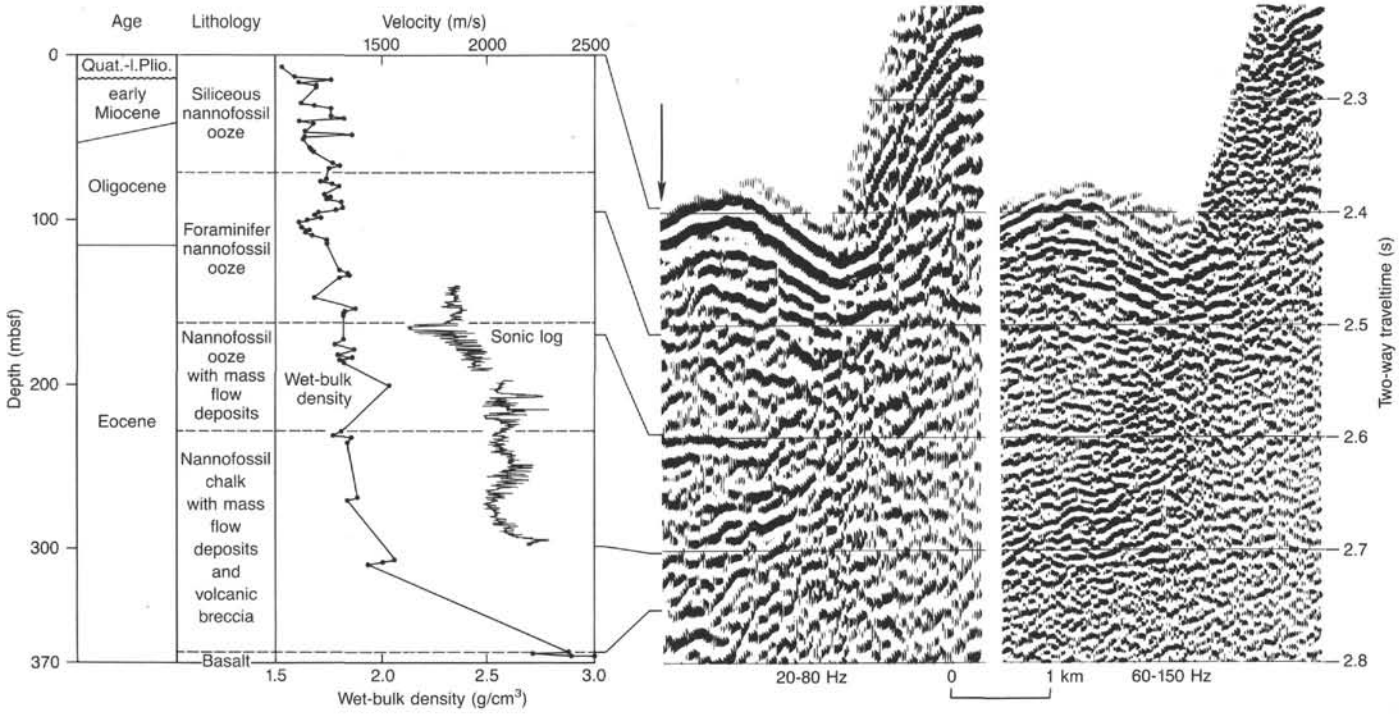

Figure 21. Summary of *P*-wave velocity (0–140 and 300–377 mbsf) and wet-bulk density (from "Physical Properties" section), sonic velocity (140–300 mbsf) and resistivity (from "Logging" section), lithology (from "Lithostratigraphy" section), and age (from "Biostratigraphy" section) of Site 703 correlated with single-channel seismic-reflection data obtained by *JOIDES Resolution* over the site location.

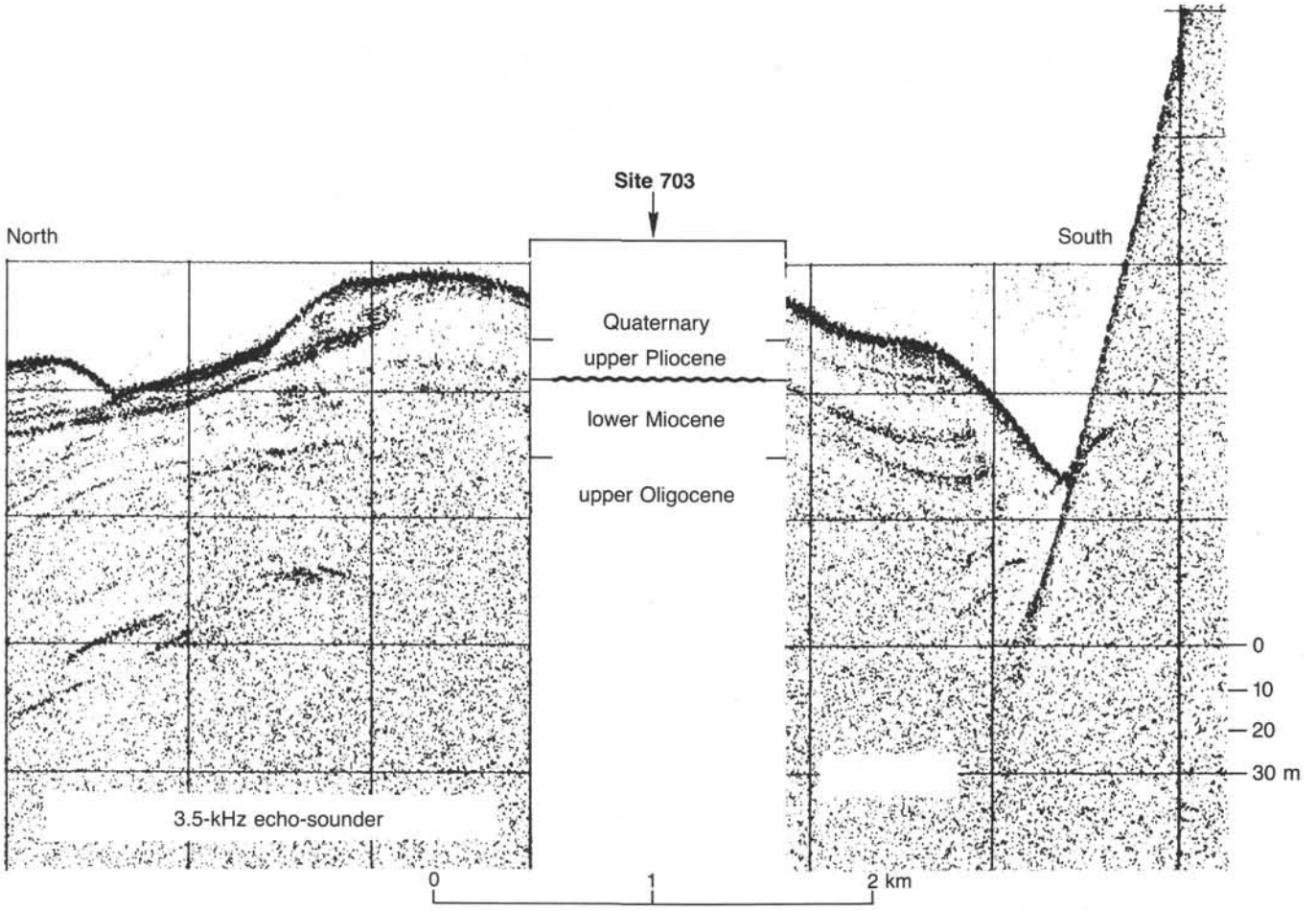

Figure 22. High-resolution (3.5-kHz) seismic-reflection profile over Site 703, recorded by *JOIDES Resolution*.

A general description of possible lithostratigraphic units can be inferred from the combined responses of the logs available. Lithostratigraphic Subunit IB (calcareous ooze, to a depth 162.4 mbsf) is the first unit logged and shows fairly uniform gamma-ray and conductivity responses. The sonic log, however, shows alternating cycles of high and low velocities. These could be interpreted as sections of subtle changes in lithology, resulting from differential compaction or micritic recrystallization. Porosities derived from the deep resistivity data and the measured porosities from the physical properties do not indicate such diagenetic changes. The sonic tool that we used has relatively short source/receiver offsets of 0.91 and 1.52 m. In an 11-in.-diameter hole, transit times that exceed 170 ms/ft and measured using this tool are not always reliable; this situation occurred in the upper unconsolidated part of the hole, where velocities are approximately 1800 m/s.

Lithostratigraphic Subunit IC consists of calcareous ooze with mass flow deposits (from 162.4 to 228.9 mbsf). This unit shows a general and gradual decrease in conductivity with depth. The top part of the subunit (162.4–169 mbsf) exhibits a characteristic high-conductivity and low-velocity response. This may be because of the presence of sand or flows, but caution must be taken in assigning a lithology from so few log responses. The next part of the subunit (169–200 mbsf) shows increasing velocity with depth, and from 170 to 190 mbsf, this part also shows increasing resistivity with depth. The sonic log is very noisy between 190 and 200 mbsf. This probable result of cycle skipping appears in the full-waveform record, where the amplitude of the first arrival is low (Fig. 23). These data will be reprocessed to obtain better estimates of arrival times. The bottom section of Subunit IC (200–228.9 mbsf) shows relatively constant velocities of approximately 2000 m/s and conductivities of less than 1000 ms/m. The entire subunit, which was poorly recovered, is disturbed by lower conductivity and high velocity peaks. These characteristics could possibly represent mass flow deposits, encompassing a poorly sorted mixture of reworked chert and sand particles. But once again, no definite lithologic recognition can be inferred from the logs alone, and care must be taken in assigning lithology where no cores were recovered. However, we can safely state that sediments were severely disturbed throughout the subunit.

Subunit ID (228.9–364 mbsf) is a chalk with mass flow deposits. Porosity and conductivity variations show that the interval has been disrupted, possibly by mass flow deposits; there is poor core recovery throughout this subunit. The bottom part (295–304 mbsf) is a gravelly volcanic sand ("Lithostratigraphy" section) that exhibits both lower conductivity and high velocity.

The lower unit logged (from a depth of 304 mbsf and downward) shows such a sharp contrast with the rest of the section as to exclude it from Subunit ID. The gamma-ray count increases suddenly, and the conductivity and sonic velocity decrease. This unit is a pumice breccia. The high gamma-ray response was expected, and it indicates the presence of minerals with a high concentration of uranium, thorium, or potassium.

Conclusions

The use of high-resolution logging tools permitted a better definition of the lithologic boundaries at Site 703. The upper

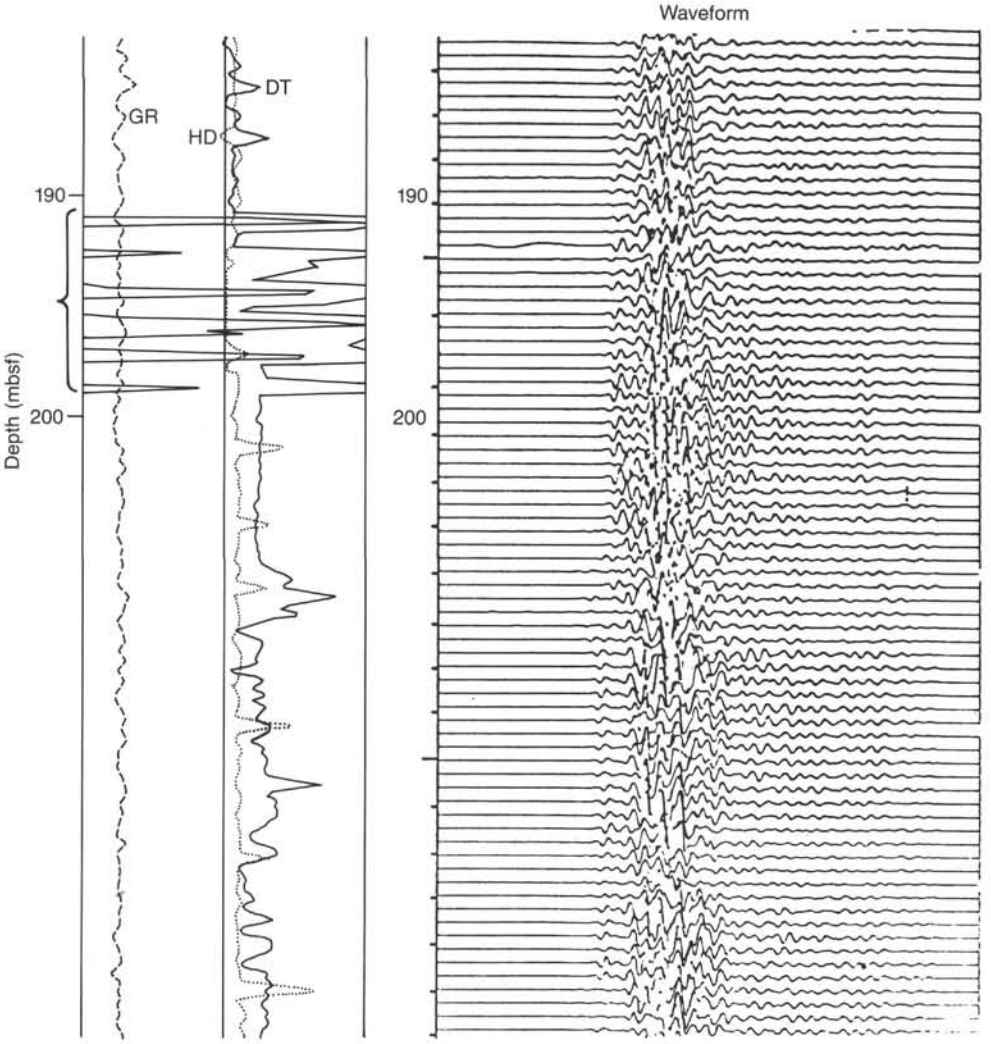

Figure 23. Record of full-waveform log from the BHC sonic tool. This figure also shows the *P*-wave arrivals in the left-hand column (interval transit times), picked by an automatic computer subroutine. Some cycle skipping can occur if the amplitude of the first arrival is low, as is the case between 190 and 200 mbsf. The full-waveform display at right is shifted upward by 11 m with respect to the transit time picks presented on the left (the data were recorded this way). Total count gamma-ray log = GR; caliper hole diameter = HD; interval transit time = DT.

part of the logs (Subunits IB and IC) shows an overall decrease in porosity. This trend is expected and resulted from compaction and possibly recrystallization. Better data analysis (e.g., the determination of lithology from log responses alone) requires more than one suite of logs.

SUMMARY AND CONCLUSIONS

Summary

Site 703 is located at 47°03.042′S, 07°53.679′W, in water depth of 1796.1 m, on the Meteor Rise, an aseismic ridge extending southeast from the Agulhas Fracture Zone. The Islas Orcadas Rise (Site 702 location) and the Meteor Rise are both bounded by lower Eocene oceanic crust generated at the Mid-Atlantic Ridge. These rises are thought to have formed at the locus of a new spreading center following a Late Cretaceous westward shift of the ridge axis in the Agulhas Basin (LaBrecque and Hayes, 1979). The major objectives of drilling at this site were to determine the nature, age, and subsidence history of the rise and to investigate the influence of the shallow Paleogene Meteor Rise, Islas Orcadas Rise, and the adjacent fracture zones on oceanic communication between the high and temperate latitudes of the South Atlantic. A review of other Site 703 objectives is given in the "Background and Objectives" section of this chapter.

Site 703 was meant to recover the older portion of the Meteor Rise sedimentary record, which would be obtainable, without a reentry hole, only where the sediment sequence thins onto basement highs. Site 704, a companion site to Site 703, was occupied nearby at a younger and thicker upper Paleogene to Neogene sequence.

The crestal area of the southern part of Meteor Rise has a rugged relief with an irregular distribution of sediments as infill of topographic lows and a complex pattern of drifts, particularly on the lee side of basement ridges and seamounts. The sediments are characterized by well-defined acoustic stratification throughout, with the upper 0–200 ms (two-way traveltime) highly reflective. The maximum total thickness may locally reach 1 s. The rapidly varying relief, lack of sufficient navigational control (transit satellite only), and severe weather conditions made

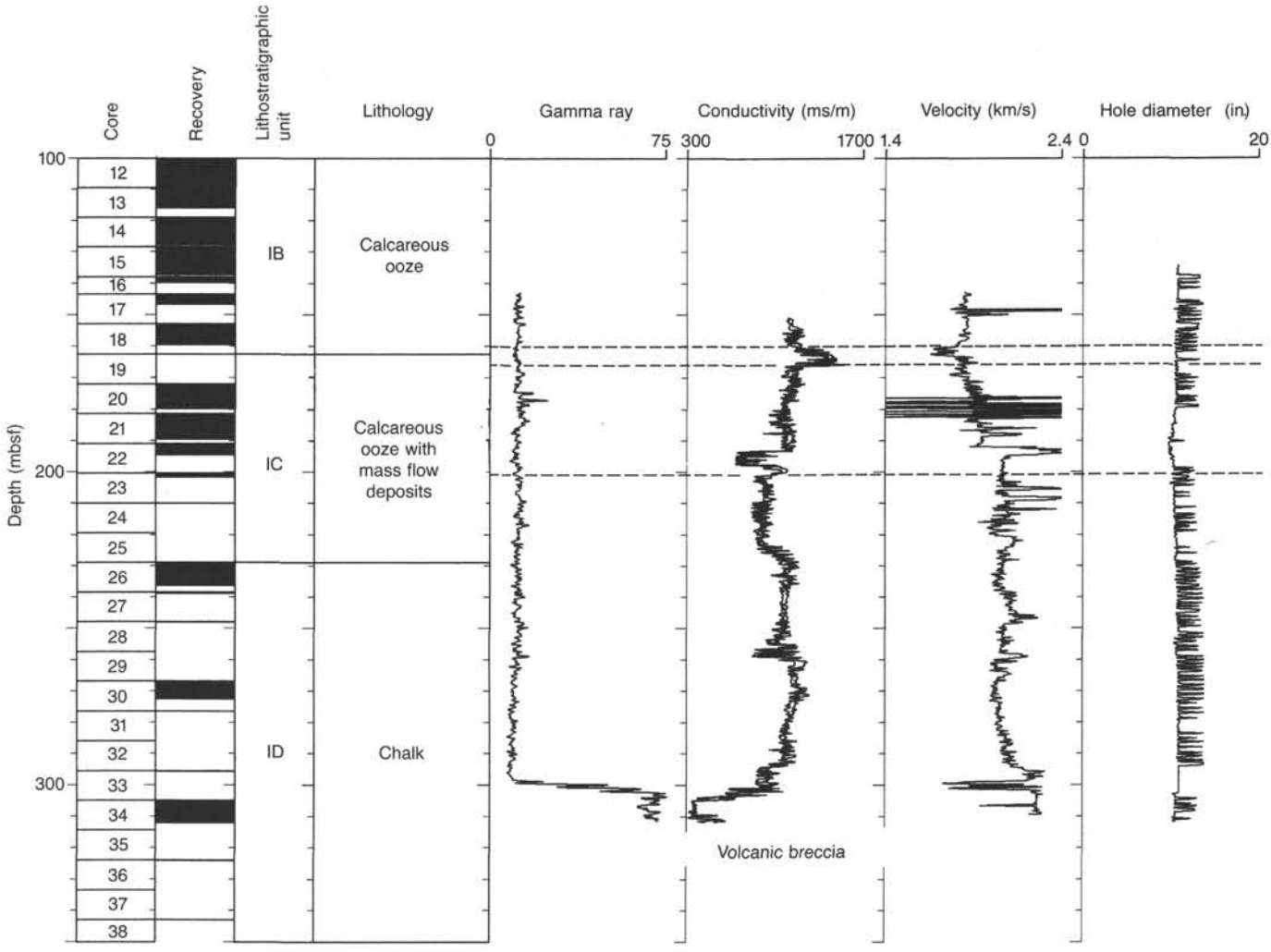

Figure 24. Logs taken while lowering the tool are not routinely made because of the lower log quality. However, this log is presented here for correlation purposes because of the lack of other runs.

attempts to reach optimum site locations very difficult. Site 703 is 2 km from the foot of a 15° slope of a seamount with an elevation 500 m higher than the site.

Site 703 consists of a single hole of 15 cores obtained with the APC to 137.9 mbsf (97.5% recovery) and 26 cores obtained with the XCB system to 377.4 mbsf total depth (24.2% recovery), with a total recovery of 51%. Additional tests of the Navidrill coring system were conducted, but no sediments were obtained. The hole was terminated when further basement penetration could not be obtained with the Navidrill or XCB systems. The hole was logged with a single run using the Schlumberger sonic, dual induction, natural gamma-ray, and caliper tools. Drilling was hampered by heavy seas, with 12 hr waiting on weather (maximum roll 15° and maximum pitch 10°).

The stratigraphic section at Site 703 consists of calcareous ooze and chalk with intervals of mass flow deposits of clay, ooze, sand/gravel, and volcanic breccia in the lower part. The predominantly calcareous ooze and chalk sequence was divided into four subunits on the basis of slight changes and diagenesis (Figs. 5 and 26). Logging results were utilized to infer subunit boundaries below 190 mbsf where recovery was poor.

Subunit IA (0–71.4 mbsf) is a siliceous- and foraminifer-bearing nannofossil ooze of latest early Oligocene to Quaternary age. The calcium carbonate content of the subunit averages over 90% with the remaining component primarily siliceous. Upper Pliocene–Quaternary sediments in the upper ~14.4 m of the subunit are a volcanic ash- and diatom-bearing foraminifer ooze with ice-rafted detritus.

Subunit IB (71.4–162.4 mbsf) is an uppermost middle Eocene to uppermost lower Oligocene foraminifer-bearing nannofossil ooze and micrite- and foraminifer-bearing nannofossil ooze. Carbonate content averages close to 90%, except between 102 and 108 mbsf (79%–82%), where there is also a pronounced physical-properties change.

Subunit IC (162.4–228.9 mbsf) is characterized by poor recovery (Fig. 26), and therefore, variations in lithology and the base of the subunit are partially inferred from the logging results. This middle Eocene subunit is composed mostly of nannofossil ooze (88%–95% carbonate), with some chert nodules and interbedded mass flow deposits of clay, foraminifer ooze, and gravelly sand.

Subunit ID (228.9–365.9 mbsf) is a middle Eocene chalk with mass flow deposits. Recovery was very poor in this interval owing to the presence of chert nodules and gravelly volcanic sand. A volcanic breccia recovered in Core 114-703A-34X consists of pumice and volcanic shards cemented by a zeolitic(?) matrix. The base of the subunit is a dolomite-bearing volcanic ash calcareous sand of questionable early Eocene age.

Unit II (364.0–365.65) consists of slightly to moderately altered porphyritic basalt or basaltic andesite and felsic pyroclas-

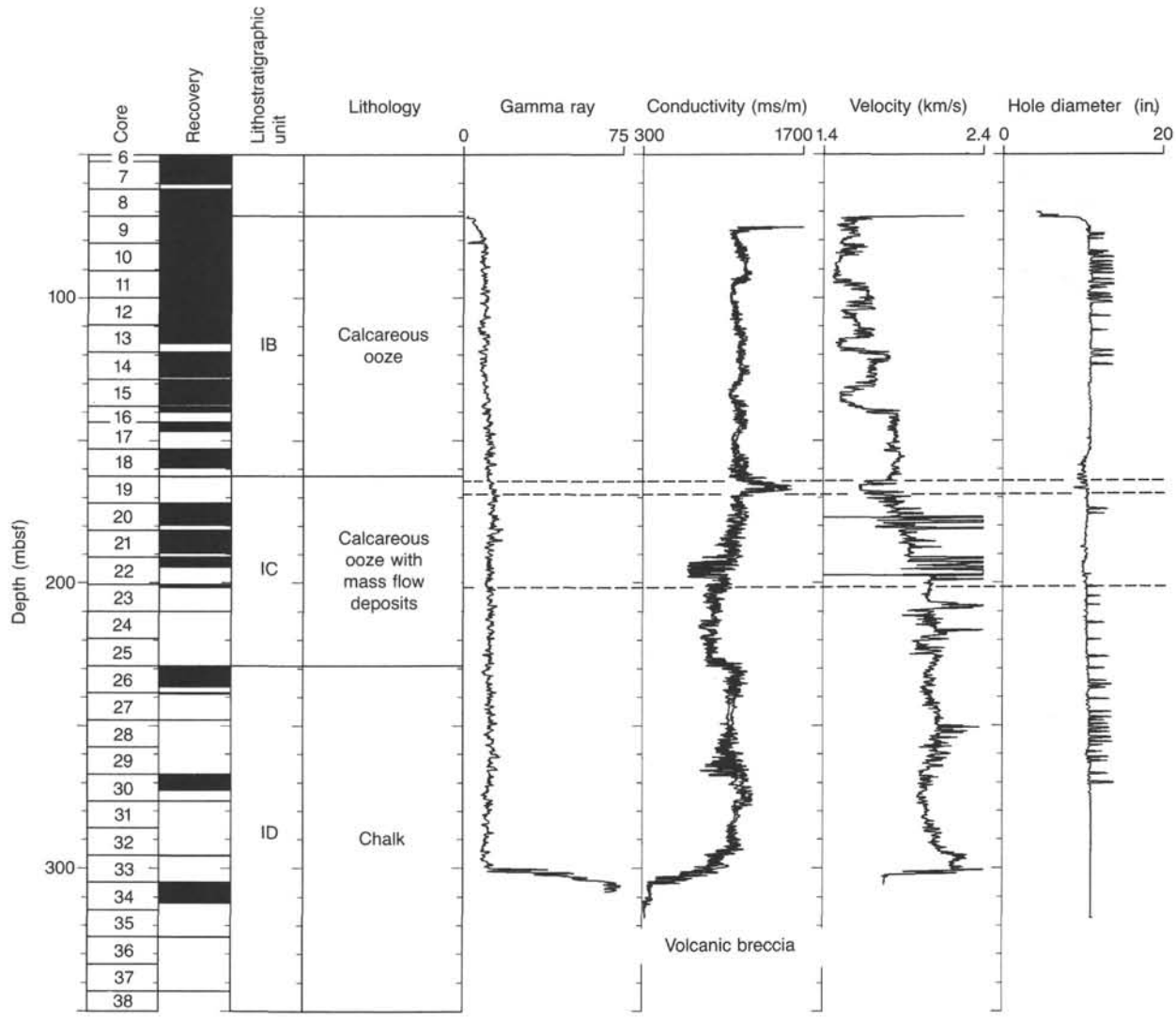

Figure 25. Main, uphole log run in Hole 703A, consisting of total count gamma-ray log (GR), resistivity logs SFLU, ILM, and ILD presented as conductivity, compressional-wave velocity from compensated sonic log, and caliper (hole diameter) log. Lithostratigraphic units are based on log responses and core descriptions (see "Lithostratigraphy" section).

tic rocks, which are fragmented and partially mixed with the base of the overlying unit. The basalt contains plagioclase phenocrysts and pyroxene microphenocrysts. The groundmass contains opaques, plagioclase, and altered pyroxene.

Conclusions

Site 703 is between the Subtropical Convergence and the ACZ (Lutjeharms and Valentine, 1984). The site received predominantly calcareous biogenic sedimentation since the early Eocene, with significant biosiliceous input in the late Eocene, the late Oligocene–early Miocene, and particularly, in the Pliocene and Quaternary.

Microfossil assemblages record a similar history of surface-water cooling during the middle Eocene to late Oligocene, as was reported in previous Leg 114 site chapters of this volume. There is some indication that surface waters remained warmer at this more easterly site during the late Paleogene, although the general middle Eocene to late Oligocene cooling trend is the same.

Paleodepth estimates based on benthic foraminifer assemblages suggest a depth >600 mbsl during the Eocene and >1000 mbsl during the Oligocene. Redeposited shallow-water microfossils occur throughout the Eocene and Oligocene section. In the Eocene, these include neritic diatoms, which suggests that the adjacent, 500-m-shallower seamount was at sea level at this time.

Because of the elevated position of this site, it is uncertain if the earliest middle Eocene age of basement is indicative of the age of the Meteor Rise proper. Redeposited microfossils are no older than Eocene, unlike for the Islas Orcadas Rise where Upper Cretaceous microfossils are reworked in the upper Paleocene.

REFERENCES

Barron, J. A., 1985. Miocene to Holocene planktic diatoms. *In* Bolli, H. M., Saunders, J. B., and Perch-Nielsen, K. (Eds.), *Plankton Stratigraphy*: Cambridge (Cambridge Univ. Press), 763–810.

Barron, J. A., Nigrini, C. A., Pujos, A., Saito, T., Thayer, F., Thomas, E., and Weinreich, N., 1985. Synthesis of biostratigraphy, central Equatorial Pacific, Deep Sea Drilling Project Leg 85: refinement of Oligocene to Quaternary biochronology—*In* Mayer, L., Thayer, F., et al., *Init Repts. DSDP*, 85: Washington (U.S. Govt. Printing Office), 905–934.

Berggren, W. A., Kent, D. V., and Flynn, J. J., 1985. Paleogene geochronology and chronostratigraphy. *In* Snelling, N. J. (Ed.), *The Chronology of the Geological Record*: Geol. Soc. London Mem., 10:141–195.

Burckle, L. H., Clarke, D. B., and Shackleton, N. J., 1978. Isochronous last-abundant-appearance datum (LAAD) of the diatom *Hemidiscus karstenii* in the sub-Antarctic. *Geology*, 6:243–246.

Chen, P. H., 1975. Antarctic radiolaria. *In* Hayes, D. E., Frakes, L. A., et al., *Init. Repts. DSDP*, 28: Washington (U.S. Govt. Printing Office), 437–513.

Ciesielski, P. F., 1975. Biostratigraphy and paleoecology of Neogene and Oligocene silicoflagellates from cores recovered during antarctic Leg 28. *In* Hayes, D. E., Frakes, L. A., et al., *Init. Repts. DSDP*, 28: Washington (U.S. Govt. Printing Office), 625–691.

_____, 1983. The Neogene and Quaternary diatom biostratigraphy of subantarctic sediments, Deep Sea drilling Leg 71. *In* Ludwig, W. J., Krasheninnikov, V. A., et al., *Init. Repts. DSDP*, 71: Washington (U.S. Govt. Printing Office), 635–666.

_____, 1985. Middle Miocene to Quaternary diatom biostratigraphy of Deep Sea Drilling Project Site 594, Chatham Rise, Southwest Pacific. *In* Kennett, J. P., von der Borch, D. D., et al., *Init. Repts. DSDP*, 90: Washington (U.S. Govt. Printing Office), 1249–1256.

Fenner, J. M., 1984. Eocene-Oligocene planktic diatom stratigraphy in the low latitudes and high southern latitudes. *Micropaleontology*, 30:319–342.

Gombos, A. M., Jr., 1983. Survey of diatoms in the upper Oligocene and lower Miocene in Holes 515B and 516F. *In* Barker, P. F., Carlson, R. L., Johnson, D. A., et al., *Init. Repts. DSDP*, 72: Washington (U.S. Govt. Printing Office), 793–804.

Gombos, A. M., Jr., and Ciesielski, P. F., 1983. Late Eocene to early Miocene diatoms from the southwest Atlantic. *In* Ludwig, W. J., Krasheninnikov, V. A., et al., *Init. Repts. DSDP*, 71: Washington (U.S. Govt. Printing Office), 583–634.

Hays, J. D., and Opdyke, N. D., 1967. Antarctic radiolaria, magnetic reversals, and climatic change. *Science*, 158:1001–1011.

Hays, J. D., and Shackleton, N. J., 1976. Globally synchronous extinction of the radiolarian *Stylatractus universus*. *Geology*, 4:649–652.

Jenkins, D. G., 1985. Southern mid-latitude Paleocene to Holocene planktic foraminifera. *In* Bolli, H. M., Saunders, J. B., and Perch-Nielsen, K. (Eds.), *Plankton Stratigraphy*: Cambridge (Cambridge Univ. Press), 263–282.

Kent, D. V., and Gradstein, F., 1985. A Cretaceous and Jurassic geochronology. *Geol. Soc. Am. Bull.*, 96:1419–1427.

LaBrecque, J. L. (Ed.), 1986. *South Atlantic Ocean and Adjacent Continental Margin Atlas 13*: Ocean Margin Drilling Program Reg. Atlas Ser., 13.

LaBrecque, J. L., and Hayes, D. E., 1979. Seafloor spreading history of the Agulhas Basin. *Earth Planet. Sci. Lett.*, 45:411–428.

Lutjeharms, J.R.E., and Valentine, H. R., 1984. Southern Ocean thermal fronts south of Africa. *Deep Sea Res.*, 31:1461–1475.

Martini, E., 1971. Standard Tertiary and Quaternary calcareous nannoplankton zonation. In Farinacci, A. (Ed.), *Proc. Planktonic Conf. II Rome 1970*: Rome (Technoscienze), 2:739–785.

Martini, E., and Müller, C., 1986. Current Tertiary and Quaternary calcareous nannoplankton stratigraphy and correlations. *Newsl. Stratigr.*, 16:99–112.

McCollum, D. W., 1975. Diatom stratigraphy of the Southern Ocean. *In* Hayes, D. E., Frakes, L. A., et al., *Init. Repts. DSDP*, 28: Washington (U.S. Govt. Printing Office), 515–572.

McGowran, B., 1986. Cainozoic oceanic and climatic events: the Indo-Pacific foraminiferal biostratigraphic records. *Palaeogr. Palaeoclimatol. Palaeoecol.*, 44:247–265.

Morkhoven, F.P.C.M. van, Berggren, W. A., and Edwards, A. S., 1986. Cenozoic cosmopolitan deep-water benthic foraminifera. *Cent. Rech. Explor. Prod. Elf Aquitaine Mem.*, 11.

Perch-Nielsen, K., 1985. Cenozoic calcareous nannofossils. *In* Bolli, H. M., Saunders, J. B., and Perch-Nielsen, K. (Eds.), *Plankton Stratigraphy*: Cambridge (Cambridge Univ. Press), 427–554.

Shaw, C. A., and Ciesielski, P. F., 1983. Silicoflagellate biostratigraphy of middle Eocene to Holocene Subantarctic sediments recovered by Deep Sea Drilling Project Leg 71. *In* Ludwig, W. J., Krasheninnikov, V. A., et al., *Init. Repts. DSDP*, 71: Washington (U.S. Govt. Printing Office), 687–737.

Weaver, F. M., 1983. Cenozoic radiolarians from the southwest Atlantic, Falkland Plateau region, Deep Sea Drilling Project Leg 71. *In* Ludwig, W. J., Krasheninnikov, V. A., et al., *Init. Repts. DSDP*, 71: Washington (U.S. Govt. Printing Office), 667–686.

Weaver, F. M., and Gombos, A. M., Jr., 1981. Southern high latitude diatom biostratigraphy. *In* Warme, J. E., Douglas, R. G., and Winterer, E. L. (Eds.), *The Deep Sea Drilling Project: A Decade of Progress*: Spec. Publ. Soc. Econ. Paleontol. Mineral., 32:445–470.

Wise, S. W., 1983. Mesozoic and Cenozoic calcareous nannofossils recovered by Deep Sea Drilling Project Leg 71 in the Falkland Plateau Region, southwest Atlantic Ocean. *In* Ludwig, W. J., Krasheninnikov, V. A., et al., *Init. Repts. DSDP*, 71: Washington (U.S. Govt. Printing Office), 481–550.

Ms 114A-110

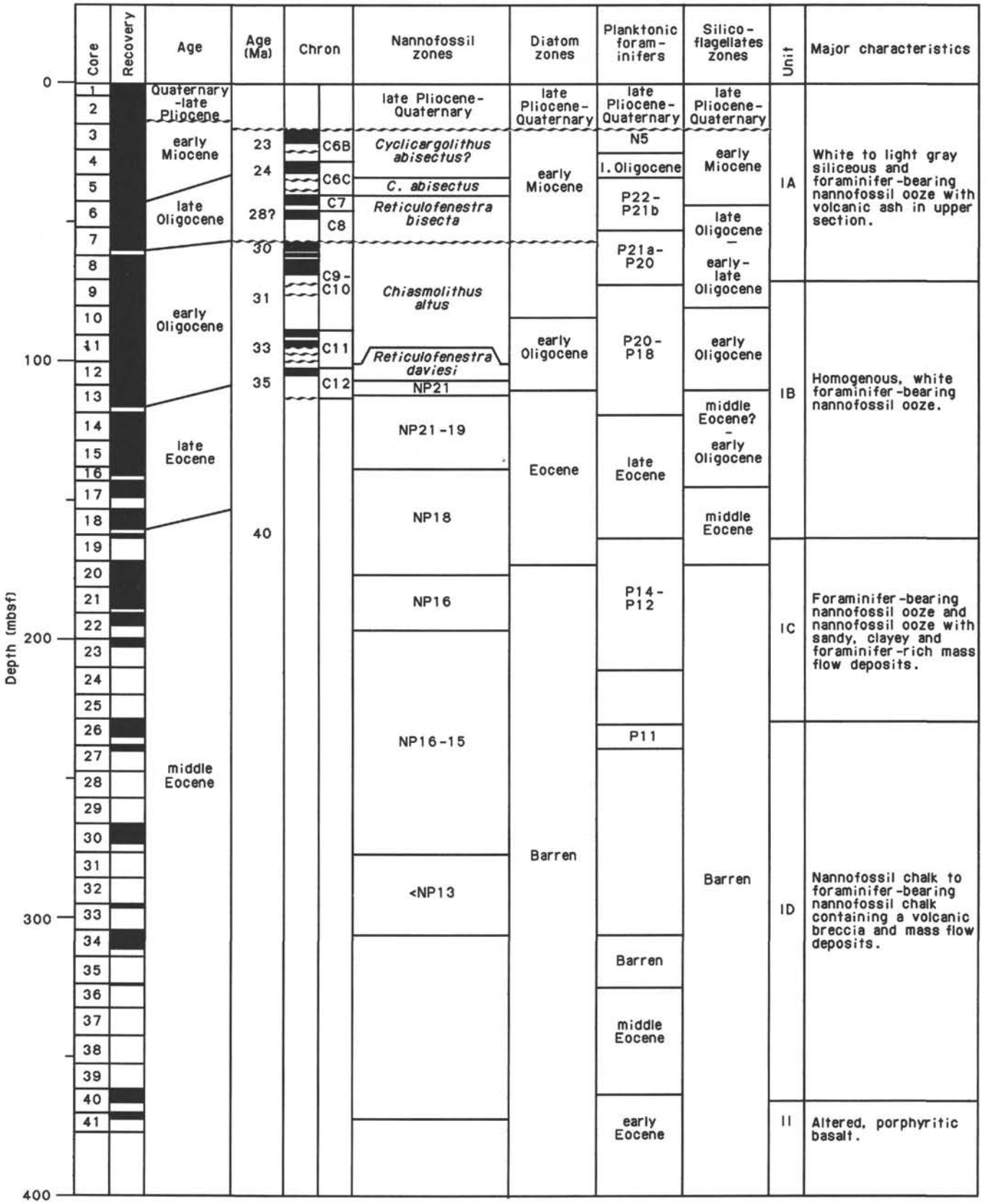

Figure 26. Summary of Site 703 data, including: depth, core recovery, age assignments, paleomagnetic polarity, biostratigraphic ages (nannofossils, diatoms, planktonic foraminifers, and silicoflagellates), lithostratigraphic units and subunits and a description of their major characteristics, relative abundance variations of smear slide constituents (volcanic ash = *, chert = solid triangles; turbidite = T), percent carbonate, and porosity.

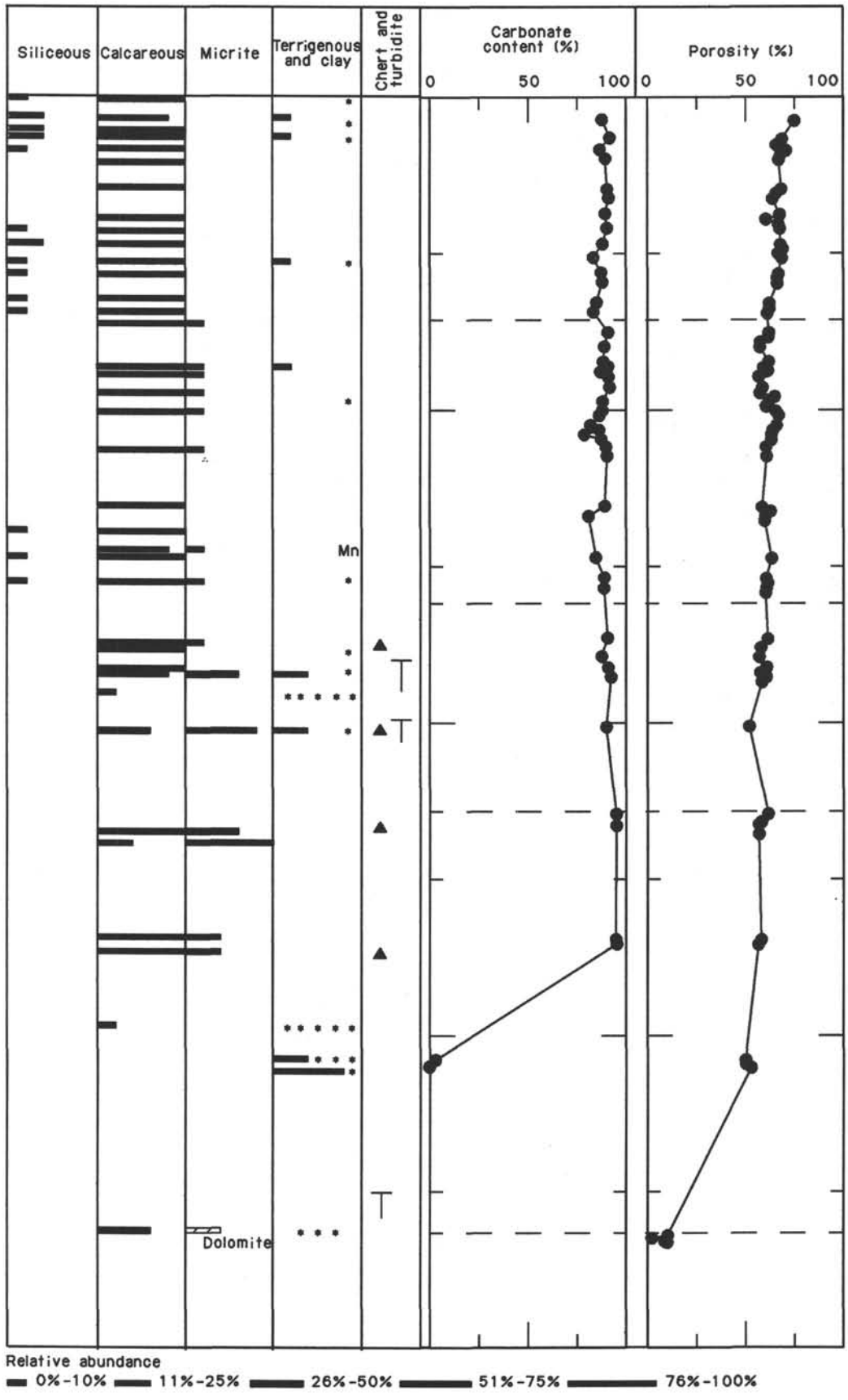

Figure 26 (continued).

Summary log for Hole 703A.

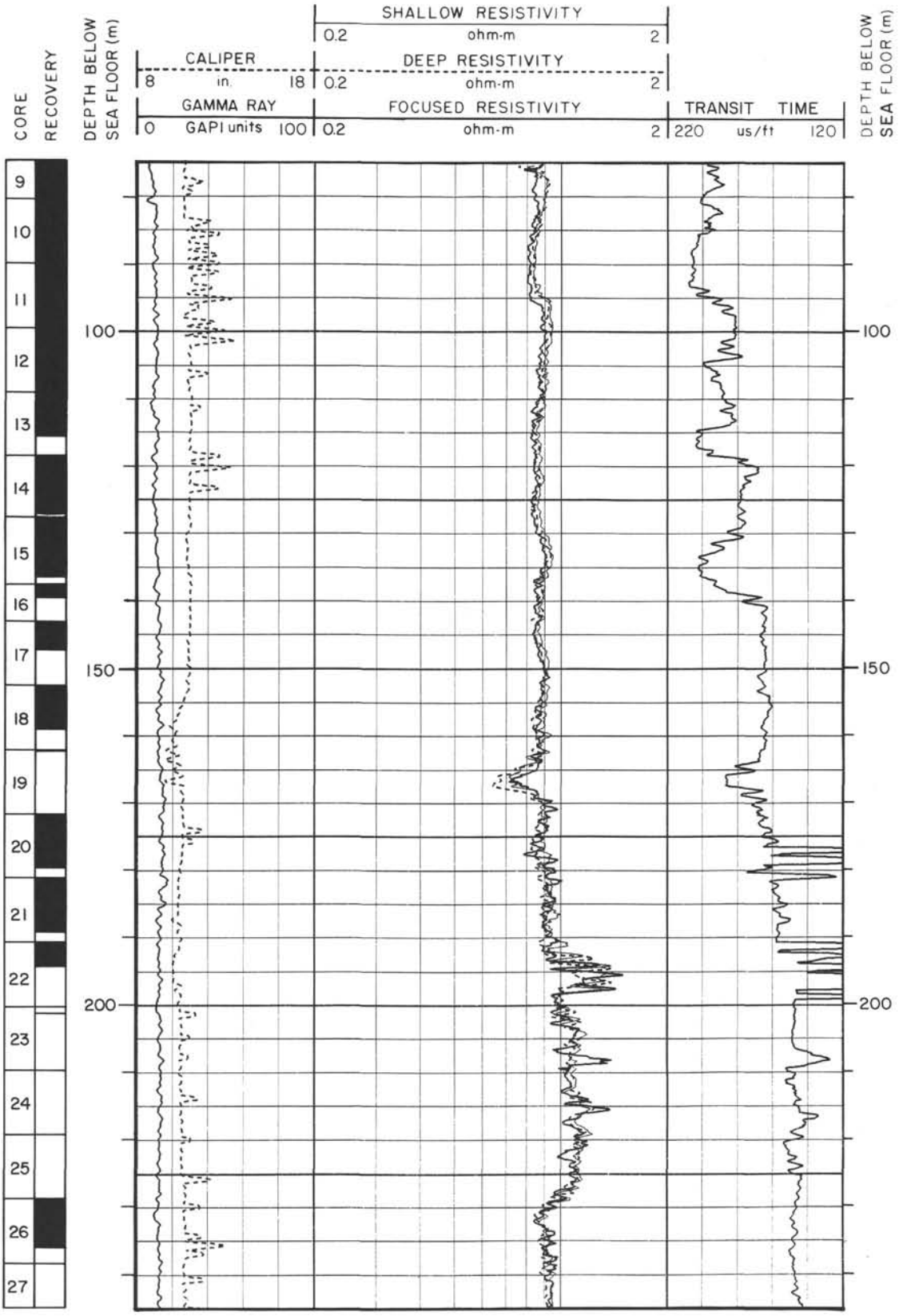

Summary log for Hole 703A (continued).

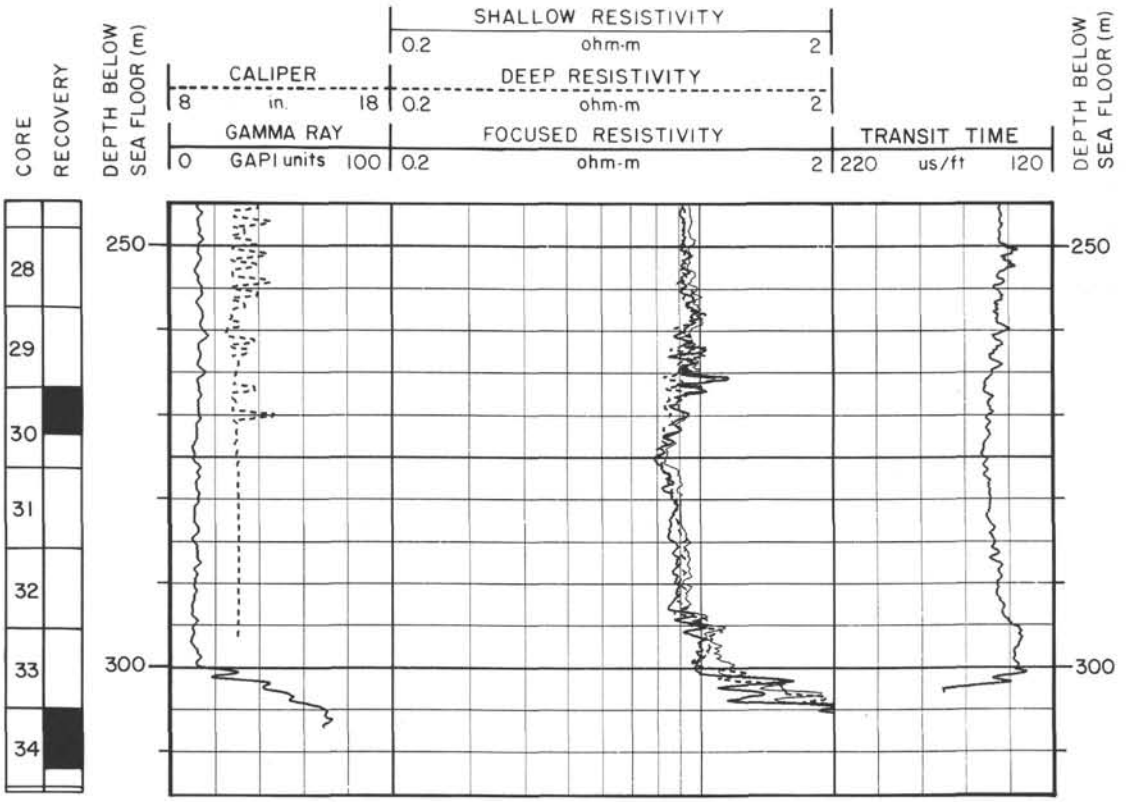

SITE 703 HOLE A CORE 1H CORED INTERVAL 1796.1-1801.0 mbsl; 0.0-4.9 mbsf

TIME-ROCK UNIT	BIOSTRAT. ZONE/ FOSSIL CHARACTER: FORAMINIFERS	NANNOFOSSILS	RADIOLARIANS	DIATOMS	SILICOFLAGELLATES	PALEOMAGNETICS	PHYS. PROPERTIES	CHEMISTRY	SECTION	METERS	GRAPHIC LITHOLOGY	DRILLING DISTURB.	SED. STRUCTURES	SAMPLES
QUATERNARY	PLEISTOCENE - HOLOCENE	UPPER PLIOCENE - LOWER PLEISTOCENE	*Stylatractus universus* (QUATERNARY)	*Coscinodiscus elliptipora-Actinocyclus ingens*	*Coscinodiscus lentiginosus* unzoned				1	0.5				*
										1.0				*
									2					
									3					
									4					
									CC					

LITHOLOGIC DESCRIPTION

VOLCANIC ASH-BEARING, NANNOFOSSIL-BEARING FORAMINIFER OOZE

Drilling disturbance: Soupy to very disturbed sediments throughout core.

Major lithology: White (10YR 8/1) volcanic ash-bearing, nannofossil-bearing foraminifer ooze.

Minor lithology:
a. Volcanic ash-bearing, diatom-bearing foraminifer ooze, light gray (10YR 7/1), Section 1, 82-99 cm.
b. Gravel, Section 3, 28-39 cm.

Volcanic ash and gravel may be downhole contaminants.

SMEAR SLIDE SUMMARY (%):

COMPOSITION:	1, 70 D	1, 98 D
Volcanic glass	10	10
Foraminifers	69	71
Nannofossils	15	5
Diatoms	1	10
Radiolarians	5	2
Sponge spicules	—	1
Silicoflagellates	—	1

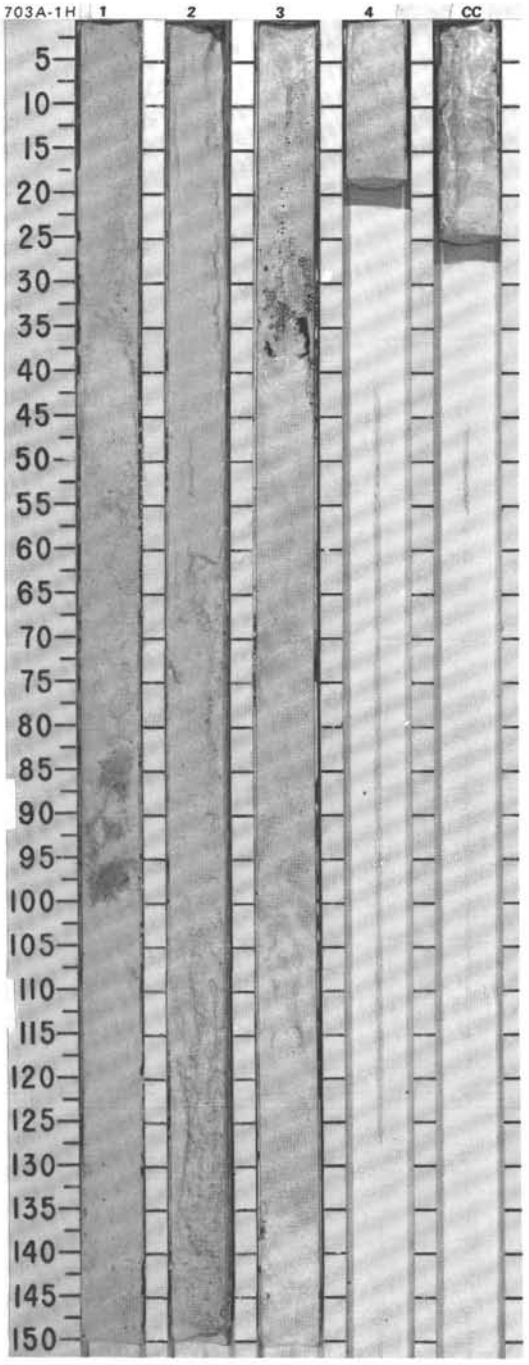

SITE 703 HOLE A CORE 2H CORED INTERVAL 1801.0 - 1810.5 mbsl; 4.9-14.4 mbsf

TIME-ROCK UNIT	BIOSTRAT. ZONE/ FOSSIL CHARACTER: FORAMINIFERS	NANNOFOSSILS	RADIOLARIANS	DIATOMS	SILICOFLAGELLATES	PALEOMAGNETICS	PHYS. PROPERTIES	CHEMISTRY	SECTION	METERS	GRAPHIC LITHOLOGY	DRILLING DISTURB.	SED. STRUCTURES	SAMPLES
UPPER PLIOCENE	QUATERNARY	UPPER PLIOCENE - LOWER PLEISTOCENE	UPPER PLIOCENE - LOWER PLEISTOCENE	*N. interfrigidaria-C. vulnificus* *Helotholus vema* (LOWER PLIOCENE)	*Coscinodiscus vulnificus*	*Coscinodiscus elliptipora-Actinocyclus ingens*	*Distephanus boliviensis* (LOWER PLIOCENE)	ϕ=68.54 Pg=2.81	ϕ=74.70 Pg=2.81		1, 2, 3, 4, 5, 6, 7, CC	0.5, 1.0			IW

LITHOLOGIC DESCRIPTION

VOLCANIC ASH-BEARING, NANNOFOSSIL-BEARING FORAMINIFER OOZE, and NANNOFOSSIL-BEARING FORAMINIFER OOZE

Drilling disturbance: Soupy to highly disturbed throughout the core.

Major lithology:

a. White (10YR 8/1) volcanic ash-bearing, nannofossil-bearing foraminifer ooze from the top of the core downhole to Section 5, 45 cm.
b. White (10YR 8/1) nannofossil-bearing foraminifer ooze from Section 5, 45 cm, to the bottom of the core.

Minor lithology: Two intervals of light gray (10YR 7/1), volcanic ash-bearing, diatom-bearing foraminifer ooze in Section 1, 65-98 cm, and Section 2, 22-40 cm.

SMEAR SLIDE SUMMARY (%):

	1, 83 D	2, 90 D	5, 20 D	6, 30 M
COMPOSITION:				
COMPOSITION:				
Clay	3	—	2	—
Volcanic glass	10	1	3	Tr
Foraminifers	74	87	84	10
Nannofossils	—	Tr	—	90
Diatoms	12	8	10	Tr
Radiolarians	1	2	1	Tr
Sponge spicules	—	—	—	Tr
Silicoflagellates	—	2	Tr	Tr

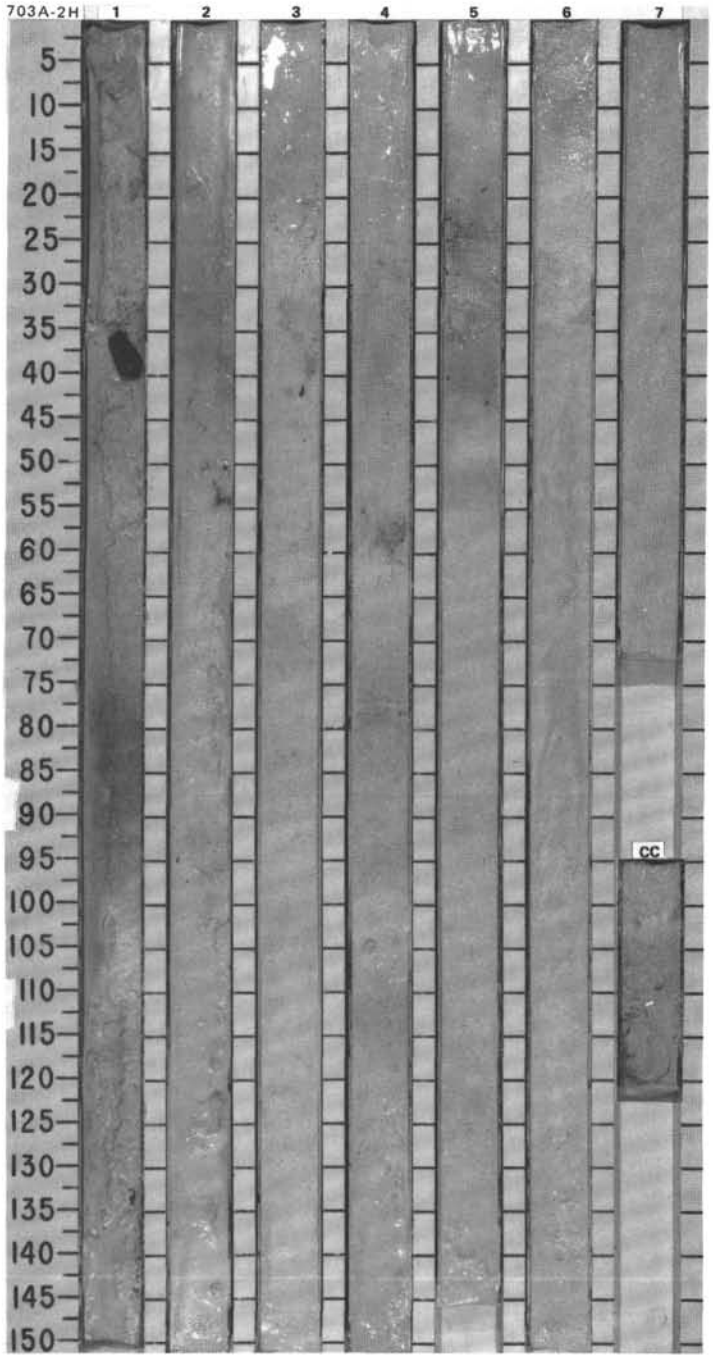

SITE 703 HOLE A CORE 3H CORED INTERVAL 1810.5-1820.0 mbsl; 14.4-23.9 mbsf

TIME-ROCK UNIT	BIOSTRAT. ZONE/ FOSSIL CHARACTER: FORAMINIFERS	NANNOFOSSILS	RADIOLARIANS	DIATOMS	SILICOFLAGELLATES	PALEOMAGNETICS	PHYS. PROPERTIES	CHEMISTRY	SECTION	METERS	GRAPHIC LITHOLOGY	DRILLING DISTURB.	SED. STRUCTURES	SAMPLES
LOWER MIOCENE	LOWER MIOCENE N5 - N6	C. abisectus Zone?	not examined	Cyrtocapsella tetrapera (LOWER MIOCENE)	Coscinodiscus rhombicus	not examined	Corbisema triacanthantha (LOWER-MIDDLE MIOCENE)		ϕ=66.88 ρ_g=67.82 ϕ=67.82 ρ_g=3.03 ϕ=70.46 ρ_g=2.94 ϕ=65.67 ρ_g=2.84	1 2 3 4 5 6 CC	0.5 1.0			* *	IW OG

LITHOLOGIC DESCRIPTION

FORAMINIFER-NANNOFOSSIL OOZE and FORAMINIFER-BEARING NANNOFOSSIL OOZE

Drilling disturbance: Soupy sediments in Section 1, 0-50 cm.

Major lithology: White (no color code) foraminifer-nannofossil ooze from the top of the core down to the base of Section 5, grading into pinkish white (7.5YR 8/2) in Section 6 and CC.

Minor lithology:
a. Gravelly foraminifer-nannofossil ooze at the top of the core with a large quartzite pebble (of ice-rafted detritus origin?). This occurrence could, however, be due to downhole contamination.
b. Volcanic ash horizon, Section 1, 75-76 cm.

SMEAR SLIDE SUMMARY (%):

	2, 70 D	6, 100 D
COMPOSITION:		
Foraminifers	30	20
Nannofossils	70	80
Diatoms	Tr	—
Radiolarians	Tr	Tr
Sponge spicules	Tr	—
Silicoflagellates	3	—

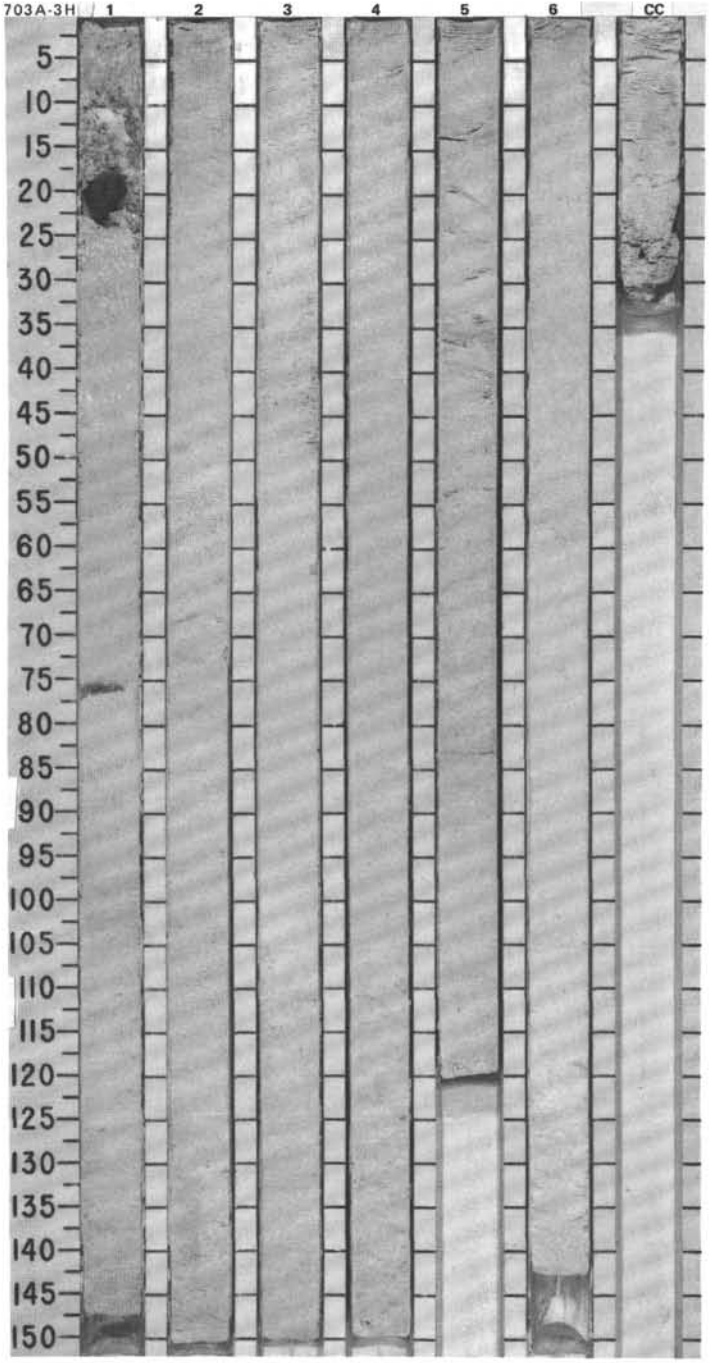

SITE 703 HOLE A CORE 4H CORED INTERVAL 1820.0-1829.5 mbsl; 23.9-33.4 mbsf

TIME-ROCK UNIT	BIOSTRAT. ZONE/ FOSSIL CHARACTER: FORAMINIFERS	NANNOFOSSILS	RADIOLARIANS	DIATOMS	SILICOFLAGELLATES	PALEOMAGNETICS	PHYS. PROPERTIES	CHEMISTRY	SECTION	METERS	GRAPHIC LITHOLOGY	DRILLING DISTURB.	SED. STRUCTURES	SAMPLES	LITHOLOGIC DESCRIPTION
LOWER MIOCENE	LOWER MIOCENE N4 - N5	*C. abisectus* Zone ?	*Cyrtocapsella tetrapera* (LOWER MIOCENE)	not examined	*Naviculopsis vegularis* (LOWER MIOCENE)		ϕ=63.78 ρ_g=2.85 ϕ=65.71 ρ_g=2.79 ϕ=68.25 ρ_g=2.69		1 2 3 4 5 6 7 CC	0.5 1.0				*	FORAMINIFER-BEARING NANNOFOSSIL OOZE Drilling disturbance: First two sections are quite badly disturbed. Gravel admixture at the top of Sections 1 and 2 could be due to ice-rafted detritus or downhole contamination. Major lithology: Featureless foraminifer-bearing ooze, white (no color code) grading into pinkish white (7.5YR 8/2) in Section 3. SMEAR SLIDE SUMMARY (%): 3, 70 D COMPOSITION: Volcanic glass Tr Foraminifers 20 Nannofossils 80 Radiolarians Tr

Rocella gelida ←

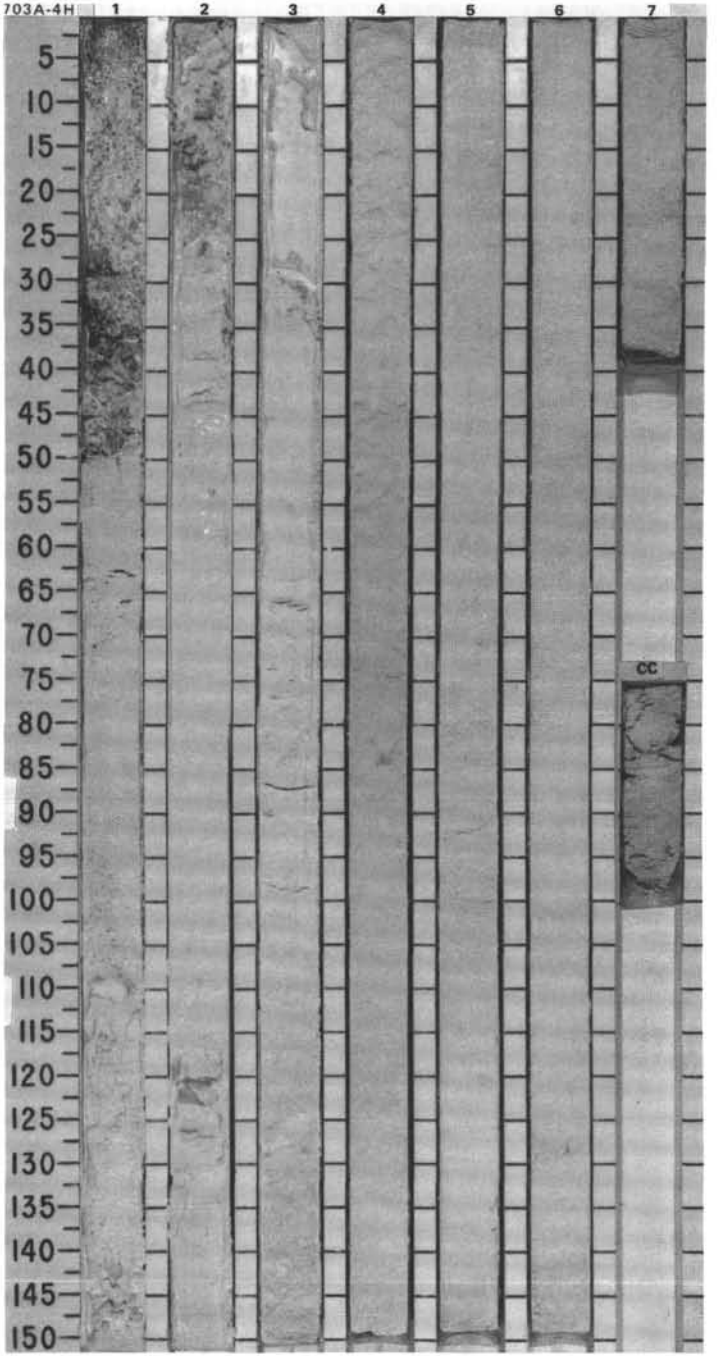

SITE 703 HOLE A CORE 5H CORED INTERVAL 1829.5-1839.0 mbsl; 33.4-42.9 mbsf

TIME-ROCK UNIT	BIOSTRAT. ZONE/ FOSSIL CHARACTER												
	FORAMINIFERS	NANNOFOSSILS	RADIOLARIANS	DIATOMS	SILICO-FLAGELLATES	PALEOMAGNETICS	PHYS. PROPERTIES	CHEMISTRY	SECTION	METERS	GRAPHIC LITHOLOGY	DRILLING DISTURB.	SED. STRUCTURES	SAMPLES
UPPER OLIGOCENE LOWER MIOCENE														
UPPER OLIGOCENE - LOWER MIOCENE	P22 - N4													
R. bisecta Zone	*C. abisectus* Zone													
	unzoned (UPPER OLIGOCENE)													
			Rocella gelida											
					Naviculopsis biapiculata (UPPER OLIGOCENE)									
						ϕ=67.55 ρ_g=2.96	ϕ=66.76 ρ_g=2.70	ϕ=60.40 ρ_g=2.86	ϕ=67.57 ρ_g=3.07						
UPPER OLIGOCENE									1	0.5				
										1.0				
									2					
											VOID			
									3					*
									4					
									5					
									6					
									7					
									CC					

LITHOLOGIC DESCRIPTION

FORAMINIFER-BEARING NANNOFOSSIL OOZE

Drilling disturbance: Generally minor, but Section 2 quite badly disturbed. Gravel at the top of the core is probably downhole contamination.

Major lithology: Pinkish white (7.5YR 8/2) foraminifer-bearing nannofossil ooze. No distinguishing features.

Minor lithology: Finely disseminated volcanic ash in the foraminifer-bearing nannofossil ooze, Section 3, 137-148 cm.

SMEAR SLIDE SUMMARY (%):

	3, 70 D
COMPOSITION:	
Foraminifers	15
Nannofossils	85
Radiolarians	Tr

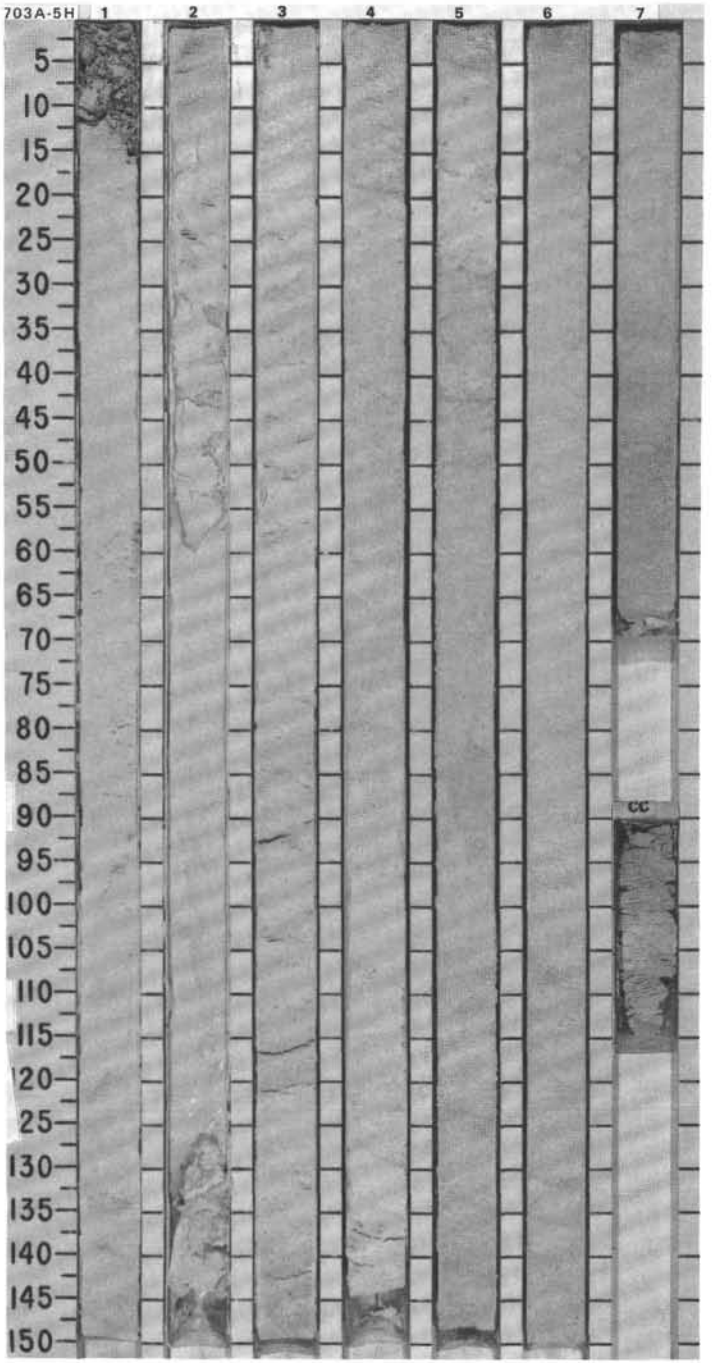

SITE 703 HOLE A CORE 6H CORED INTERVAL 1839.0-1848.5 mbsl; 42.9-52.4 mbsf

TIME-ROCK UNIT	BIOSTRAT. ZONE/ FOSSIL CHARACTER: FORAMINIFERS	NANNOFOSSILS	RADIOLARIANS	DIATOMS	PALEOMAGNETICS	PHYS. PROPERTIES	CHEMISTRY	SECTION	METERS	GRAPHIC LITHOLOGY	DRILLING DISTURB.	SED. STRUCTURES	SAMPLES	LITHOLOGIC DESCRIPTION
UPPER OLIGOCENE	UPPER OLIGOCENE - LOWER MIOCENE P22 - N4	*R. bisecta* Zone	*Rocella gelida*	*Corbisema archangelskiana* (UPPER OLIGOCENE)		ϕ=68.56 ρ_g=2.81 ϕ=66.80 ρ_g=2.75 ϕ=68.94 ρ_g=2.83 ϕ=67.87 ρ_g=2.78		1 2 3 4 5 6 7 CC	0.5 1.0		O		* * IW OG	SILICEOUS-BEARING, FORAMINIFER-BEARING NANNOFOSSIL OOZE Drilling disturbance: Soupy gravel/sediment mixture at the top of the core. Major lithology: Pinkish white (5YR 8/2) siliceous-bearing, foraminifer-bearing nannofossil ooze. Minor mottling due to bioturbation. SMEAR SLIDE SUMMARY (%): 1, 80 D / 3, 40 D COMPOSITION: Volcanic glass Tr Tr Foraminifers 15 10 Nannofossils 75 75 Diatoms 8 12 Radiolarians 2 2 Sponge spicules — Tr Micrite Tr Tr

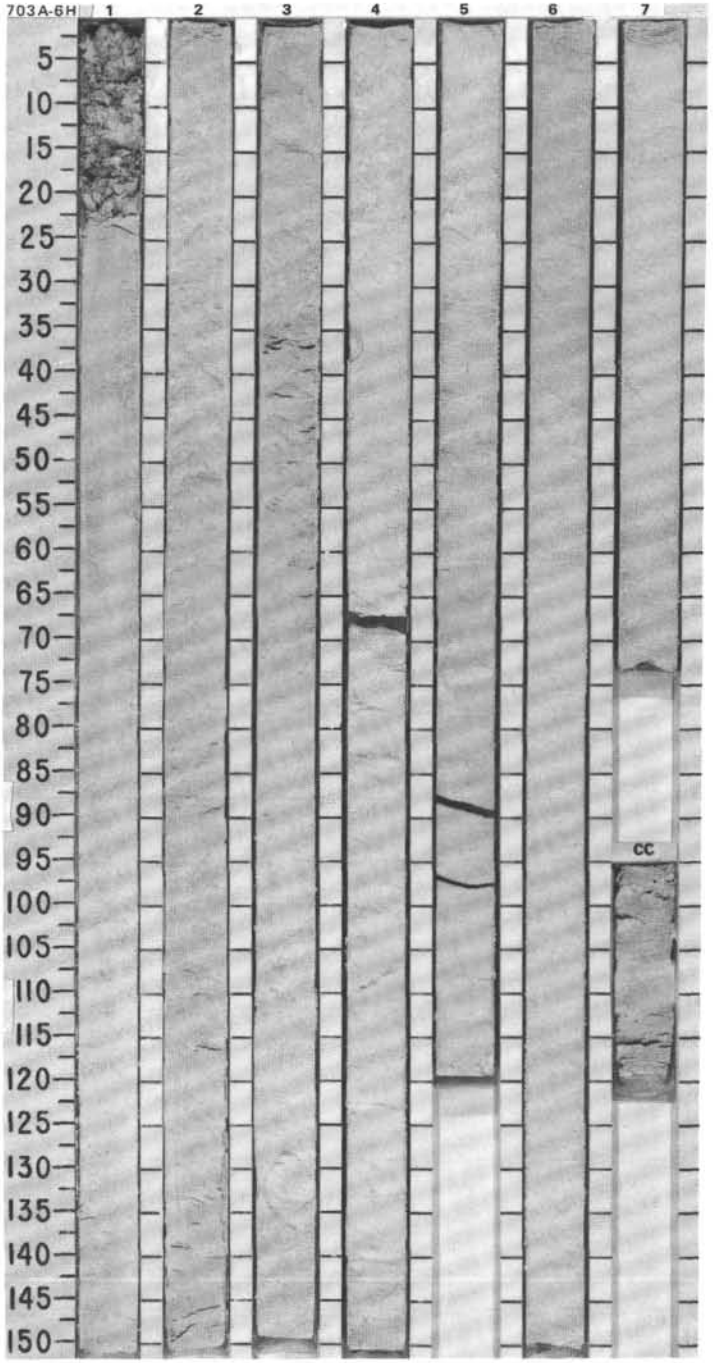

SITE 703 HOLE A CORE 7H CORED INTERVAL 1848.5-1858.0 mbsl; 52.4-61.9 mbsf

TIME-ROCK UNIT: UPPER OLIGOCENE
BIOSTRAT. ZONE/FOSSIL CHARACTER: FORAMINIFERS: LOWER OLIGOCENE; P20 - P21a; UPPER OLIGOCENE; P21b
NANNOFOSSILS: *C. altus* Zone; not examined; *R. bisecta* Zone
RADIOLARIANS: *Rocella vigilans*; unzoned
DIATOMS: not examined; *Rocella gelida*
SILICOFLAGELLATES: *Corbisema archangelskiana* (UPPER OLIGOCENE)
PALEOMAGNETICS
PHYS. PROPERTIES: ϕ=66.20 ρ_g=2.83; ϕ=66.04 ρ_g=2.80; ϕ=66.75 ρ_g=2.80
CHEMISTRY
SECTION: 1, 2, 3, 4, 5, 6, CC
METERS: 0.5, 1.0
GRAPHIC LITHOLOGY
DRILLING DISTURB.
SED. STRUCTURES
SAMPLES

LITHOLOGIC DESCRIPTION

SILICEOUS-BEARING FORAMINIFER-NANNOFOSSIL OOZE

Drilling disturbance: Gravel slurry at the top of the core is probably downhole contamination. Sediment is biscuited throughout core.

Major lithology: Siliceous-bearing foraminifer-nannofossil ooze, pinkish white (5YR 8/2). Minor mottling due to bioturbation in Section 3, 90-150 cm. Fine lithic fragments are sparsely disseminated throughout the core.

Minor lithology: Siliceous, foraminifer-bearing nannofossil ooze, pinkish white (5YR 8/2).

SMEAR SLIDE SUMMARY (%):

	1, 80 D	2, 50 D
COMPOSITION:		
Clay	5	—
Volcanic glass	1	1
Foraminifers	26	15
Nannofossils	57	76
Diatoms	9	15
Radiolarians	2	2
Sponge spicules	—	Tr
Micrite	—	1

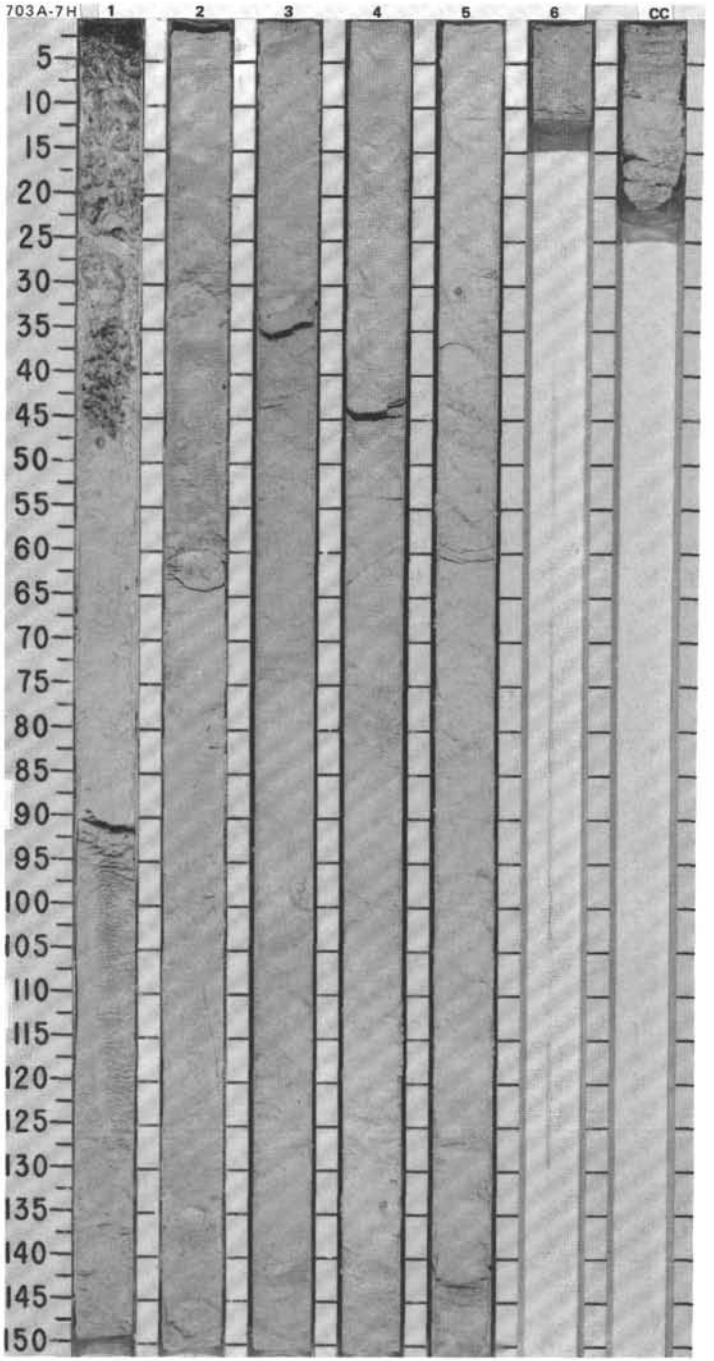

SITE 703 HOLE A CORE 8H CORED INTERVAL 1858.0-1867.5 mbsl; 61.9-71.4 mbsf

TIME-ROCK UNIT: LOWER OLIGOCENE

BIOSTRAT. ZONE/FOSSIL CHARACTER:
- FORAMINIFERS: LOWER OLIGOCENE P20 - P21a
- NANNOFOSSILS: *C. altus* Zone
- RADIOLARIANS: unzoned
- DIATOMS: OLIGOCENE
- SILICOFLAGELLATES: undetermined

PALEOMAGNETICS

PHYS. PROPERTIES: ϕ=61.16 ρ_g=2.75 ϕ=62.23 ρ_g=2.82 ϕ=62.16 ρ_g=2.67

CHEMISTRY

SECTION: 1, 2, 3, 4, 5, 6, CC

METERS: 0.5, 1.0

GRAPHIC LITHOLOGY

DRILLING DISTURB.

SED. STRUCTURES

SAMPLES

LITHOLOGIC DESCRIPTION

FORAMINIFER-BEARING NANNOFOSSIL OOZE

Drilling disturbance: 5 cm of gravel slurry (downhole contamination) at the top of the core.

Major lithology: Foraminifer-bearing nannofossil ooze, light gray (5YR 7/1) grading into white (5Y 8/1), in Section 3, 110 cm. Small (0.5 mm) lithic fragments sparsely disseminated throughout core. Faint mottling due to bioturbation in Section 1, 3-5.

Minor lithology: Siliceous-bearing, foraminifer-bearing nannofossil ooze, pinkish white (5YR 8/2) at the top of the core (Section 1, 5-60 cm).

SMEAR SLIDE SUMMARY (%):

	2, 80 D	6, 60 D
COMPOSITION:		
Volcanic glass	2	1
Accessory minerals	Tr	—
Foraminifers	12	15
Nannofossils	80	77
Diatoms	5	5
Sponge spicules	—	Tr
Micrite	1	2

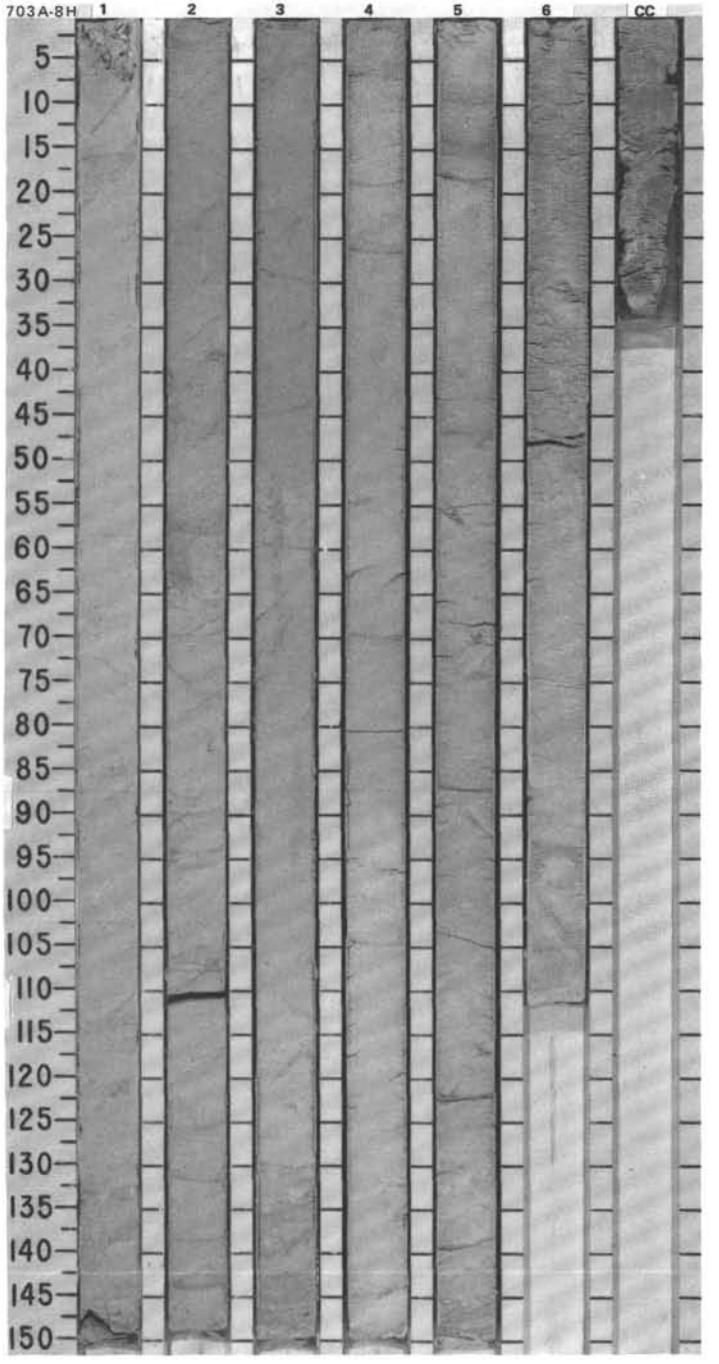

SITE 703 HOLE A CORE 9H CORED INTERVAL 1867.5-1877.0 mbsl; 71.4-80.9 mbsf

TIME-ROCK UNIT	BIOSTRAT. ZONE/ FOSSIL CHARACTER: FORAMINIFERS	NANNOFOSSILS	RADIOLARIANS	DIATOMS	SILICOFLAGELLATES	PALEOMAGNETICS	PHYS. PROPERTIES	CHEMISTRY	SECTION	METERS	GRAPHIC LITHOLOGY	DRILLING DISTURB.	SED. STRUCTURES	SAMPLES
LOWER OLIGOCENE	LOWER OLIGOCENE	P20 - P21a	*C. altus* Zone	unzoned	OLIGOCENE	undetermined	ϕ=57.46 ρ_g=2.71 ϕ=57.61 ρ_g=2.74 ϕ=61.76 ρ_g=2.77 ϕ=62.08 ρ_g=2.90		1 2 3 4 5 6 7 CC	0.5 1.0	VOID			IW OG *

LITHOLOGIC DESCRIPTION

FORAMINIFER-BEARING NANNOFOSSIL OOZE

Drilling disturbance: Soupy sediments in Section 1.

Major lithology: White (no color code) foraminifer-bearing nannofossil ooze. Mn discoloration (spots) sparsely distributed throughout core. Some Mn-colored banding in Section 6 at 47, 59, 86, and 103 cm.

SMEAR SLIDE SUMMARY (%):

	2, 70 D
COMPOSITION:	
Foraminifers	20
Nannofossils	71
Diatoms	Tr
Radiolarians	Tr
Sponge spicules	1
Micrite	8

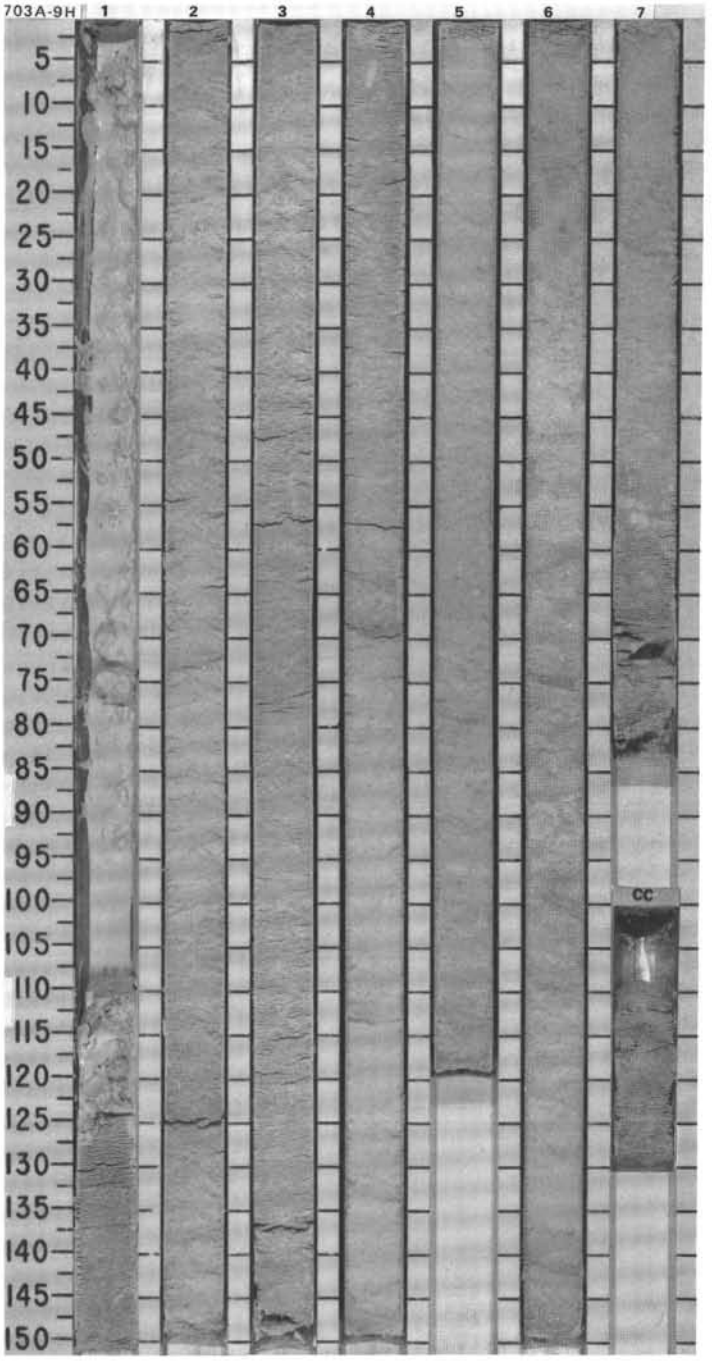

SITE 703 HOLE A CORE 10H CORED INTERVAL 1877.0-1886.5 mbsl; 80.9-90.4 mbsf

TIME-ROCK UNIT	BIOSTRAT. ZONE/ FOSSIL CHARACTER: FORAMINIFERS	NANNOFOSSILS	RADIOLARIANS	DIATOMS	SILICO-FLAGELLATES	PALEOMAGNETICS	PHYS. PROPERTIES	CHEMISTRY	SECTION	METERS	GRAPHIC LITHOLOGY	DRILLING DISTURB.	SED. STRUCTURES	SAMPLES
LOWER OLIGOCENE	LOWER OLIGOCENE P18 - P20	*C. altus* Zone	unzoned	LOWER OLIGOCENE	undetermined		ϕ=56.92 ρ_g=2.79 ϕ=61.35 ρ_g=2.73 ϕ=59.34 ρ_g=2.66 ϕ=61.98 ρ_g=2.77		1	0.5				
										1.0				
									2					
									3					*
									4					
									5					*
									6					
									7					
									CC					

LITHOLOGIC DESCRIPTION

FORAMINIFER-BEARING NANNOFOSSIL OOZE

Drilling disturbance: First two sections badly disturbed with soupy sediments.

Major lithology: Foraminifer-bearing nannofossil ooze, white (no color code) with pale green (5Y 7/2) discoloration, in Section 5, 70–84 cm.

SMEAR SLIDE SUMMARY (%):

	3, 80 D	5, 75 D
COMPOSITION:		
Quartz	—	Tr
Clay	—	5
Volcanic glass	—	Tr
Foraminifers	10	10
Nannofossils	85	83
Micrite	5	2

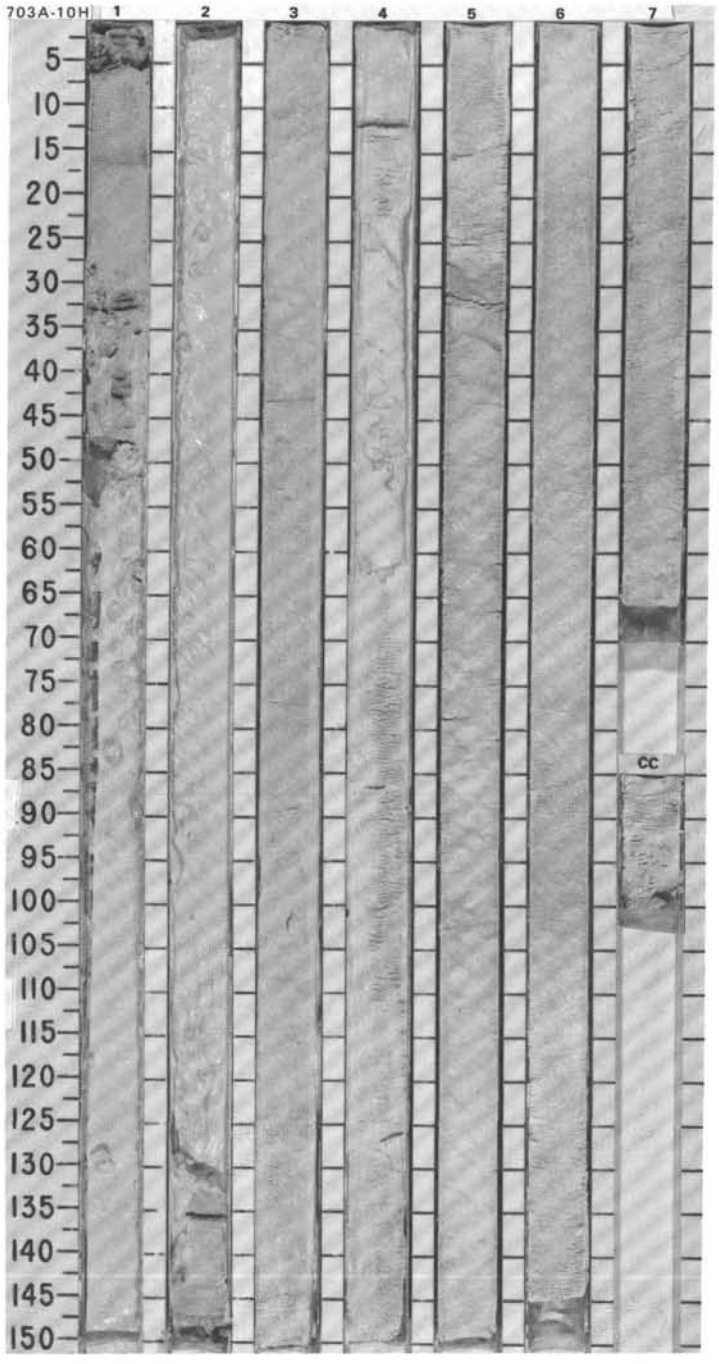

SITE 703 HOLE A CORE 11H CORED INTERVAL 1886.5-1896.0 mbsl; 90.4-99.9 mbsf

TIME-ROCK UNIT	FORAMINIFERS	NANNOFOSSILS	RADIOLARIANS	DIATOMS	SILICO-FLAGELLATES	PALEOMAGNETICS	PHYS. PROPERTIES	CHEMISTRY	SECTION	METERS	GRAPHIC LITHOLOGY	DRILLING DISTURB.	SED. STRUCTURES	SAMPLES
LOWER OLIGOCENE	LOWER OLIGOCENE P18 - P20	*C. altus* Zone	unzoned	LOWER OLIGOCENE	undetermined		ϕ=60.66 ρ_g=2.74 ϕ=62.03 ρ_g=2.75 ϕ=64.95 ρ_g=2.78 ϕ=57.50 ρ_g=2.71 ϕ=58.78 ρ_g=2.83		1 2 3 4 5 6 7 CC	0.5 1.0			* *	

LITHOLOGIC DESCRIPTION

NANNOFOSSIL OOZE

Drilling disturbance: Some gravel at the bottom of the CC may be downhole contamination.

Major lithology: White nannofossil ooze (no color code). Faint mottling due to bioturbation in Sections 4 and 5.

Minor lithology: Foraminifer-bearing nannofossil ooze, white (no color code), in Section 4.

SMEAR SLIDE SUMMARY (%):

	4, 63 M	1, 75 D
COMPOSITION:		
Volcanic glass	3	Tr
Foraminifers	12	7
Nannofossils	78	86
Radiolarians	Tr	2
Sponge spicules	Tr	—
Micrite	7	5

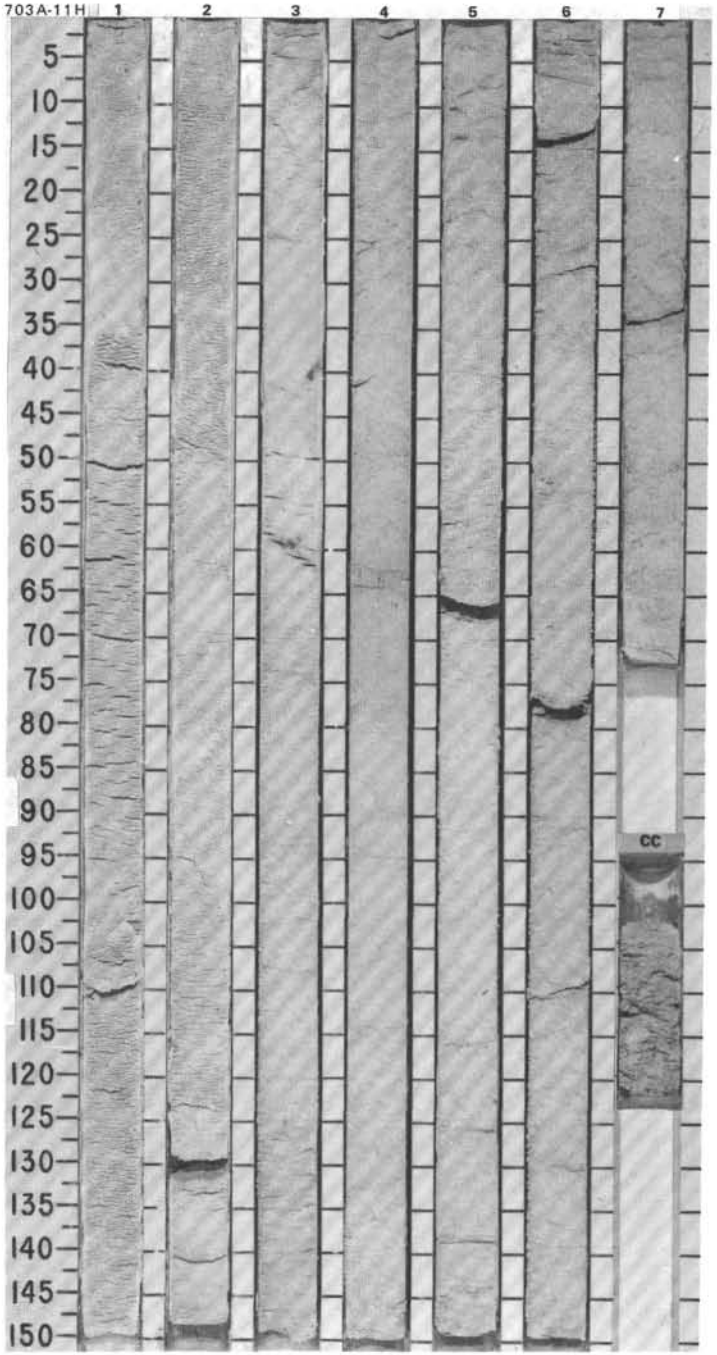

SITE 703 HOLE A CORE 12H CORED INTERVAL 1896.0-1905.5 mbsl; 99.9-109.4 mbsf

TIME-ROCK UNIT: LOWER OLIGOCENE

BIOSTRAT. ZONE/FOSSIL CHARACTER:
- FORAMINIFERS: LOWER OLIGOCENE — P18 - P20
- NANNOFOSSILS: not examined — *R. davisei* Zone — not examined
- RADIOLARIANS: unzoned
- DIATOMS: LOWER OLIGOCENE
- SILICOFLAGELLATES: undetermined

PALEOMAGNETICS

PHYS. PROPERTIES: ϕ=63.37 ρ_g=2.65 | ϕ=64.09 ρ_g=2.75 | ϕ=66.03 ρ_g=2.69 | ϕ=67.00 ρ_g=2.71 | ϕ=65.50 ρ_g=2.78

CHEMISTRY

SECTION: 1, 2, 3, 4, 5, 6, 7, CC

METERS: 0.5, 1.0

GRAPHIC LITHOLOGY: VOID, VOID

DRILLING DISTURB.

SED. STRUCTURES

SAMPLES: IW, OG

LITHOLOGIC DESCRIPTION

FORAMINIFER-BEARING NANNOFOSSIL OOZE

Drilling disturbance: Lower half of Section 2 and whole of Section 3 badly disturbed by partly soupy sediments.

Major lithology: White (no color code) foraminifer-bearing nannofossil ooze. Faint bioturbation at the top of Section 1.

SMEAR SLIDE SUMMARY (%):

	1, 75 D
COMPOSITION:	
Foraminifers	10
Nannofossils	82
Diatoms	Tr
Micrite	8

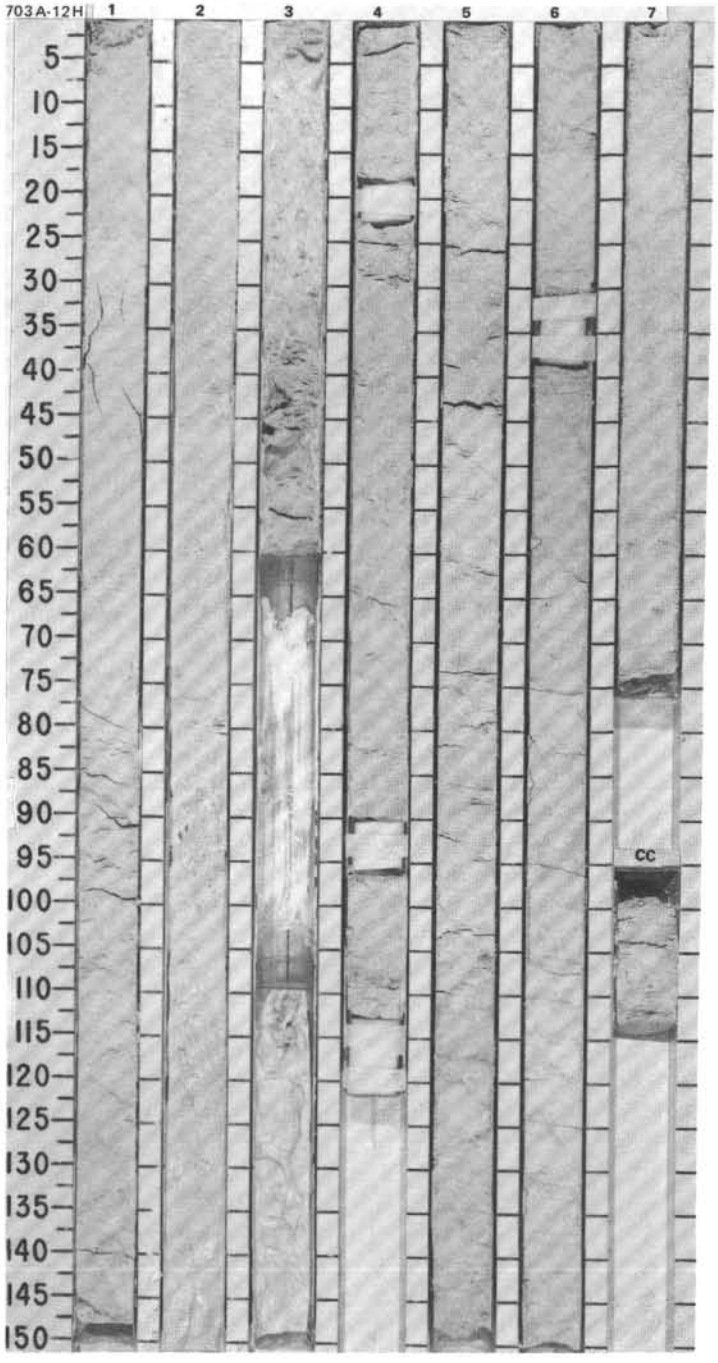

SITE 703 HOLE A CORE 13H CORED INTERVAL 1905.5-1915.0 mbsl; 109.4-118.9 mbsf

TIME-ROCK UNIT: ↑ UPPER EOCENE / LOWER OLIGOCENE

BIOSTRAT. ZONE/FOSSIL CHARACTER: FORAMINIFERS: LOWER OLIGOCENE P18 - P20; NANNOFOSSILS: not examined; RADIOLARIANS: unzoned; DIATOMS: EOCENE; SILICOFLAGELLATES: (LOWER OLIGOCENE - MIDDLE EOCENE)

PALEOMAGNETICS: *Mesocena occidentalis-Mesocena apiculata* (subzone)

PHYS. PROPERTIES: ϕ=61.03 ρ_g=2.69; ϕ=60.70 ρ_g=2.72

CHEMISTRY

SECTION: 1, 2, 3, 4, CC

METERS: 0.5, 1.0

GRAPHIC LITHOLOGY: VOID

DRILLING DISTURB.: *

SED. STRUCTURES

SAMPLES

LITHOLOGIC DESCRIPTION

FORAMINIFER-BEARING NANNOFOSSIL OOZE

Drilling disturbance: Slight biscuiting in the first section.

Major lithology: White (no color code) foraminifer-bearing nannofossil ooze. No distinguishing features.

SMEAR SLIDE SUMMARY (%):

	4, 70 D
COMPOSITION:	
Clay	Tr
Volcanic glass	Tr
Foraminifers	10
Nannofossils	83
Diatoms	Tr
Radiolarians	Tr
Sponge spicules	Tr
Micrite	7

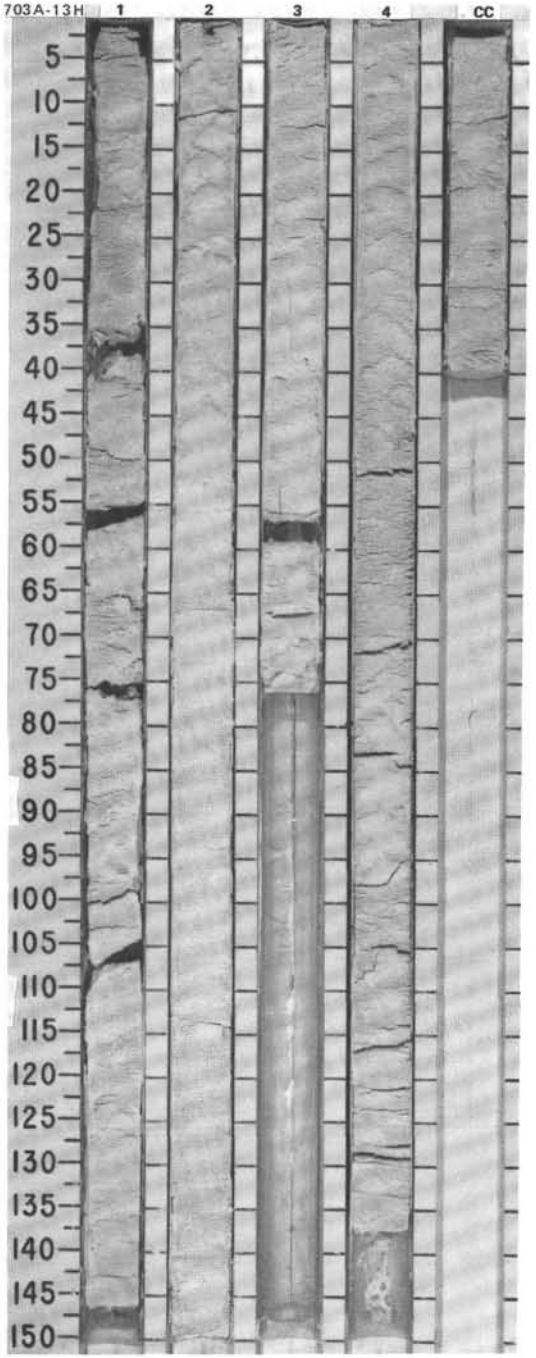

SITE 703 HOLE A CORE 14H CORED INTERVAL 1915.0-1924.5 mbsl; 118.9-128.4 mbsf

TIME-ROCK UNIT	BIOSTRAT. ZONE/ FOSSIL CHARACTER: FORAMINIFERS	NANNOFOSSILS	RADIOLARIANS	DIATOMS	SILICO-FLAGELLATES	PALEOMAGNETICS	PHYS. PROPERTIES	CHEMISTRY	SECTION	METERS	GRAPHIC LITHOLOGY	DRILLING DISTURB.	SED. STRUCTURES	SAMPLES	LITHOLOGIC DESCRIPTION
UPPER EOCENE	UPPER EOCENE	NP 19-21	unzoned		*Mesocena occidentalis-Mesocena apiculata* (subzone) (LOWER OLIGOCENE - MIDDLE EOCENE)				1	0.5					Foraminifer-bearing nannofossil ooze. Drilling disturbance: Whole core consists white soupy mixture of sediment and gravel. Major lithology: Nannofossil ooze (no color code) and gravel (probably downhole contamination).
										1.0					
									2						
									3						
									4						
									5						
									6						
									CC						

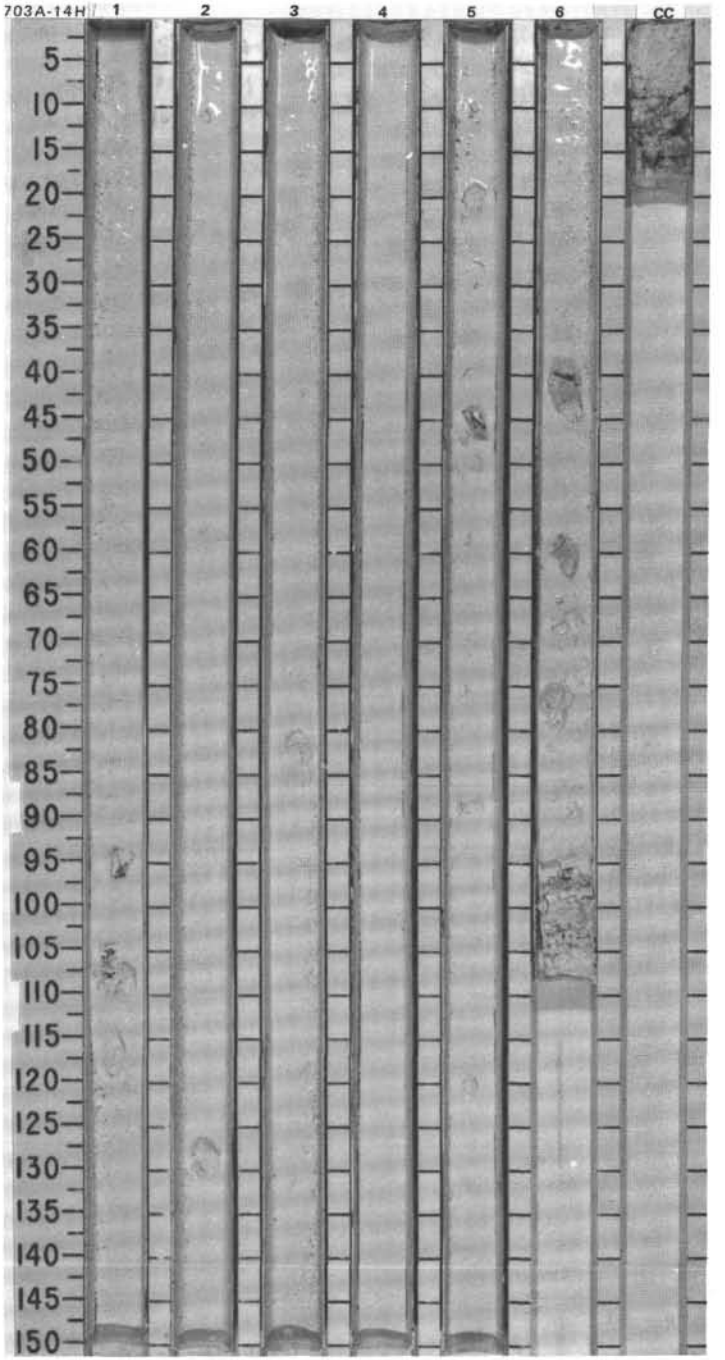

SITE 703 HOLE A CORE 15H CORED INTERVAL 1924.5-1934.0 mbsl; 128.4-137.9 mbsf

TIME-ROCK UNIT	BIOSTRAT. ZONE/ FOSSIL CHARACTER: FORAMINIFERS	NANNOFOSSILS	RADIOLARIANS	DIATOMS	SILICO-FLAGELLATES	PALEOMAGNETICS	PHYS. PROPERTIES	CHEMISTRY	SECTION	METERS	GRAPHIC LITHOLOGY	DRILLING DISTURB.	SED. STRUCTURES	SAMPLES
UPPER EOCENE	UPPER EOCENE	NP 19-21	unzoned	EOCENE	*Mesocena occidentalis-M. apiculata* (subzone)		ϕ=60.02 ρ_g=2.83 ϕ=60.44 ρ_g=2.96 ϕ=62.89 ρ_g=2.91 ϕ=58.70 ρ_g=2.71		1 2 3 4 5 6 CC	0.5 1.0				IW OC

LITHOLOGIC DESCRIPTION

MICRITE-BEARING, FORAMINIFER-BEARING NANNOFOSSIL OOZE

Drilling disturbance: Soupy sediments in Section 1.

Major lithology: White (no color code), micrite-bearing, foraminifer-bearing nannofossil ooze.

SMEAR SLIDE SUMMARY (%):

	2, 70 D
COMPOSITION:	
Foraminifers	10
Nannofossils	80
Diatoms	Tr
Radiolarians	Tr
Sponge spicules	Tr
Micrite	10

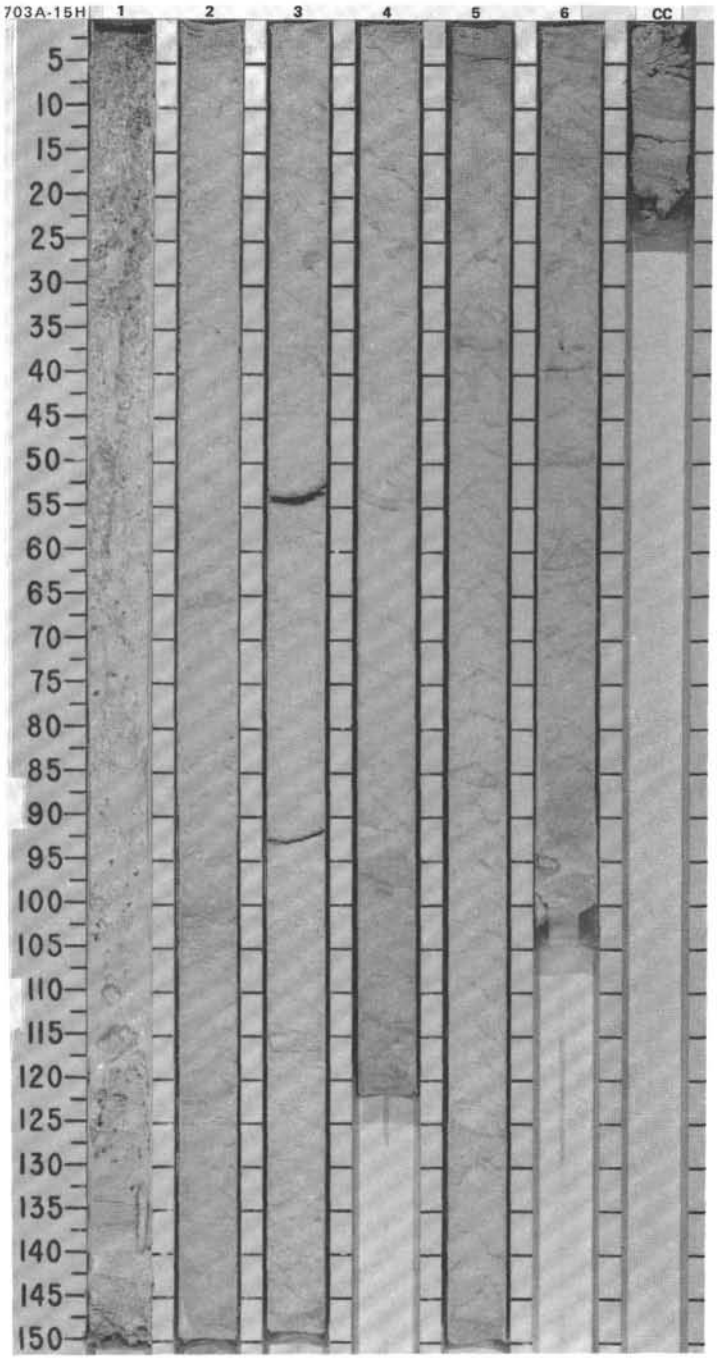

SITE 703 HOLE A CORE 16X CORED INTERVAL 1934.0-1939.5 mbsl; 137.9-143.4 mbsf

TIME-ROCK UNIT	BIOSTRAT. ZONE/ FOSSIL CHARACTER: FORAMINIFERS	NANNOFOSSILS	RADIOLARIANS	DIATOMS	SILICOFLAGELLATES	PALEOMAGNETICS	PHYS. PROPERTIES	CHEMISTRY	SECTION	METERS	GRAPHIC LITHOLOGY	DRILLING DISTURB.	SED. STRUCTURES	SAMPLES	LITHOLOGIC DESCRIPTION
UPPER EOCENE	UPPER EOCENE P15 - P16	NP 18	unzoned	EOCENE	*Mesocena occidentalis-Mesocena apiculata* (subzone) (LOWER OLIGOCENE - MIDDLE EOCENE)				1 CC	0.5 1.0				*	MICRITE-BEARING, FORAMINIFER-BEARING NANNOFOSSIL OOZE Drilling disturbance: Slight biscuiting of sediment. Major lithology: White (no color code), micrite-bearing, foraminifer-bearing nannofossil ooze with a pale green (5G 7/2) band in the CC, 25-27 cm. SMEAR SLIDE SUMMARY (%): 1, 80 D COMPOSITION: Foraminifers 20 Nannofossils 61 Diatoms 3 *Radiolarians* Tr Sponge spicules 1 Silicoflagellates Tr Micrite 15

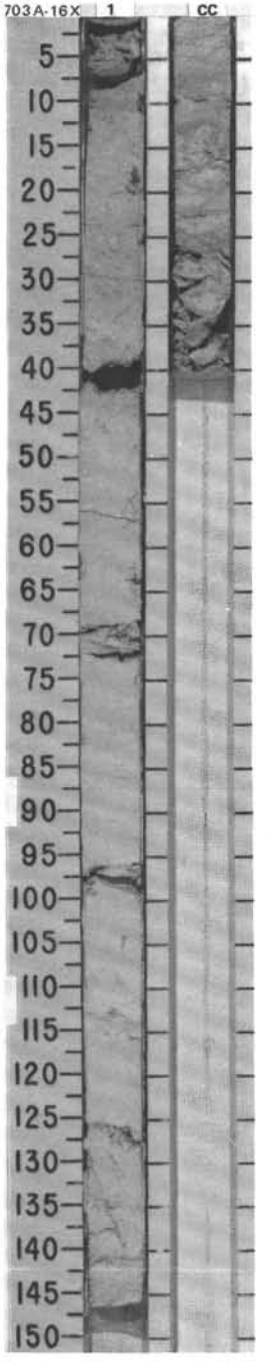

SITE 703 HOLE A CORE 17X CORED INTERVAL 1939.5-1949.0 mbsl; 143.4-152.9 mbsf

TIME-ROCK UNIT	BIOSTRAT. ZONE/ FOSSIL CHARACTER: FORAMINIFERS	NANNOFOSSILS	RADIOLARIANS	DIATOMS	SILICOFLAGELLATES	PALEOMAGNETICS	PHYS. PROPERTIES	CHEMISTRY	SECTION	METERS	GRAPHIC LITHOLOGY	DRILLING DISTURB.	SED. STRUCTURES	SAMPLES
UPPER EOCENE	UPPER EOCENE P15	NP 18	unzoned	EOCENE	*Dictyocha stelliformis-Mesocena apiculata* (subzone) (MIDDLE EOCENE)		ϕ=63.45 ρ_g=2.74		1	0.5				*
										1.0				
									2					
									3					*
									CC					

LITHOLOGIC DESCRIPTION

FORAMINIFER-BEARING NANNOFOSSIL OOZE

Drilling disturbance: Slight biscuiting in the upper 50 cm of Section 3. Three cm of gravel at the top of the core (downhole contamination).

Major lithology: White (no color code) foraminifer-bearing nannofossil ooze. Mn-stained layers in Section 1, 46, 84, and 148 cm; Section 2, 29 and 124 cm; and Section 3, 89-92 cm (light gray, 5Y 7/1). Also sparsely distributed Mn spotting throughout the core.

SMEAR SLIDE SUMMARY (%):

	1, 46 M	3, 60 D
COMPOSITION:		
Volcanic glass	Tr	Tr
Accessory minerals:		
Mn nodules	40	—
Foraminifers	—	20
Nannofossils	55	75
Diatoms	—	4
Radiolarians	—	1
Sponge spicules	—	Tr
Silicoflagellates	—	1
Micrite	5	—

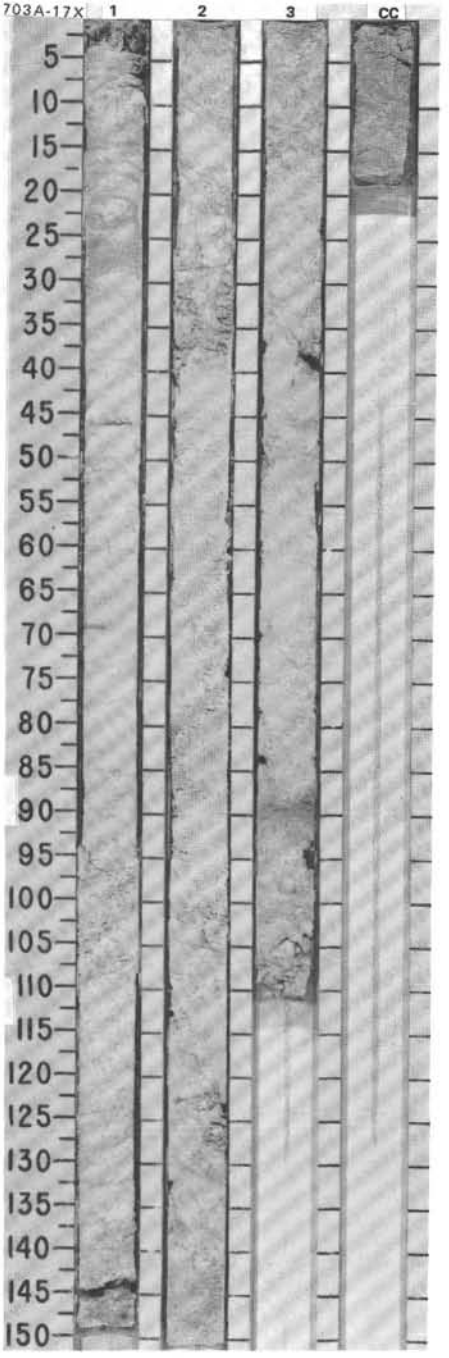

SITE 703 HOLE A CORE 18X CORED INTERVAL 1949.0-1958.5 mbsl; 152.9-162.4 mbsf

TIME-ROCK UNIT	BIOSTRAT. ZONE/ FOSSIL CHARACTER: FORAMINIFERS	NANNOFOSSILS	RADIOLARIANS	DIATOMS	SILICOFLAGELLATES	PALEOMAGNETICS	PHYS. PROPERTIES	CHEMISTRY	SECTION	METERS	GRAPHIC LITHOLOGY	DRILLING DISTURB.	SED. STRUCTURES	SAMPLES
UPPER EOCENE	UPPER EOCENE P15	NP 18	unzoned	EOCENE	*Dictyocha stelliformis-Mesocena apiculata* (subzone)	ϕ=60.50 ρ_g=2.90	ϕ=60.90 ρ_g=2.84	ϕ=61.48 ρ_g=2.86	ϕ=60.73 ρ_g=2.80		1	0.5 1.0			IW OG
											2				
											3				
											4	VOID			*
											5				
											CC				

LITHOLOGIC DESCRIPTION

FORAMINIFER-BEARING NANNOFOSSIL OOZE

Drilling disturbance: Biscuiting of the whole core. Five cm of gravel (downhole contamination) at the top of the core.

Major lithology: Foraminifer-bearing nannofossil ooze, generally white (no color code) with a light gray (5Y 7/1) interval at the top of Section 2, 0-15 cm. Mn-stained layers in Section 1, 24 cm; Section 2, 16, 32, and 55 cm; Section 3, 73-77 cm; and Section 4, 123-130 cm.

SMEAR SLIDE SUMMARY (%):

	4, 60 D
COMPOSITION:	
Volcanic glass	1
Foraminifers	20
Nannofossils	72
Diatoms	3
Radiolarians	1
Sponge spicules	1
Silicoflagellates	Tr
Micrite	2

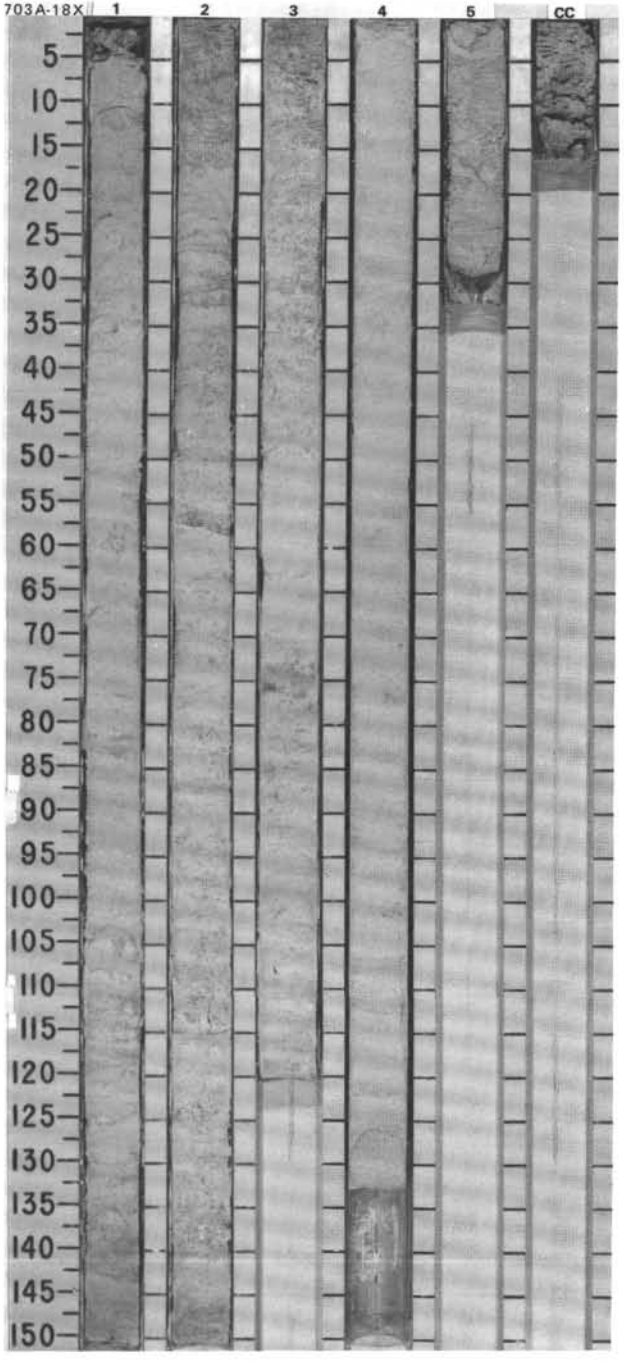

SITE 703 HOLE A CORE 19X CORED INTERVAL 1958.5-1968.0 mbsl; 162.4-171.9 mbsf

TIME-ROCK UNIT	BIOSTRAT. ZONE/ FOSSIL CHARACTER: FORAMINIFERS	NANNOFOSSILS	RADIOLARIANS	DIATOMS	SILICO-FLAGELLATES	PALEOMAGNETICS	PHYS. PROPERTIES	CHEMISTRY	SECTION	METERS	GRAPHIC LITHOLOGY	DRILLING DISTURB.	SED. STRUCTURES	SAMPLES	LITHOLOGIC DESCRIPTION
MIDDLE EOCENE	*G. index* Zone	UPPER MIDDLE EOCENE ◀ P14 ┘	NP 18	unzoned	EOCENE	*Dictyocha stelliformis* (MIDDLE EOCENE)				CC					FORAMINIFER-BEARING NANNOFOSSIL OOZE Drilling disturbance: Downhole contamination from metamorphic and sandstone pebbles. Major lithology: Light greenish gray (5GY 7/1) foraminifer-bearing nannofossil ooze.

SITE 703 HOLE A CORE 20X CORED INTERVAL 1968.0-1977.5 mbsl; 171.9-181.4 mbsf

TIME-ROCK UNIT: MIDDLE EOCENE — UPPER MIDDLE EOCENE

BIOSTRAT. ZONE/FOSSIL CHARACTER: *G. index* Zone P12 - P14

FORAMINIFERS: not examined

NANNOFOSSILS: NP 18 — NP 16

RADIOLARIANS: Barren

DIATOMS: Barren

SILICOFLAGELLATES: Barren

PALEOMAGNETICS

PHYS. PROPERTIES: ϕ=57.24 ρ_g=2.83; ϕ=58.19 ρ_g=2.79; ϕ=61.66 ρ_g=2.89

CHEMISTRY

SECTION: 1, 2, 3, 4, 5, CC

METERS: 0.5, 1.0

GRAPHIC LITHOLOGY: VOID; VOID

DRILLING DISTURB.

SED. STRUCTURES

SAMPLES: *; *

LITHOLOGIC DESCRIPTION

NANNOFOSSIL OOZE

Drilling disturbance: Biscuiting throughout Sections 1-3 and part of Section 4.

Major lithology: White (no color code) nannofossil ooze with Mn-stained horizons at Section 1, 15, 29, and 90 cm; Section 2, 71, 81, 82, and 99 cm; Section 3, 62 cm; Section 4, 30 cm; and Section 5, 8, 10, 56, 69, 76, and 81 cm. Some altered volcanic shards in Section 5, 52 cm.

Minor lithology: Chert nodule, Section 2, 108-111 cm.

SMEAR SLIDE SUMMARY (%):

	2, 70 D	5, 50 M
COMPOSITION:		
Feldspar	—	1
Volcanic glass	Tr	5
Foraminifers	5	5
Nannofossils	93	89
Micrite	2	—

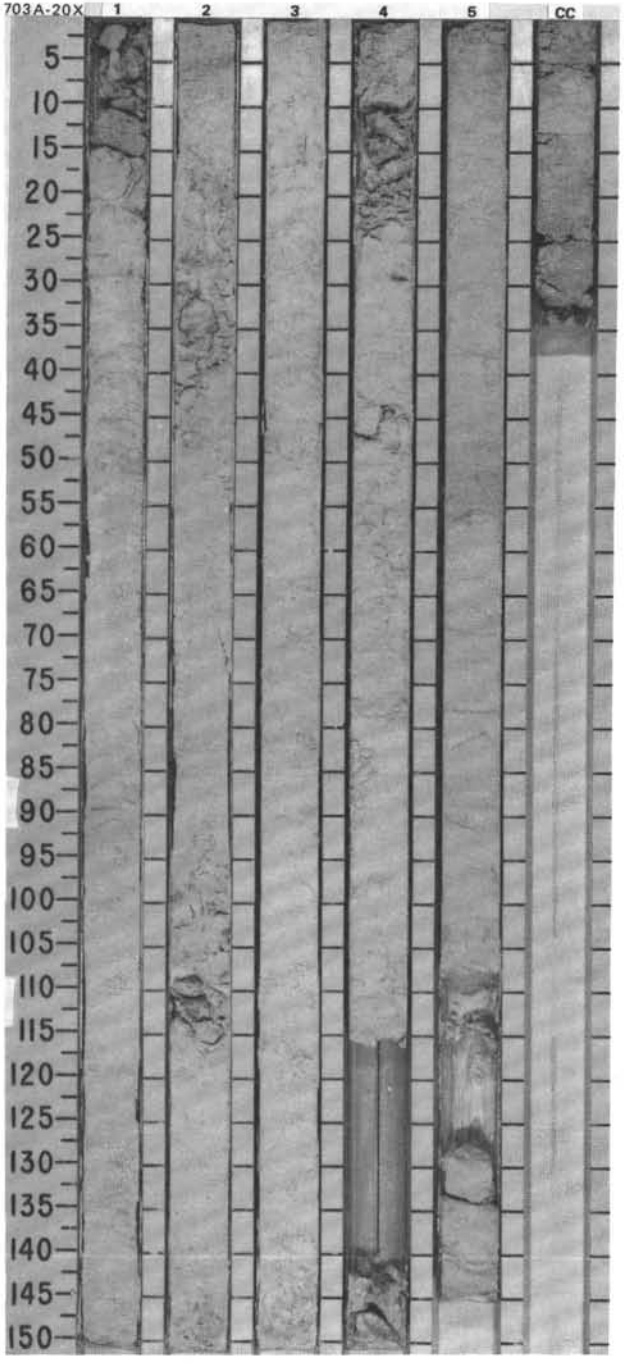

SITE 703 HOLE A CORE 21X CORED INTERVAL 1977.5-1987.0 mbsl; 181.4-190.9 mbsf

TIME-ROCK UNIT: MIDDLE EOCENE — UPPER MIDDLE EOCENE

BIOSTRAT. ZONE/FOSSIL CHARACTER:
- FORAMINIFERS: *G. index* Zone
- NANNOFOSSILS: P12 - P14; NP 16
- RADIOLARIANS: Barren
- DIATOMS: Barren
- SILICOFLAGELLATES: Barren

PALEOMAGNETICS

PHYS. PROPERTIES: ρ_g=2.79, ϕ=58.65; ρ_g=2.88, ϕ=60.89; ρ_g=2.90, ϕ=57.95; ρ_g=2.81, ϕ=61.05

CHEMISTRY

SECTION: 1, 2, 3, 4, 5, 6, CC

METERS: 0.5, 1.0

GRAPHIC LITHOLOGY: VOID; VOID; VOID

DRILLING DISTURB.

SED. STRUCTURES

SAMPLES: IW, OG

LITHOLOGIC DESCRIPTION

NANNOFOSSIL OOZE

Drilling disturbance: Biscuiting or broken-up sections throughout.

Major lithology: White (no color code) nannofossil ooze with a sparse concentration of altered volcanic ash giving rise to pale yellow (5Y 8/3) coloration in Section 5, 35-48 cm.

Minor lithology: Pinkish white (7.5YR 8/2) clay-bearing nannofossil ooze which is more indurated than the pure nannofossil ooze in Section 1 (Section 1, 34-44 and 93-102 cm, and Section 2, 20-39 cm). Also two intervals of white (2.5Y 8/2) nannofossil-foraminifer chalk exhibiting normal grading in Section 2, 54-67 and 91-120 cm.

SMEAR SLIDE SUMMARY (%):

	1, 64 M	2, 24 M
COMPOSITION:		
Clay	—	10
Volcanic glass	1	Tr
Foraminifers	50	7
Nannofossils	49	53
Micrite	—	30

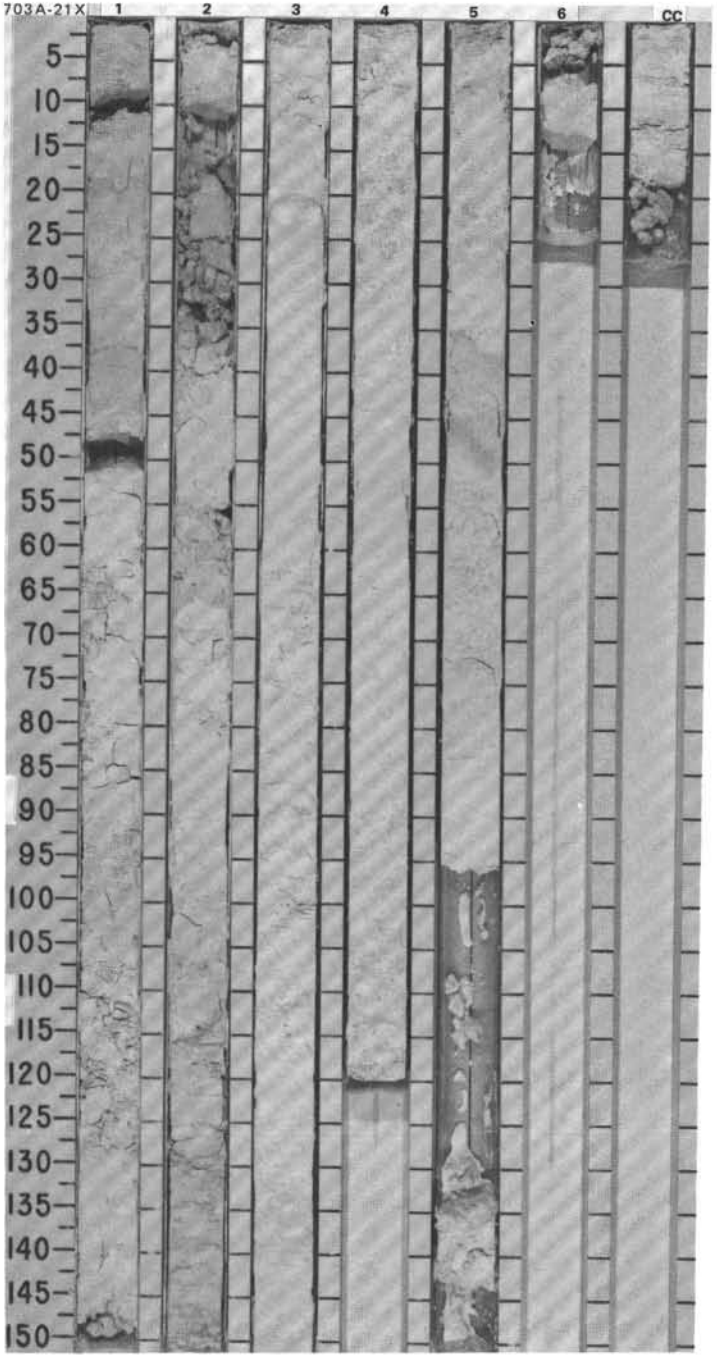

SITE 703 HOLE A CORE 22X CORED INTERVAL 1987.0-1996.5 mbsl; 190.9-200.4 mbsf

TIME-ROCK UNIT	BIOSTRAT. ZONE/ FOSSIL CHARACTER: FORAMINIFERS	NANNOFOSSILS	RADIOLARIANS	DIATOMS	SILICOFLAGELLATES	PALEOMAGNETICS	PHYS. PROPERTIES	CHEMISTRY	SECTION	METERS	GRAPHIC LITHOLOGY	DRILLING DISTURB.	SED. STRUCTURES	SAMPLES	LITHOLOGIC DESCRIPTION
MIDDLE EOCENE	G. *index* Zone UPPER MIDDLE EOCENE	P12 - P14	NP 16	Barren	Barren	Barren									

GRAVELLY VOLCANIC SAND

Drilling disturbance: Sand has probably been washed during coring.

Major lithology: Gravelly volcanic sand consisting predominantly of glass shards, pumice, fragments of volcanic rock, chert, and granite, with an admixture of nannofossil ooze. No primary sedimentary structures observable.

SMEAR SLIDE SUMMARY (%):

	2, 47 D
TEXTURE:	
Sand	100
COMPOSITION:	
Volcanic glass	98
Accessory minerals	2

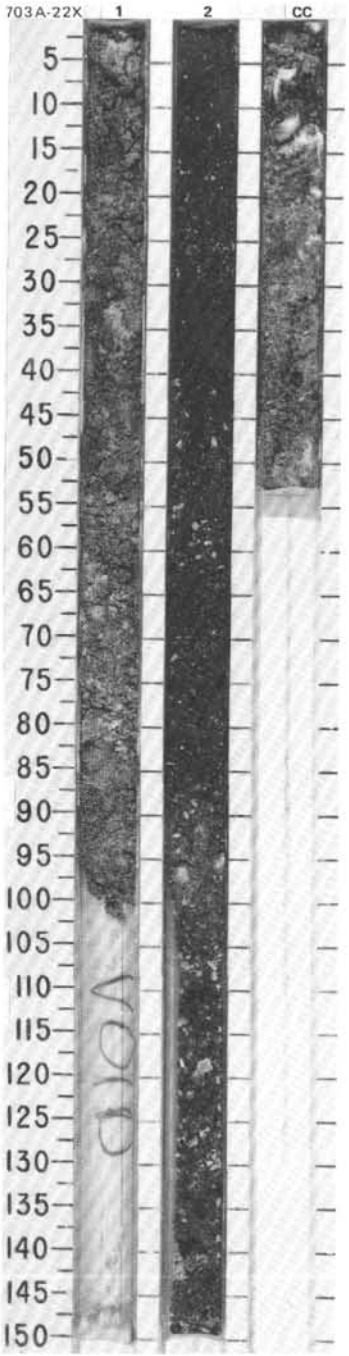

SITE 703 HOLE A CORE 23X CORED INTERVAL 1996.5-2006.0 mbsl; 200.4-209.9 mbsf

TIME-ROCK UNIT	BIOSTRAT. ZONE/FOSSIL CHARACTER: FORAMINIFERS	NANNOFOSSILS	RADIOLARIANS	DIATOMS	SILICOFLAGELLATES	PALEOMAGNETICS	PHYS. PROPERTIES	CHEMISTRY	SECTION	METERS	GRAPHIC LITHOLOGY	DRILLING DISTURB.	SED. STRUCTURES	SAMPLES
MIDDLE EOCENE	*G. index* Zone UPPER MIDDLE EOCENE P12 - P14	NP 15-16	unzoned	Barren	Barren		ϕ=52.24 ρ_g=2.79		1 CC	0.5 1.0				*

LITHOLOGIC DESCRIPTION

CLAY-BEARING, NANNOFOSSIL-BEARING MICRITIC CHALK

Drilling disturbance: Biscuiting throughout.

Major lithology: White (no color code), clay-bearing, nannofossil-bearing micritic chalk.

Minor lithology: Chert nodules, dark brown (7.5YR 3/2), to pinkish gray (7.5YR 7/2), to greenish gray (5Y 5/1), at the top of the core and bottom of the CC.

SMEAR SLIDE SUMMARY (%):

	1, 42 D
COMPOSITION:	
Clay	*10*
Volcanic glass	1
Foraminifers	5
Nannofossils	25
Micrite	59

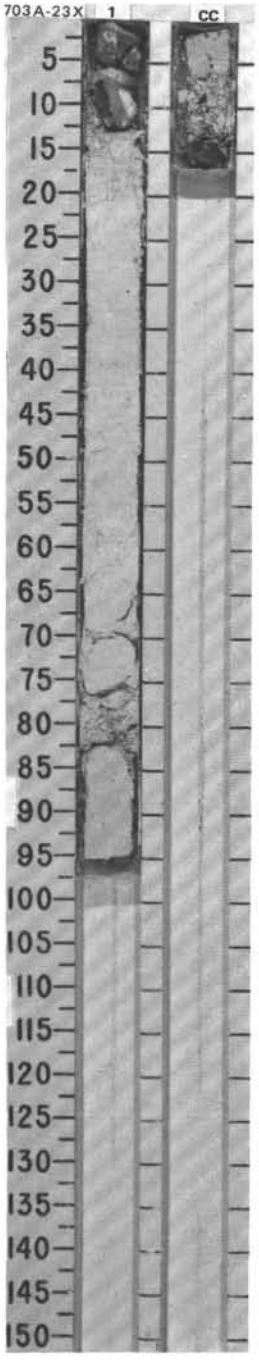

SITE 703 HOLE A CORE 24X CORED INTERVAL 2006.0-2015.5 mbsl; 209.9-219.4 mbsf

TIME-ROCK UNIT	BIOSTRAT. ZONE/ FOSSIL CHARACTER: FORAMINIFERS	NANNOFOSSILS	RADIOLARIANS	DIATOMS	SILICO-FLAGELLATES	PALEOMAGNETICS	PHYS. PROPERTIES	CHEMISTRY	SECTION	METERS	GRAPHIC LITHOLOGY	DRILLING DISTURB.	SED. STRUCTURES	SAMPLES	LITHOLOGIC DESCRIPTION
MIDDLE EOCENE	*G. index* Zone UPPER MIDDLE EOCENE P12 - P14	NP 15-16	Barren	Barren	Barren				CC		●●●●●●●●				GRAVEL Drilling disturbance: No recovery apart from a few pebbles in the CC which are probably due to downhole contamination.

703A-25X NO RECOVERY

SITE 703 HOLE A CORE 26X CORED INTERVAL 2025.0-2034.5 mbsl; 228.9-238.4 mbsf

TIME-ROCK UNIT	BIOSTRAT. ZONE/ FOSSIL CHARACTER: FORAMINIFERS	NANNOFOSSILS	RADIOLARIANS	DIATOMS	SILICOFLAGELLATES	PALEOMAGNETICS	PHYS. PROPERTIES	CHEMISTRY	SECTION	METERS	GRAPHIC LITHOLOGY	DRILLING DISTURB.	SED. STRUCTURES	SAMPLES
MIDDLE EOCENE														
	G. index Zone	NP 15-16	Barren	Barren	Barren		ϕ=57.17 ρ_g=2.76	ϕ=57.06 ρ_g=2.81	ϕ=58.53 ρ_g=2.64	ϕ=61.84 ρ_g=2.92	1	0.5 1.0				
	LOWER MIDDLE EOCENE	P11 - P12									2				OG IW	
											3					
											4					
											5				*	
											CC					

LITHOLOGIC DESCRIPTION

MICRITIC NANNOFOSSIL CHALK

Drilling disturbance: Soupy sediment in Section 1. Biscuiting throughout.

Major lithology: Micritic nannofossil chalk, white (no color code). *Zoophycos* burrow in Section 1, 113 cm.

Minor lithology: Chert nodule in Section 4, 29–36 cm.

SMEAR SLIDE SUMMARY (%):

	5, 70 D
COMPOSITION:	
Calcite/dolomite	1
Accessory minerals	Tr
Foraminifers	8
Nannofossils	74
Micrite	18

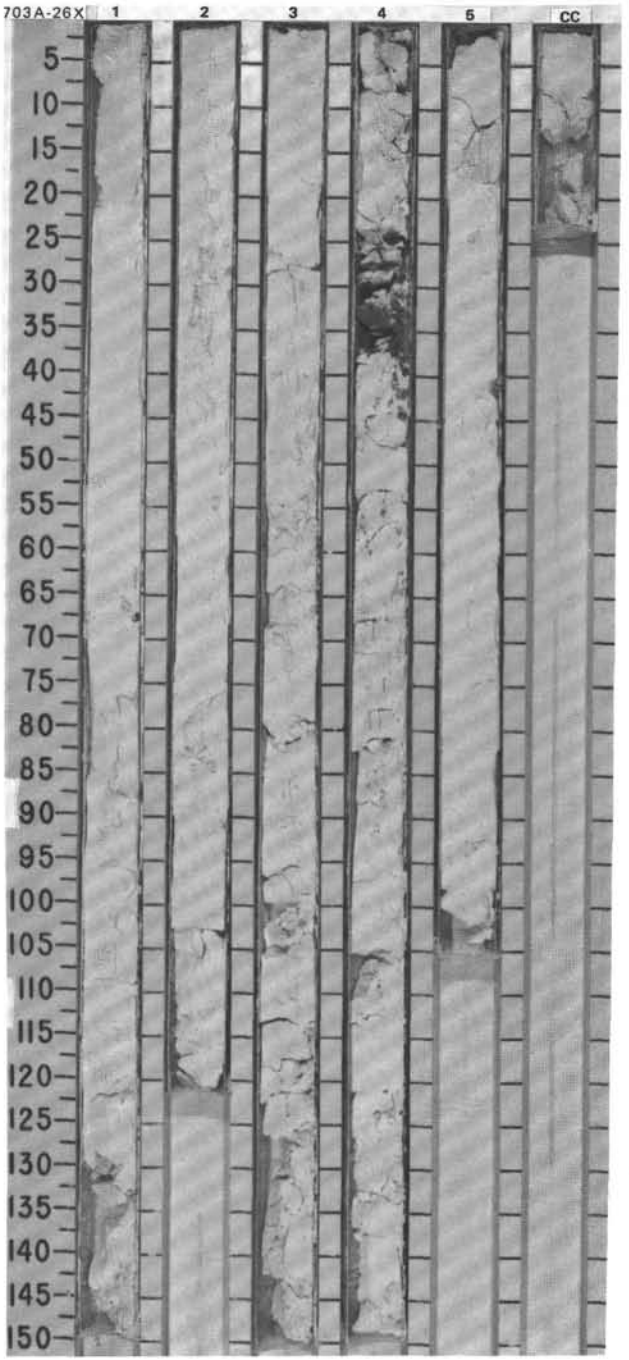

SITE 703 HOLE A CORE 27X CORED INTERVAL 2034.5-2044.0 mbsl; 238.4-247.9 mbsf

TIME-ROCK UNIT	BIOSTRAT. ZONE/ FOSSIL CHARACTER: FORAMINIFERS	NANNOFOSSILS	RADIOLARIANS	DIATOMS	SILICOFLAGELLATES	PALEOMAGNETICS	PHYS. PROPERTIES	CHEMISTRY	SECTION	METERS	GRAPHIC LITHOLOGY	DRILLING DISTURB.	SED. STRUCTURES	SAMPLES	LITHOLOGIC DESCRIPTION
MIDDLE EOCENE		NP 15-16	Barren	Barren	Barren				CC		●●●●●●●●	X		*	CHERT Major lithology: Chert. Minor lithology: White (no color code) foraminifer-bearing micritic chalk. SMEAR SLIDE SUMMARY (%): CC, 6 D COMPOSITION: Feldspar 1 Foraminifers 12 Micrite 87

SITE 703 HOLE A CORE 28X CORED INTERVAL 2044.0-2053.5 mbsl; 247.9-257.4 mbsf

TIME-ROCK UNIT	BIOSTRAT. ZONE/ FOSSIL CHARACTER: FORAMINIFERS	NANNOFOSSILS	RADIOLARIANS	DIATOMS	SILICOFLAGELLATES	PALEOMAGNETICS	PHYS. PROPERTIES	CHEMISTRY	SECTION	METERS	GRAPHIC LITHOLOGY	DRILLING DISTURB.	SED. STRUCTURES	SAMPLES	LITHOLOGIC DESCRIPTION
MIDDLE EOCENE		NP 15-16	Barren	Barren	Barren				CC		●●●●●●●●				LITHIC FRAGMENTS Drilling disturbance: No recovery apart from two lithic fragments due to downhole contamination.

703A-29X NO RECOVERY

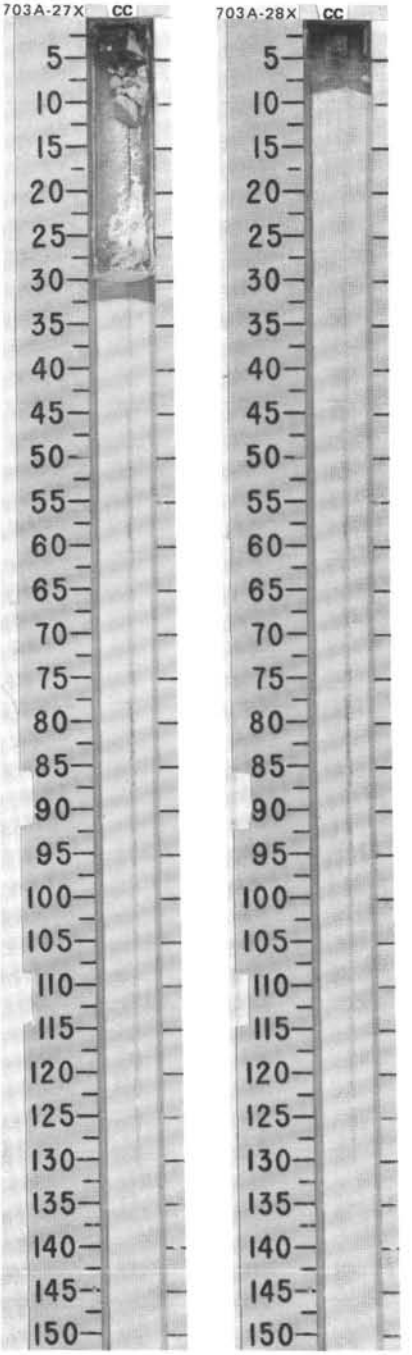

SITE 703 HOLE A CORE 30X CORED INTERVAL 2063.0-2072.5 mbsl: 266.9-276.4 mbsf

TIME-ROCK UNIT	BIOSTRAT. ZONE/FOSSIL CHARACTER: FORAMINIFERS	NANNOFOSSILS	RADIOLARIANS	DIATOMS	SILICOFLAGELLATES	PALEOMAGNETICS	PHYS. PROPERTIES	CHEMISTRY	SECTION	METERS	GRAPHIC LITHOLOGY	DRILLING DISTURB.	SED. STRUCTURES	SAMPLES	LITHOLOGIC DESCRIPTION
MIDDLE EOCENE		NP 15-16	Barren	Barren	Barren		ϕ=56.87 ρ_g=2.84 ϕ=58.44 ρ_g=2.98		1 2 3 4 CC	0.5 1.0	VOID	○		* * * IW OG	MICRITE-BEARING, FORAMINIFER-BEARING NANNOFOSSIL CHALK

Drilling disturbance: Soupy sediments in Sections 1 and 2.

Major lithology: White (no color code) to light gray (5Y 7/1) micrite-bearing, foraminifer-bearing nannofossil chalk. Section 3, 0-80 cm, and CC, slightly mottled.

Minor lithology: Chert fragments at the top of the core.

SMEAR SLIDE SUMMARY (%):

	1, 70 D	2, 29 D	3, 81 D	3, 120 D
COMPOSITION:				
Calcite/dolomite	1	2	3	2
Foraminifers	—	10	12	10
Nannofossils	79	73	70	78
Micrite	20	15	15	10

703A-31X NO RECOVERY

703A-32X NO RECOVERY

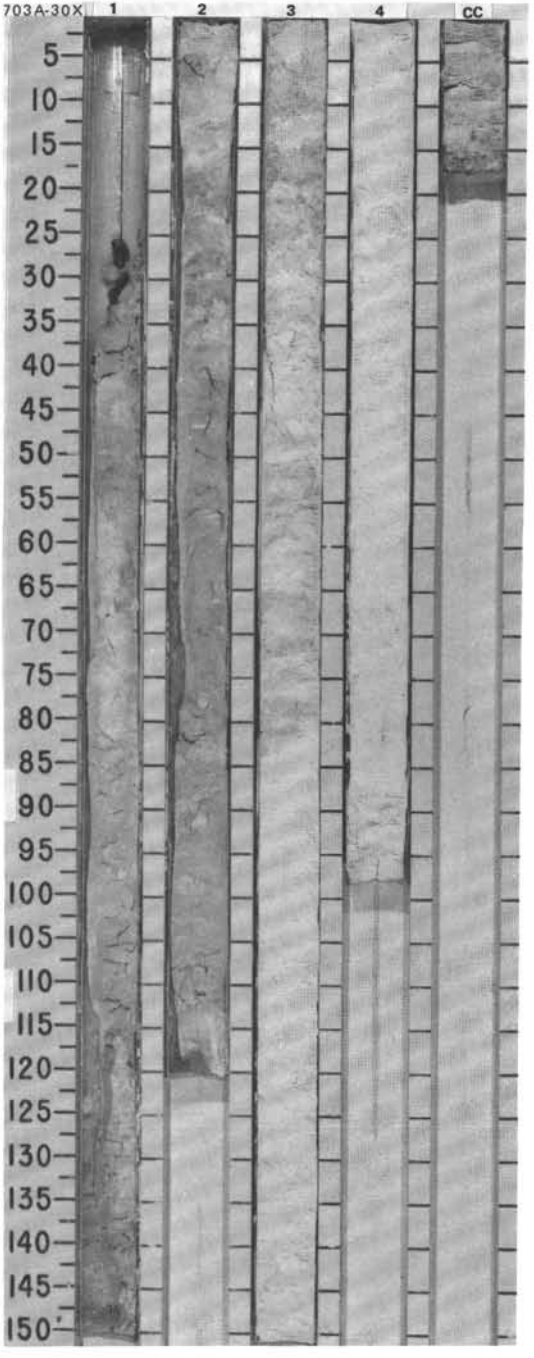

SITE 703 HOLE A CORE 33X CORED INTERVAL 2091.5-2101.0 mbsl; 295.4-304.9 mbsf

TIME-ROCK UNIT	BIOSTRAT. ZONE/ FOSSIL CHARACTER: FORAMINIFERS	NANNOFOSSILS	RADIOLARIANS	DIATOMS	SILICOFLAGELLATES	PALEOMAGNETICS	PHYS. PROPERTIES	CHEMISTRY	SECTION	METERS	GRAPHIC LITHOLOGY	DRILLING DISTURB.	SED. STRUCTURES	SAMPLES	LITHOLOGIC DESCRIPTION
MIDDLE EOCENE		NP 13?	Barren	Barren	Barren				CC					*	GRAVELLY VOLCANIC SAND

Major lithology: Gravelly volcanic sand with an admixture of chert, basalt, and quartz gravel as well as granodiorite pebble (downhole contamination?).

SMEAR SLIDE SUMMARY (%):

	CC D	CC D
COMPOSITION:		
Feldspar	2	5
Volcanic glass	90	85
Accessory minerals	5	10

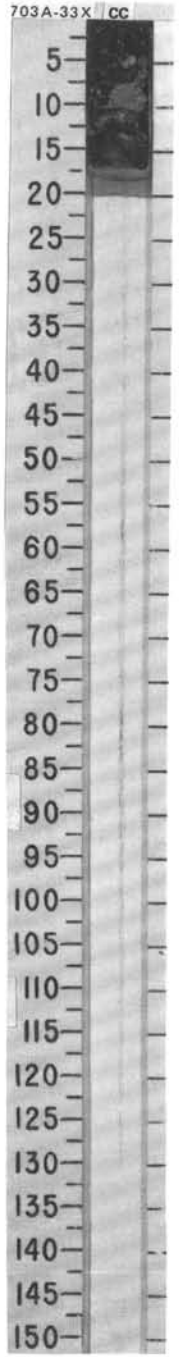

SITE 703 HOLE A CORE 34X CORED INTERVAL 2101.0-2110.5 mbsl; 304.9-314.4 mbsf

TIME-ROCK UNIT	BIOSTRAT. ZONE/ FOSSIL CHARACTER: FORAMINIFERS	NANNOFOSSILS	RADIOLARIANS	DIATOMS	SILICOFLAGELLATES	PALEOMAGNETICS	PHYS. PROPERTIES	CHEMISTRY	SECTION	METERS	GRAPHIC LITHOLOGY	DRILLING DISTURB.	SED. STRUCTURES	SAMPLES
	Barren	Barren	Barren	Barren	Barren	ϕ=53.13 ρ_g=2.92	ϕ=50.49 ρ_g=2.97	ϕ=50.36 ρ_g=2.89	1	0.5 1.0		X		*
									2			X		
									3			X	// //	
									4			X		
									5			X		TW
									CC			X		

LITHOLOGIC DESCRIPTION

VOLCANIC BRECCIA

Drilling disturbance: Entire core is fragmented and biscuited.

Major lithology: Volcanic breccia, generally yellow (5Y 8/6) to olive yellow (5Y 6/6), but reddish brown (5YR 5/5) to light yellowish brown (10YR 6/4) in Section 1. The breccia is highly altered and, where not highly disturbed by the drilling process, indurated. It consists of pumice with volcanic glass shards. A few large indurated pieces in Section 3, 55-62 cm exhibit bedding with coarse-grained yellow (5Y 8/6) layers containing 2-3-mm-sized fragments of pumice alternating with finer-grained dark gray to brown (2.5Y 4/2) layers (0.5 mm). In Sections 4 and 5, the pumice is partly cemented by a white (2.5Y 8/2), fine-grained, non-carbonate matrix.

SMEAR SLIDE SUMMARY (%):

	1, 1 D	1, 144 D	CC D
COMPOSITION:			
Feldspar	4	20	8
Rock fragments	—	5	—
Clay	20	60	63
Volcanic glass	65	5	4
Accessory minerals	11	10	15
Nannofossils	Tr	—	—

703A-35X NO RECOVERY

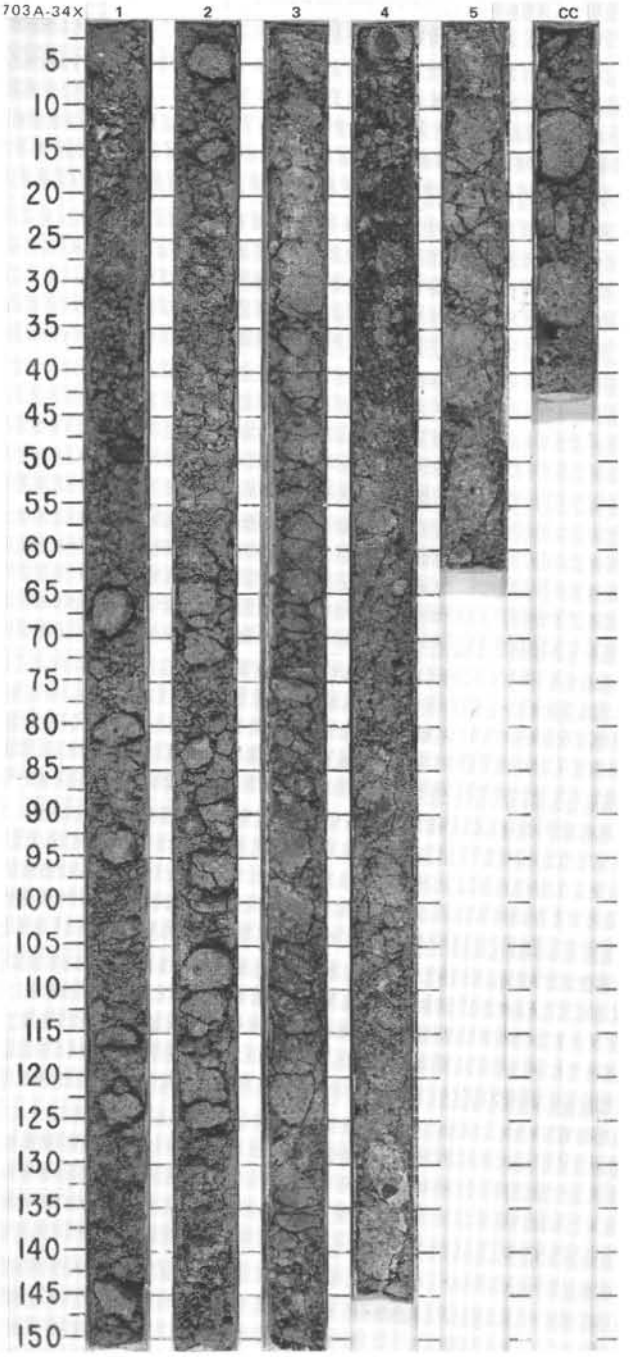

SITE 703 HOLE A CORE 36X CORED INTERVAL 2120.0-2129.5 mbsl: 323.9-333.4 mbsf

TIME-ROCK UNIT	BIOSTRAT. ZONE/ FOSSIL CHARACTER: FORAMINIFERS	NANNOFOSSILS	RADIOLARIANS	DIATOMS	SILICOFLAGELLATES	PALEOMAGNETICS	PHYS. PROPERTIES	CHEMISTRY	SECTION	METERS	GRAPHIC LITHOLOGY	DRILLING DISTURB.	SED. STRUCTURES	SAMPLES	LITHOLOGIC DESCRIPTION
	Barren	Barren	Barren	Barren	Barren				CC						GRAVEL

Drilling disturbance: No recovery apart from drilling breccia in the CC.

Major lithology: Gravel consisting of mudstone, granodiorite, quartz, greenschist, pumice and other volcanic material, and chert mixed with a fine-grained, floury, pale yellow (5Y 7/4) matrix which is similar to the matrix of the volcanic breccia in 114-703A-34X.

703A-37X NO RECOVERY

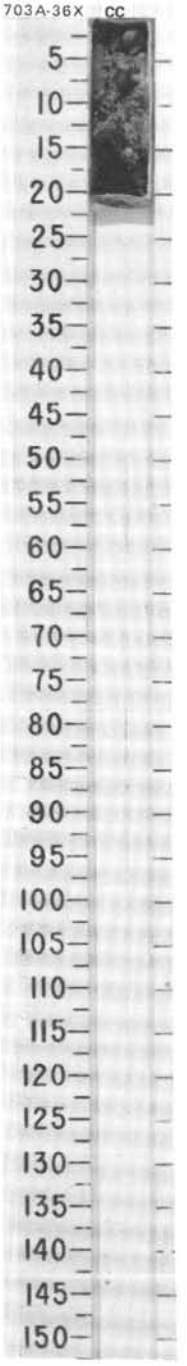

SITE 703 HOLE A CORE 38X CORED INTERVAL 2139.0-2148.5 mbsl; 342.9-352.4 mbsf

TIME-ROCK UNIT	BIOSTRAT. ZONE/ FOSSIL CHARACTER: FORAMINIFERS	NANNOFOSSILS	RADIOLARIANS	DIATOMS	SILICO-FLAGELLATES	PALEOMAGNETICS	PHYS. PROPERTIES	CHEMISTRY	SECTION	METERS	GRAPHIC LITHOLOGY	DRILLING DISTURB.	SED. STRUCTURES	SAMPLES	LITHOLOGIC DESCRIPTION
		Barren	Barren	Barren	Barren				CC						GRAVEL Major lithology: A single fine-grained porphyritic rhyolite(?) pebble was found in CC.

SITE 703 HOLE A CORE 39X CORED INTERVAL 2148.5-2158.0 mbsl; 352.4-361.9 mbsf

TIME-ROCK UNIT	BIOSTRAT. ZONE/ FOSSIL CHARACTER: FORAMINIFERS	NANNOFOSSILS	RADIOLARIANS	DIATOMS	SILICO-FLAGELLATES	PALEOMAGNETICS	PHYS. PROPERTIES	CHEMISTRY	SECTION	METERS	GRAPHIC LITHOLOGY	DRILLING DISTURB.	SED. STRUCTURES	SAMPLES	LITHOLOGIC DESCRIPTION
		Barren	Barren	Barren	Barren				CC						GRAVEL Major lithology: Two pebbles were recovered. One is a porphyritic acidic volcanic rock, the other (2 × 1 × 2 cm) is a vesicular, porphyritic rhyolite(?).

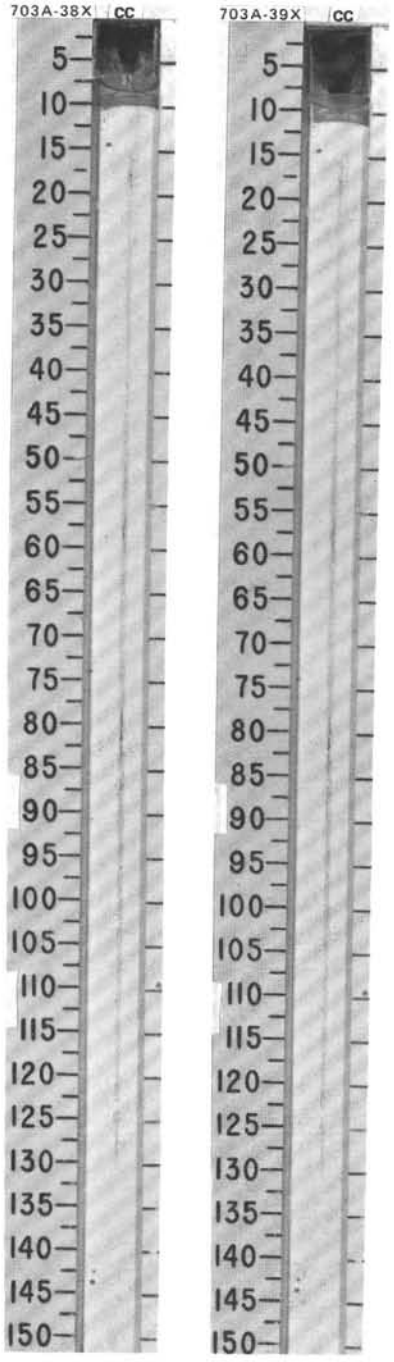

SITE 703 HOLE A CORE 40X CORED INTERVAL 2158.0-2167.5 mbsl; 361.9-371.4 mbsf

TIME-ROCK UNIT	BIOSTRAT. ZONE/ FOSSIL CHARACTER: FORAMINIFERS	NANNOFOSSILS	RADIOLARIANS	DIATOMS	SILICO-FLAGELLATES	PALEOMAGNETICS	PHYS. PROPERTIES	CHEMISTRY	SECTION	METERS	GRAPHIC LITHOLOGY	DRILLING DISTURB.	SED. STRUCTURES	SAMPLES	LITHOLOGIC DESCRIPTION
MIDDLE EOCENE LOWER MIDDLE EOCENE *A. primitiva* Zone	P10 - P11	Barren	Barren	Barren	Barren	ϕ=8.93 ρ_g=2.84 ϕ=2.55 ρ_g=2.74 ϕ=10.55 ρ_g=3.01			1 2 3	0.5 1.0					DOLOMITE-BEARING, VOLCANIC ASH CALCAREOUS SAND, and BASALT

Drilling disturbance: Sand and basalt are intermixed in Section 3. Sand has probably been washed in during drilling process.

Major lithologies: Dolomite-bearing, volcanic ash calcareous sand of mixed color (white, 2.5Y 8/2, to light olive brown, 2.5Y 5/4), and highly altered amygdaloidal porphyritic basalt.

SMEAR SLIDE SUMMARY (%):

	1, 80 D
COMPOSITION:	
Volcanic glass	30
Dolomite	15
Foraminifers	15
Nannofossils	40

SITE 703 HOLE A CORE 41X CORED INTERVAL 2167.5-2175.5 mbsl; 371.4-377.4 mbsf

TIME-ROCK UNIT	BIOSTRAT. ZONE/ FOSSIL CHARACTER: FORAMINIFERS	NANNOFOSSILS	RADIOLARIANS	DIATOMS	SILICO-FLAGELLATES	PALEOMAGNETICS	PHYS. PROPERTIES	CHEMISTRY	SECTION	METERS	GRAPHIC LITHOLOGY	DRILLING DISTURB.	SED. STRUCTURES	SAMPLES	LITHOLOGIC DESCRIPTION
	Barren	Barren	Barren	Barren	Barren				CC						BASALT

Major lithology: Core consists of a number of pieces of highly altered amygdaloidal basalt.